

An Experiment to Search for $\left\{ \begin{matrix} \nu_\mu \\ \nu_e \end{matrix} \right\} \rightarrow \nu_\tau$ Neutrino Oscillations
 Using an Enriched $(\nu_e/\bar{\nu}_e)$ Beam

U. Camerini, C. Canada, D. Cline, G. Bauer, W. Fry, R. Loveless

R. March, M. Mohammadi, A. More, D.D. Reeder, H. Wachsmuth

University of Wisconsin, Madison, Wisconsin

C. Kourkoumelis, A. Markou, L.K. Resvanis

University of Athens, Athens, Greece

R. Huson, J. Schmidt, W. Smart, R. Stefanski, E. Treadwell

Fermilab, Batavia, Illinois

F. Bobbisut, E. Calimani, G. Puglierin, A. Sconsa, M. Baldo-Ceolin

Instituto di Fisica, Università di Padova, Padova, Italy*

ABSTRACT

We propose to construct an enriched $\nu_e/\bar{\nu}_e$ beam using K^0_L decays and the sign selected bare target beam elements. The $(\nu_e/\bar{\nu}_e)$ beam and the 15' bubble chamber filled with heavy neon will be used to search for ν_τ interactions arising from $\nu_e \rightarrow \nu_\tau$ or $\nu_\mu \rightarrow \nu_\tau$ neutrino oscillations. Using the present analysis of neutrino oscillations from Barger, et al., we find that $\lesssim 250$ ν_τ interactions could be observed in a 500,000 picture exposure depending on the neutrino mixing parameters. If oscillations are observed, this experiment would also establish the existence of the ν_τ neutrino. The energy of the primary proton beam is 400 GeV, although as an energy saving alternative this experiment could also be operated at a reduced machine energy of 200 GeV with an increased repetition rate.

*Università di Padova's participation is subject to Italian authorities' approval.

Contents

1. Introduction
2. Search for $\nu_\tau + \bar{\tau}^-$ in the bubble chamber
3. The enriched $\nu_e/\bar{\nu}_e$ beam using the BTSS beam
4. Event Rates and Detection Efficiency
5. Appendices
 - A. Possible Indications of Neutrino Oscillations, V. Barger, et al
 - B. Mass and Mixing Scales of Neutrino Oscillations, V. Barger, et.al.

1. Introduction

A recent analysis of existing neutrino oscillation data suggested the possibility that neutrino oscillations may have been observed, but no conclusive evidence exists at present (Appendix A)¹. The most interesting possibility suggested by this analysis is that $\nu_e \rightarrow \nu_\tau$ oscillations may exist with a fairly large mixing angle and δm^2 ^{1,2}. All previous experiments were insensitive to this kind of oscillation because of low ν_e flux or very large ν_μ flux that produces a large background. We propose to construct an enriched ν_e , $\bar{\nu}_e$ beam with a large ν_e/ν_μ ratio, compared to ordinary beams, in order to carry out a conclusive search for $\nu_e \rightarrow \nu_\tau$ oscillations. Figure 1 shows the range of sensitivity required to deserve $\nu_e \rightarrow \nu^\tau$ for the two solutions suggested in the analysis of Barger, et al^{1,2}. We emphasize that 10 - 30 GeV (ν_e , $\bar{\nu}_e$) beams with long flight paths (> 1 KM) and considerable purity from large ν_μ , $\bar{\nu}_\mu$ flux are necessary to establish the signal of $\nu_e \rightarrow \nu_\tau$. Also the present data allow $P(\nu_e \rightarrow \nu_\tau)$ between the lower and upper kinks given by beam dump experiments (Fig. 1).

We propose to construct a K^0_L beam in the normal neutrino decay channel. Using the Bare Target Sign Selected train load, a modest, inexpensive beam defining system is available^{3,4,5}. This system is shown schematically in Figure 2. The most suitable detector to perform this search is the 15' bubble chamber with a neon-hydrogen filling.

The use of the heavy liquid bubble chamber has the following well-known advantages:

- 1) excellent identification of electrons with both sign and momentum determination.
- 2) good efficiency in observing and measuring neutrino interactions down to very low energies ~ 500 MeV/c.
- 3) excellent visibility of the vertex. It might be possible to see the τ lepton decay vertex depending on τ momentum spectra and lifetime. The addition of the high resolution camera to the stereo triad would considerably enhance this possibility.
- 4) unbiased data taking. The detection of events is independent of the kinematic characteristics and/or the event energy.

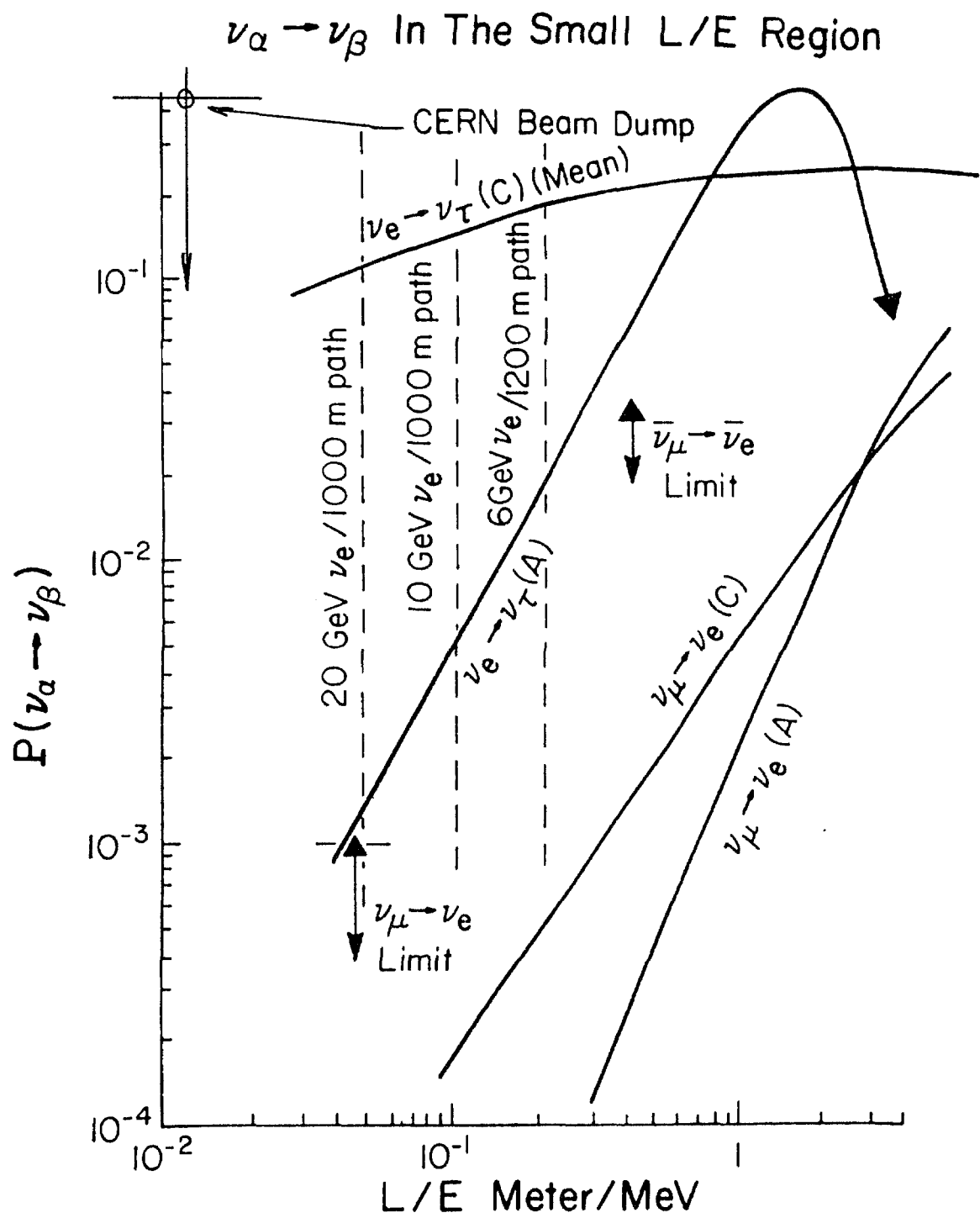


FIGURE 1

Special $\nu_e, \bar{\nu}_e$ Beam
For Neutrino Oscillation Search

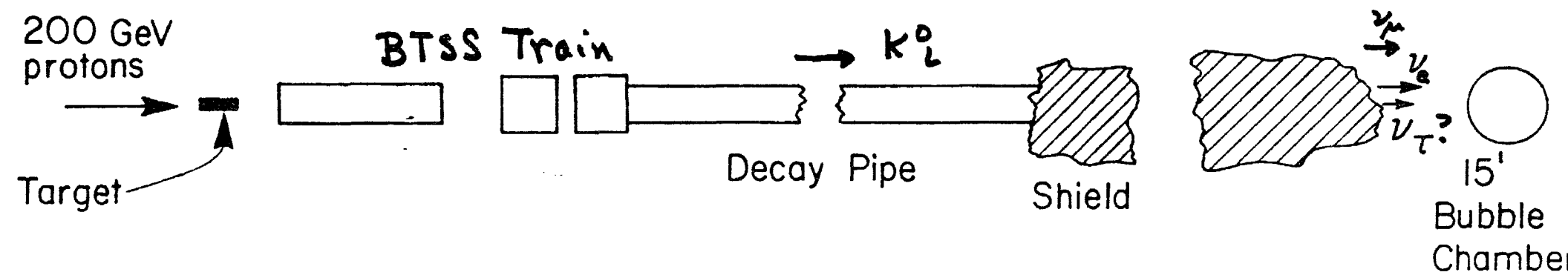
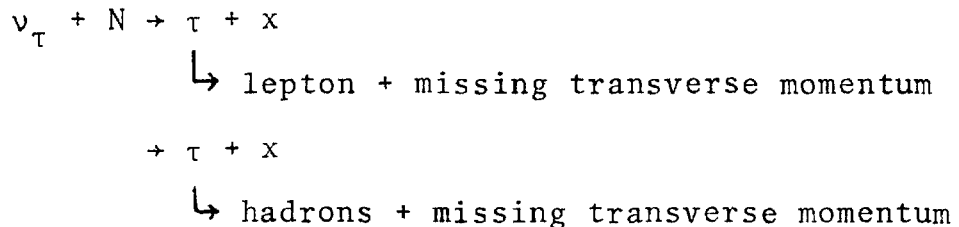


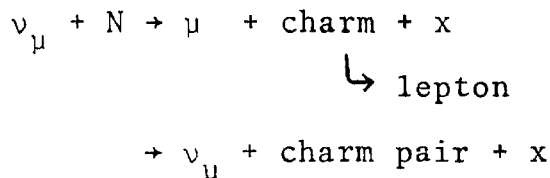
FIGURE 2

2. The Search for $\nu_\tau \rightarrow \tau$ in the Bubble Chamber

We propose to detect the presence of ν_τ , $\bar{\nu}_\tau$ in the ν_e , ν_μ beam through the signature

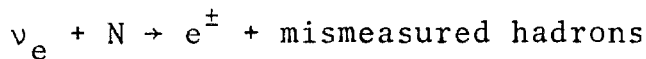


This is schematically shown in Figure 3. Albright et al.⁶ and Barger et al.⁷ have made extensive calculations for the backgrounds to these signatures from charmed particle production (i.e.)



In normal neutrino beams the ratio of ν_μ flux to ν_e flux is about 100 to 1. This is about the same ratio as the ratio of lepton pair production by ν_μ through charm. About one order of magnitude smaller there appears to be evidence for events with same sign leptons which may be due to charm pair production. At some level all of these processes may contribute to fake $\nu_\tau \rightarrow \tau$ events. Thus it is essential to reduce the large ν_μ flux in a ν_e beam to reduce these backgrounds. The missing transverse momentum distributions for τ^\pm production and decay are shown in Figure 4 for leptonic and $\nu_\tau + \text{hadronic}$ decays.

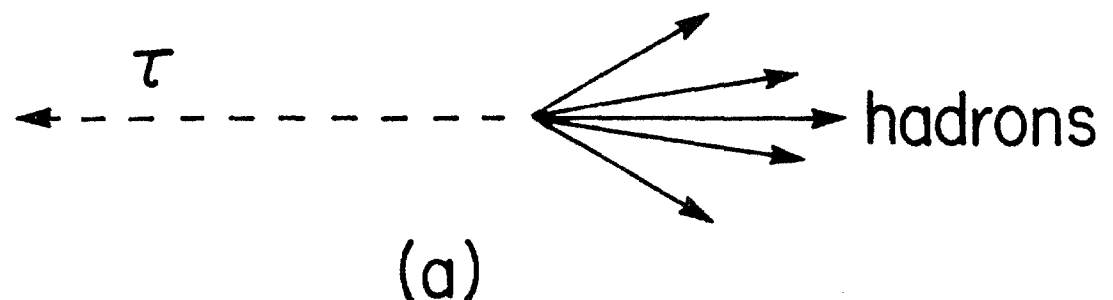
We have estimated the expected background contribution for



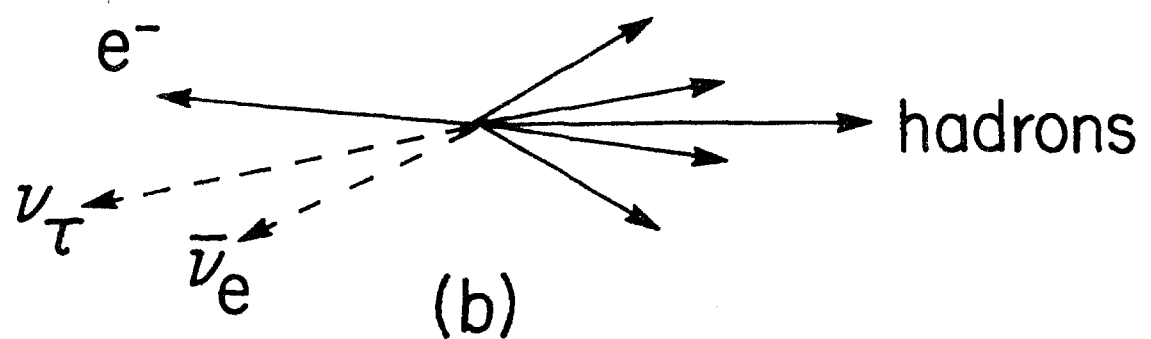
from existing data and find that less than 3×10^{-3} of ν_e , $\bar{\nu}_e$ interactions should have a "fake" missing $P\perp$. Thus it appears possible to identify τ^\pm to this level in the bubble chamber.

The expected cross section and y distribution for production at these low energies are shown in Figure 5 and Figure 6 respectively⁸. The characteristic y distribution might provide additional evidence that τ^\pm have been observed. The relevant variable in neutrino oscillations is L/E_ν (the ν path length/neutrino energy). Since the path length is fixed, the important measurements are the rates as a function of neutrino energy. No other detector combines the sensitivity and precision at low neutrino energies as does the heavy liquid bubble chamber.

τ Signatures



(a)



(b)

FIGURE 3

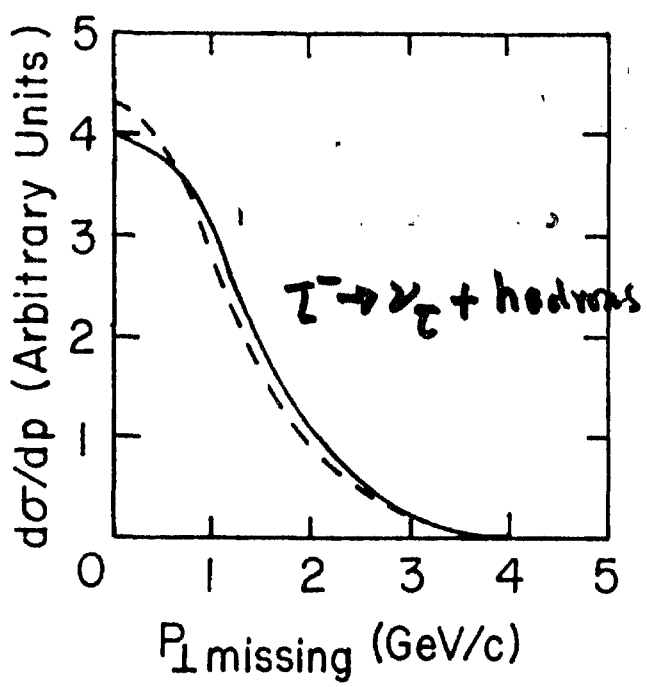
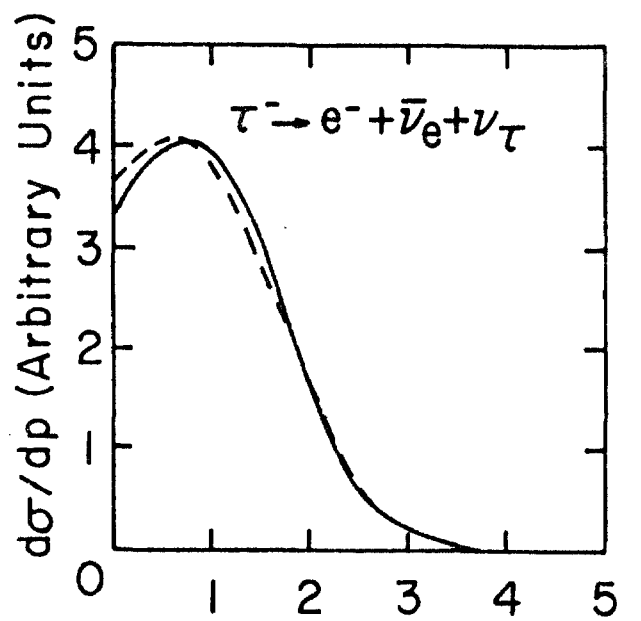


FIGURE 4

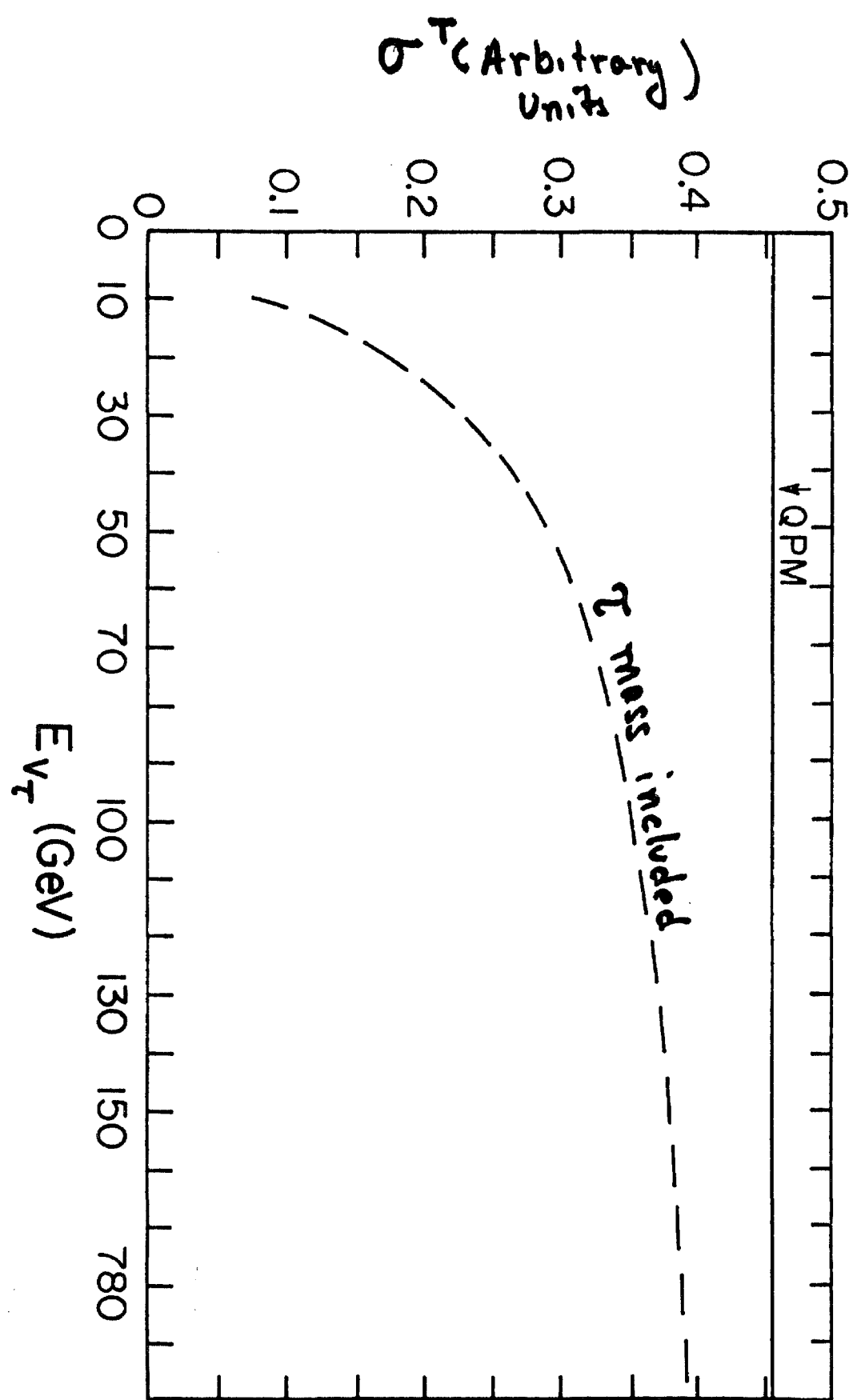


FIGURE 5

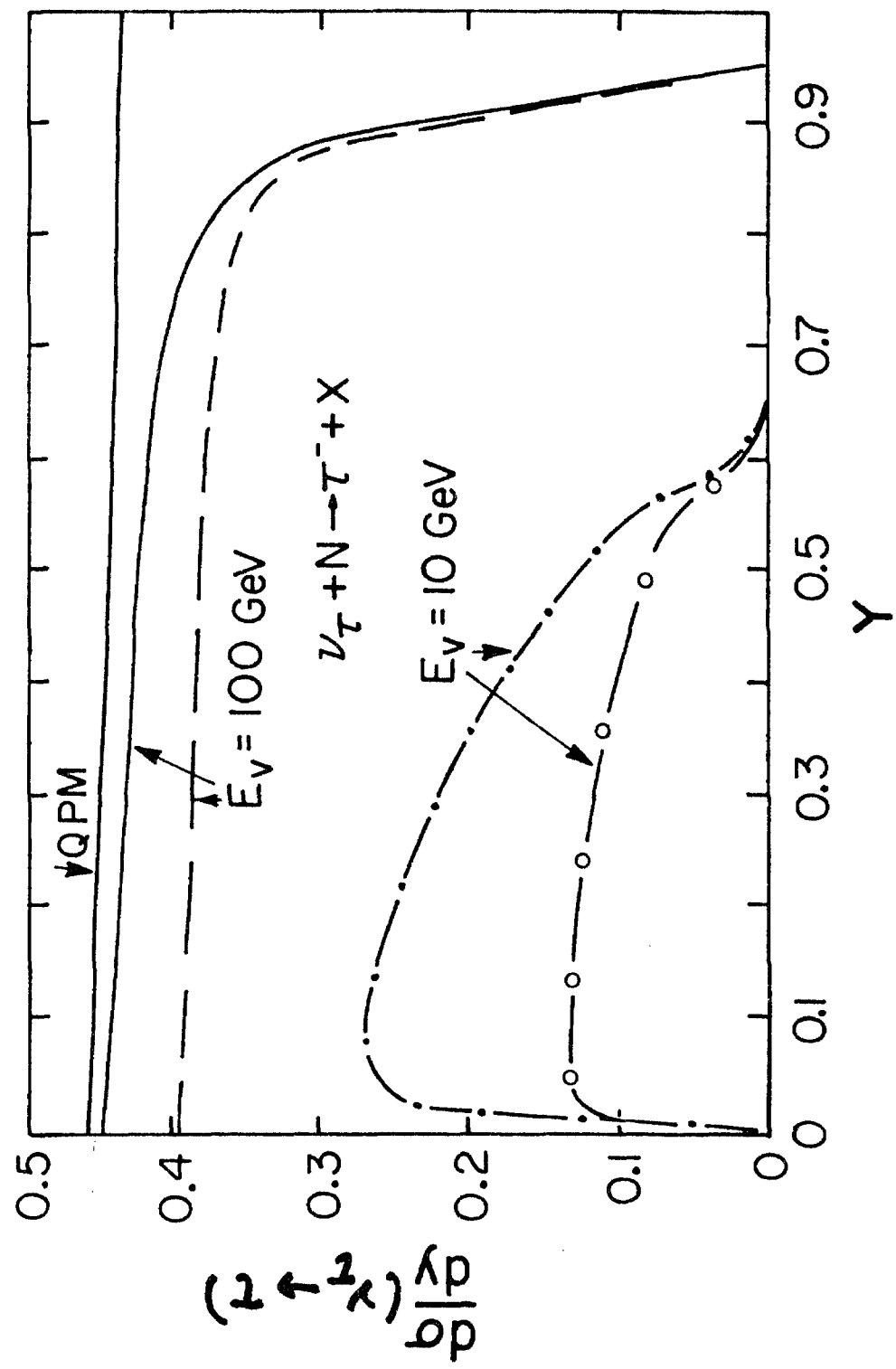


FIGURE 6

3. The Enriched $\nu_e/\bar{\nu}_e$ Beam

We propose to use K_L^0 decay to provide an enriched $\nu_e/\bar{\nu}_e$ beam. Practical beams were discussed some time ago. We follow closely the description by Mori, et al^{4,5}:

The Sign Selected Bare Target (SSBT) train used for the HPWF neutrino experiment can easily be modified for an electron neutrino beam. Figure 7 gives a schematic layout of the arrangement⁴. A modification required for the SSBT Beam is to move the dump a few inches to allow the K_L^0 beam to enter the decay pipe.

Figure 8 shows a calculated electron neutrino or antineutrino flux from the $K_L^0 \rightarrow \pi^- e^+ \nu_e$ (or $\pi^+ e^- \bar{\nu}_e$) decay by a Monte Carlo program. The incident proton energy is 400 GeV. The K_L^0 production is assumed to be the average K^+ and K^- production. Stefanski-White parameterization was used. Figure 9, 10 shows the spectra for 200 GeV protons. The muon neutrino background from the π^+ and K^+ decays is also shown in Figure 9, 10. This background is relatively independent of the incident proton energy. The muon antineutrino background from the π^- and K^- decays is substantially smaller than the muon neutrino background. The muon neutrino or antineutrino flux from the $K_L^0 \rightarrow \pi^- \mu^+ \nu_\mu$ (or $\pi^+ \mu^- \bar{\nu}_\mu$) is 70% of the electron neutrino or antineutrino flux from the K_L^0 decay. The muon neutrino or antineutrino backgrounds from pion decays of the $K_S^0 \rightarrow \pi^+ \pi^-$ are estimated to be relatively small in the present arrangement.

In summary, computed electron neutrino fluxes for the present electron neutrino beams are shown in Figures 8, 9, 10 for the incident proton energies of 400 and 200 GeV.

BTSS Beam Set For K_L^0

C1: MAGNET (M1) PROTECTION COLLIMATOR

C2, C3, C4: ± 2 MRAD XY COLLIMATORS (NO COOLING)

DUMPS: 3 METER LONG ALUMINUM BLOCKS (WATER COOLED)

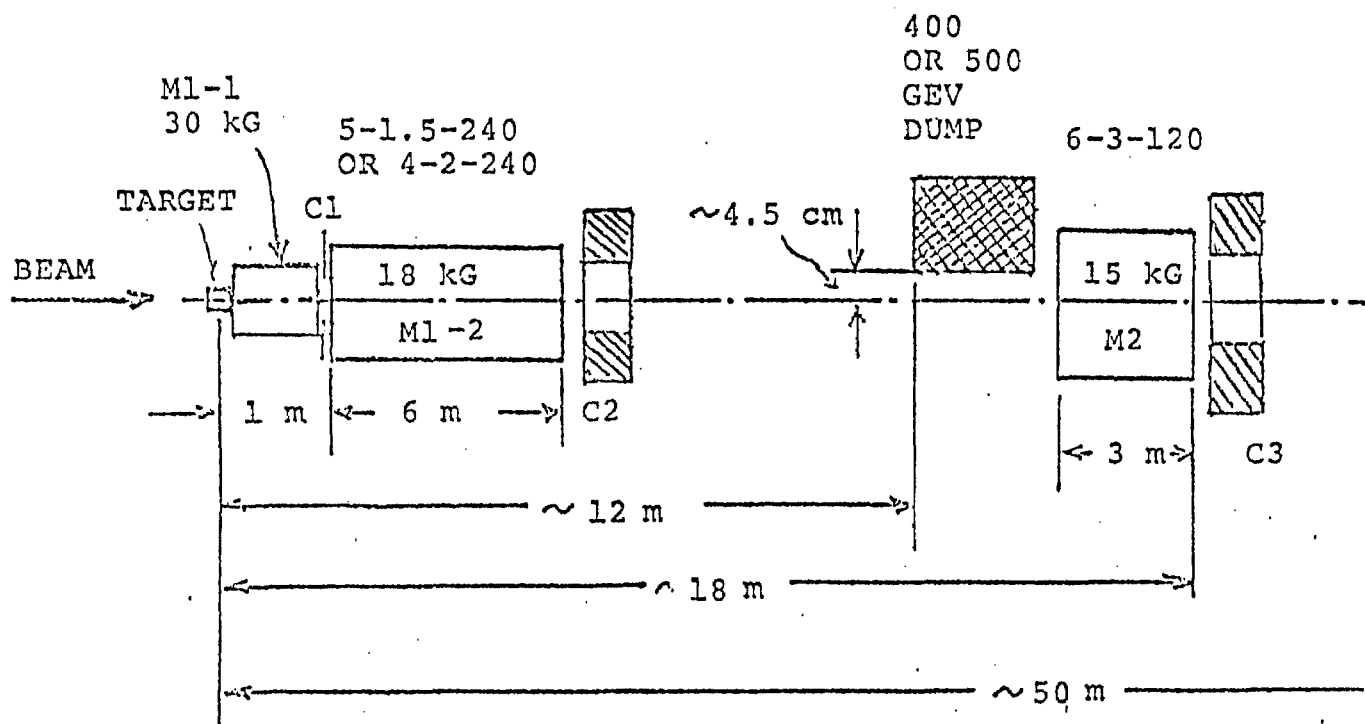


FIGURE 7

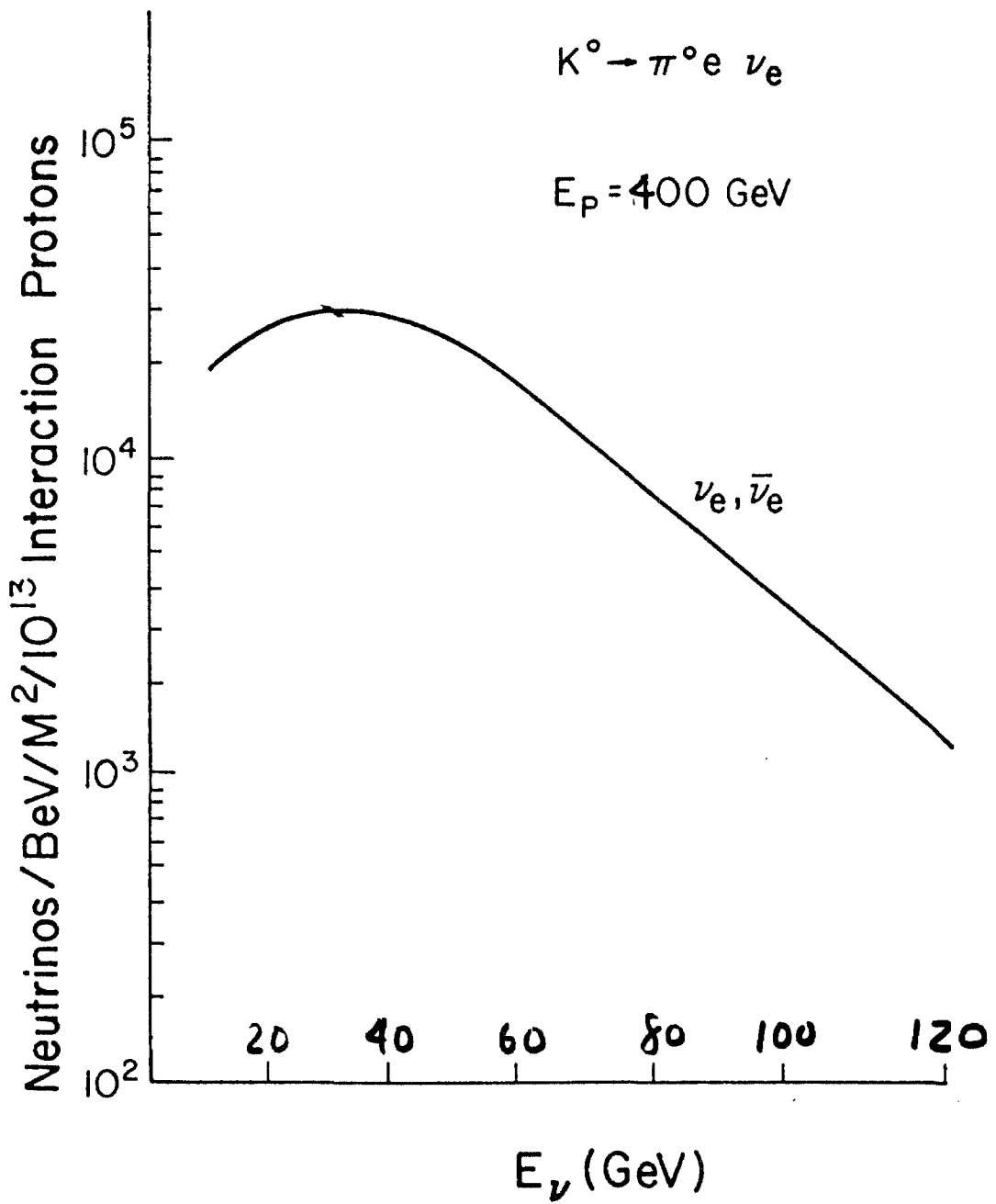


FIGURE 8

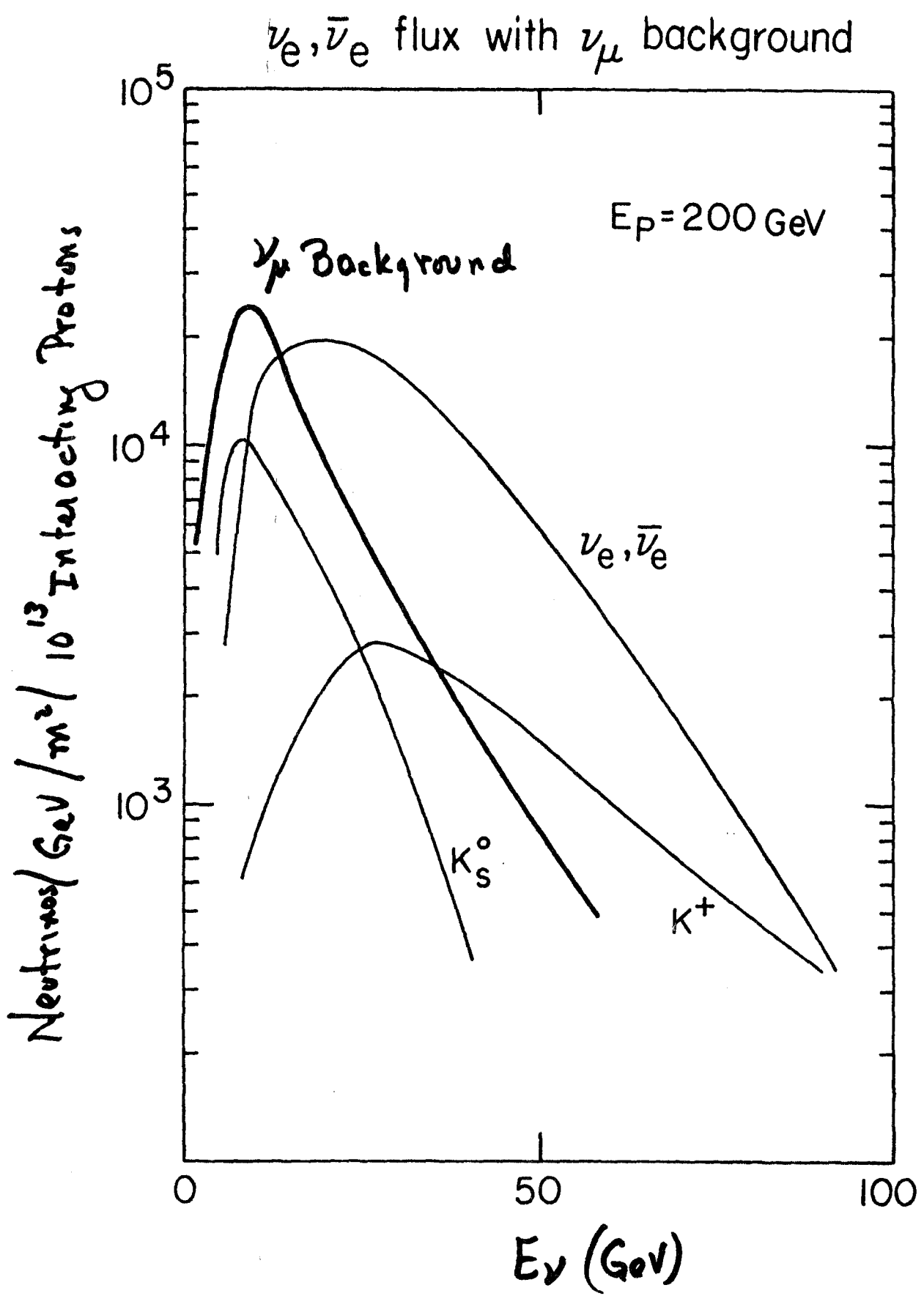


FIGURE 9

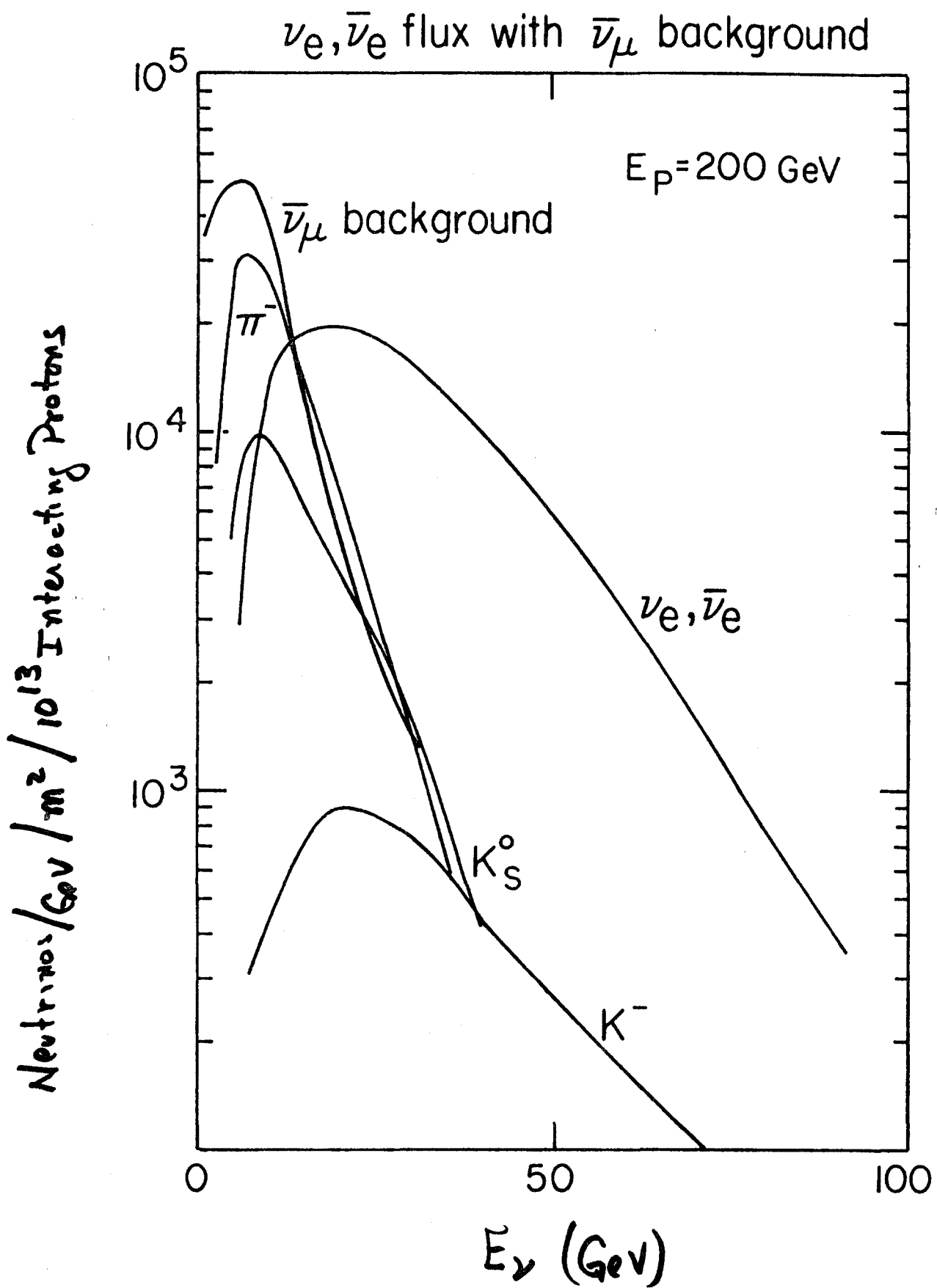


FIGURE 10

4. Event Rates and Detection Efficiency

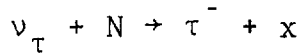
We propose to fill the bubble chamber with a heavy neon mixture, about 15 tons of neon in the fiducial volume, we also assume 2×10^{13} protons per pulse. In a 500,000 picture exposure we expect 2000 ν_e interactions and 1000 $\bar{\nu}_e$ interactions for 400 GeV operation using the spectra shown in Figure 8. We expect comparable numbers for 200 GeV operation.

However, the operation of the machine in a dedicated experiment at 200 GeV primary beam energy could have several important advantages.

- i) About $3-3.5 \times 10^{13}$ proton could reliably be delivered on target with a ~ 3 second cycle time with no flat-top.
- ii) The accelerator power requirements are greatly reduced.
- iii) Such a run of about six weeks would result in $\sim 3 \times 10^{19}$ protons on target or more than 5000 ν_e events. The short duration of the run will minimize the bubble chamber operational costs and enable a prompt analysis of the data.

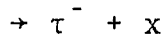
The threshold cross section behavior of τ^\pm production will suppress the low energy ν_τ , $\bar{\nu}_\tau$ rates as shown in Figure 5.

The expected detection efficiency for τ^\pm identification depends on the backgrounds in the bubble chamber. In principle all the decay modes of the τ^\pm could be detected either through



↳ charged lepton + missing P_T

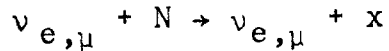
or



↳ hadron jet + missing P_T

} double jet events

The latter process is separated from the ordinary neutral current processes



through the two jet signature.

For solution C we expect ≈ 250 detected τ events and for solution A $\approx (5-10)$ events. We believe that the background rates are sufficiently low to be able to clearly separate the signal from the background in either case.

References

1. V. Barger et al., to be published in Phys. Letters; D. Cline "The Search for Neutrino Oscillations: Present Experimental Data and Future Definitive Experiments", talk given at the New Hampshire Grand Unification Conference, April, 1980.
2. V. Barger et al., "Mass and Mixing Scales of Neutrino Oscillations", submitted to Phys. Rev. Letters, April, 1980.
3. K. Winter, D. Treille, R. Turlay, ECFA 300 GeV Study, Vol. II (1972).
4. S. Mori, S. Pruss, and R. Stefanski, TM-725 (April, 1977).
5. S. Mori, "Improved Electron Neutrino Beam", TM-769.
6. C. Albright, R. Shrock, and J. Smith, "Tests for Observing Tau Neutrino Interactions in a Beam Dump Experiment", PU-C00-3077-96.
7. V. Barger and R. Phillips, Phys. Letters 74B, 393 (1978).
8. K. Bonnardt, "Lepton Mass Effects in Production of Hearing Leptons by Neutrinos in Deep Inelastic Processes", Karlsruhe Preprint, TKP79-5 (1979).

POSSIBLE INDICATIONS OF NEUTRINO OSCILLATIONS

V. Barger, K. Whisnant

Physics Department, University of Wisconsin, Madison, Wisconsin 53706 USA

D. Cline

Physics Department, University of Wisconsin, Madison, Wisconsin 53706 USA
and Fermilab, Batavia, Illinois 60510 USA

R. J. N. Phillips

Rutherford Laboratory, Chilton, Didcot, Oxon, England

ABSTRACT

We analyze neutrino oscillations of the ν_e , ν_μ , ν_τ system. Presently available reactor antineutrino data contain indications of oscillations, that have hitherto escaped attention, corresponding to an eigenmass squared difference of $\delta m^2 = 1 \text{ eV}^2$. Two other classes of oscillation solutions are contrasted and further experimental tests are indicated. All the δm^2 must be greater than 10^{-3} eV^2 to explain solar and deep mine observations.

The interesting possibility of neutrino oscillations has long been recognized¹ but no clear signal has yet been established.² In this Letter we observe, however, that the reactor antineutrino data of Reines et al.^{3,4} are consistent with an oscillation effect of shorter wavelength than hitherto considered. Solar neutrino observations and deep mine neutrino data reinforce the indication that neutrino oscillations occur, and constrain their parameters.

Neutrino oscillations depend on differences in mass m_i between the neutrino mass eigenstates ν_i . The latter are related to the weak charged current eigenstates ν_α (distinguished by Greek suffices) through a unitary transformation $|\nu_\alpha\rangle = U_{\alpha i} |\nu_i\rangle$. Starting with an initial neutrino ν_α of energy E , the probability for finding a neutrino ν_β after a path length L can be compactly written (for $E^2 \gg m_i^2$):

$$P(\nu_\alpha \rightarrow \nu_\beta) = \delta_{\alpha\beta} + \sum_{i < j} 2|U_{\alpha i} U_{\beta i} U_{\alpha j} U_{\beta j}| [(\cos(\Delta_{ij} - \phi_{\alpha\beta ij})) - \cos\phi_{\alpha\beta ij}] \quad (1)$$

where $\phi_{\alpha\beta ij} = \arg(U_{\alpha i}^* U_{\beta i}^* U_{\alpha j} U_{\beta j})$ and $\Delta_{ij} = \frac{1}{2}(m_i^2 - m_j^2)L/E$. For a diagonal transition or an off-diagonal transition with CP conservation (U real), we obtain the simple formula

$$P(\nu_\alpha \rightarrow \nu_\beta) = \delta_{\alpha\beta} - \sum_{i < j} 4U_{\alpha i} U_{\beta i}^* U_{\alpha j}^* U_{\beta j} \sin^2(\frac{1}{2}\Delta_{ij}) . \quad (2)$$

With L/E in m/MeV and m_i in eV units, the oscillation argument in radians is

$$\frac{1}{2}\Delta_{ij} = 1.27 \delta m_{ij}^2 L/E \quad (3)$$

where $\delta m_{ij}^2 \equiv m_i^2 - m_j^2$. For antineutrinos replace U by U^* above.

The oscillations are periodic in L/E . Oscillations arising from a given δm_{ij}^2 can be most readily mapped out at L/E values of order $1/\delta m_{ij}^2$. The

experimentally accessible ranges of L/E in m/MeV are $\sim 10^{10}$ (solar), $\sim 10-10^5$ (deep mine), 1-7 (low energy accelerators), 1-20 (reactors), 0.3-3. (meson factories), and 0.01-0.05 (high energy accelerators). After many cycles, detectors cannot measure L or E precisely enough to resolve individual oscillations and are sensitive only to average values. In the limit $L/E \gg (m_i^2 - m_j^2)^{-1}$ for all $i \neq j$, the average asymptotic values are given by

$$\langle P(\nu_\alpha \rightarrow \nu_\beta) \rangle = \sum_i |U_{\alpha i} U_{\beta i}^*|^2. \quad (4)$$

Since only ν_e , ν_μ , and ν_τ neutrino types are known, we specialize to a three neutrino world. The matrix U can then be parameterized in the form introduced by Kobayashi and Maskawa,⁵ in terms of angles $\theta_1, \theta_2, \theta_3$ with ranges $(0, \pi/2)$ and phase δ with range $(-\pi, \pi)$. In our present analysis we neglect CP violation (thus $\delta = 0$ or $\pm \pi$). To limit the regions of the θ_i , δm_{ij}^2 parameter space, we consider first the constraints placed by solar, deep mine and accelerator data.

Solar neutrino observations and deep mine experiments: The solar neutrino data⁶ suggest that $\langle P(\nu_e \rightarrow \nu_e) \rangle \simeq 0.3-0.5$ at $L/E \sim 10^{10}$ m/MeV. For three neutrinos, Eq. (4) gives

$$\langle P(\nu_e \rightarrow \nu_e) \rangle = c_1^4 + s_1^4 c_3^4 + s_1^4 s_3^4 \quad (5)$$

where $c_i = \cos \theta_i$ and $s_i = \sin \theta_i$. The minimum value of Eq. (5) is 1/3 and this requires $c_1 = 1/\sqrt{3}$, $c_3 = 1/\sqrt{2}$. For $\langle P(\nu_e \rightarrow \nu_e) \rangle$ to be near its minimum, all mass differences must satisfy $\delta m^2 \gg 10^{-10}$ eV². At this minimum all transition averages are specified, independent of θ_2 ; in particular $\langle P(\nu_\mu \rightarrow \nu_\mu) \rangle = 1/2$. In fact, there are indications from deep mine experiments⁷⁻⁹ that $\langle P(\nu_\mu \rightarrow \nu_\mu) \rangle \sim 1/2$ (see footnote f in Table 1). Since the ν_μ

neutrinos detected in deep mines have traversed terrestrial distances, this measurement suggests that all $\delta m^2 \gtrsim 10^{-3} \text{ eV}^2$. Based on these considerations we may suppose that the true solution is not far from the above θ_1 , θ_3 values. If we only require $\langle P(\nu_e \rightarrow \nu_e) \rangle < 0.5$, then θ_1 and θ_3 are constrained to a region approximated by the triangle $\theta_1 > 35^\circ$, $\theta_3 > \theta_1 - 45^\circ$, and $\theta_3 < 135^\circ - \theta_1$.

$\nu_\mu \rightarrow \nu_e$, ν_τ oscillations: Stringent experimental limits exist on these transitions $^{10-13}$ at L/E in the range 0.01 to 0.3 m/MeV (see Table 1). For $\delta m^2 \ll 1 \text{ eV}^2$, these oscillations do not appear until $L/E \gg 1 \text{ m/MeV}$. With a single $\delta m^2 \gtrsim 1 \text{ eV}^2$, these oscillations can be suppressed by choice of θ_2 (if θ_1, θ_3 are taken as above).

Reactor $\bar{\nu}_e$ -oscillations: The $\bar{\nu}_e$ flux at distances $L = 6 \text{ m}$ and 11.2 m from a reactor core center was measured by Reines et al., ^{3,4} using the known cross section for the inverse beta-decay reaction $\bar{\nu}_e p \rightarrow e^+ n$. The reactor $\bar{\nu}_e$ flux at the core has been calculated using semi-empirical methods.¹⁴⁻¹⁷ The ratio of measured flux at L to the calculated flux measures $P(\bar{\nu}_e \rightarrow \bar{\nu}_e)$. Neutrino oscillation interpretations of the data thereby depend on the calculated spectrum about which there is some uncertainty.

Figure 1 shows a comparison of the measured $\bar{\nu}_e$ flux at $L = 6 \text{ m}$ and $L = 11.2 \text{ m}$ with calculated spectra. We note that the Avignone-1978 calculated flux¹⁶ accommodates best the $L = 6 \text{ m}$ measurements for $E_{\bar{\nu}_e} > 6 \text{ MeV}$. The data for $P(\bar{\nu}_e \rightarrow \bar{\nu}_e)$ obtained with the Avignone-1978¹⁶ and Davis et al.¹⁷ calculated spectra are shown in Fig. 2. The horizontal error bars in Fig. 2 take into account the finite size of the reactor core source. We observe that $P(\bar{\nu}_e \rightarrow \bar{\nu}_e)$ seems to follow an oscillation pattern with one node in the range of L/E covered by the measurements. The possibility of such a solution

in which a short wavelength oscillation occurs was not considered by Reines et al.³ in their analysis of the 11.2 m data based on a similar calculated spectrum.¹⁵

The oscillation in Fig. 2 is well-described by the formula

$P(\bar{\nu}_e \rightarrow \bar{\nu}_e) = 1 - 0.44 \sin^2(1.27 L/E)$. This corresponds to a mass difference $\delta m^2 = 1 \text{ eV}^2$, which we can arbitrarily identify as δm^2_{13} . A non-zero δm^2_{12} with $\delta m^2_{12} \ll \delta m^2_{13}$, is required to bring $\langle P(\bar{\nu}_e \rightarrow \bar{\nu}_e) \rangle$ down asymptotically to the solar neutrino result. The value of δm^2_{12} is not tightly constrained, other than the indication from deep mine measurements of $\langle P(\bar{\nu}_\mu \rightarrow \bar{\nu}_\mu) \rangle$ that $\delta m^2_{12} \gtrsim 10^{-3} \text{ eV}^2$. A solution which accommodates all known constraints is

$$\begin{array}{ccccccc} \delta m^2_{13} & \delta m^2_{12} & \theta_1 & \theta_2 & \theta_3 & \delta \\ \text{SOLUTION A:} & 1.0 \text{ eV}^2 & 0.05 \text{ eV}^2 & 45^\circ & 25^\circ & 30^\circ & 0^\circ . \end{array} \quad (5)$$

The predictions for subasymptotic transition probabilities are shown in Fig. 3.

A more conservative interpretation of the reactor $\bar{\nu}_e$ data could be that $P(\bar{\nu}_e \rightarrow \bar{\nu}_e)$ falls to around 0.7-0.8 in the range of L/E considered, but that oscillatory behavior is not established. If so, two other classes of solution are possible: Class B, where $\bar{\nu}_e \rightarrow \bar{\nu}_e$ is suppressed by the onset of a long wavelength oscillation, that may have its first node well beyond $L/E = 1 \text{ m/MeV}$; Class C, where $\bar{\nu}_e \rightarrow \bar{\nu}_e$ is suppressed by a short wavelength oscillation, that may have many nodes below $L/E = 1 \text{ m/MeV}$. Illustrative solutions of these classes are as follows (we emphasize that their parameters are less constrained than in Class A).

	δm_{13}^2	δm_{12}^2	θ_1	θ_2	θ_3	δ	
<u>SOLUTION B:</u>	0.15 eV^2	0.05 eV^2	55°	0°	45°	0°	(6)
<u>SOLUTION C:</u>	10 eV^2	0.05 eV^2	45°	25°	30°	0°	.

We note that equivalent solutions to Eqs. (5) and (6) are obtained with $\delta m_{13}^2 \leftrightarrow \delta m_{12}^2$, $\delta = \pi$, and $\theta_3 \rightarrow \frac{\pi}{2} - \theta_3$ with θ_1 , θ_2 unchanged. Table 1 presents a capsule summary of the present experimental limits on oscillations and summarizes predictions of solutions A, B and C for existing and planned experiments. For the L/E range of the CERN beam dump experiment,¹⁹ a $\delta m^2 \gtrsim 10 \text{ eV}^2$ is required to yield an e/μ ratio that is significantly less than unity.^{2b} In solution C, which has a δm^2 in that range, the mixing angles are nearly the same as those contained in ref. 2b. Solution A has the same mixing matrix as solution C, but the smaller value of δm_{13}^2 leads to visible oscillations in reactor experiments rather than in high energy beam dump experiments.

New reactor experiments: Reactor measurements³ in the L/E range 5-20 m/MeV could provide information on δm_{12}^2 . For $\delta m_{12}^2 \ll 0.05 \text{ eV}^2$ solutions A and C predict no appreciable deviation from a $1/r^2$ fall-off of the average flux at $L/E > 5 \text{ m/MeV}$.

New meson factory experiments: Since the decays of stopped μ^+ mesons provide well-known ν_e and $\bar{\nu}_\mu$ spectra, meson factory experiments at $L/E \sim 1-3 \text{ m/MeV}$ ²⁴ could confirm the existence of $\nu_e \rightarrow \nu_e$ oscillations and place further constraints on $\bar{\nu}_\mu \rightarrow \bar{\nu}_e$ oscillations.

Summary: Reactor $\bar{\nu}_e$ data provide indications of neutrino oscillations with mass scale $\delta m^2 = 1 \text{ eV}^2$. Solar and deep mine results suggest that the other mass scale is in the range $\delta m^2 \gtrsim 10^{-3} \text{ eV}^2$.

Acknowledgements

This research was supported in part by the University of Wisconsin Research Committee with funds granted by the Wisconsin Alumni Research Foundation, and in part by the Department of Energy under contract DE-AC02 76ER00881, COO-881-135.

By acceptance of this article, the publisher and/or recipient acknowledges the U. S. Government's right to retain a nonexclusive, royalty-free license in and to any copyright covering this paper.

REFERENCES

1. B. Pontecorvo, Soviet Phys. JETP 53, 1717 (1967); V. Gribov and B. Pontecorvo, Phys. Lett. 28B, 493 (1969).
2. For thorough recent reviews of theory and experiment see (a) S.M. Bilenky and B. Pontecorvo, Phys. Reports 41, 225 (1978); (b) A. de Rujula et al., CERN TH-2788 (1979).
3. F. Reines, Unification of Elementary Forces and Gauge Theories (eds. D. B. Cline and F. E. Mills), Harwood Academic Publishers, p. 103 (1978); F. Reines, private communication to D. Cline of $E > 5.5$ MeV data (1978); S. Y. Nakamura et al., Proc. of the Inter. Neutrino Conf., Aachen (ed. by H. Faissner et al.), Vieweg (1977).
4. F. Nezrick and E. Reines, Phys. Rev. 142, 852 (1966).
5. M. Kobayashi and T. Maskawa, Prog. Theor. Phys. 49, 652 (1973). We follow the convention in V. Barger and S. Pakvasa, Phys. Rev. Lett. 42, 1585 (1979).
6. R. Davis Jr., J. C. Evans and B. T. Cleveland, Proc. of the Conf. on Neutrino Physics, ed. by E. C. Fowler (Purdue Univ. Press, 1978).
7. M. R. Krishnaswamy et al., Proc. Phys. Soc. Lond. A323, 489 (1971).
8. M. F. Crouch et al., Phys. Rev. D18, 2239 (1978).
9. L. V. Volkova and G. T. Zatsepin, Sov. J. Nucl. Phys. 14, 117 (1972).
10. E. Bellotti et al., Lett. Nuovo Cim. 17, 553 (1976).
11. J. Blietschau et al., Nucl. Phys. B133, 205 (1978).
12. S. E. Willis et al., Phys. Rev. Lett. 44, 522 (1980).
13. A. M. Cnops et al., Phys. Rev. Lett. 40, 144 (1978).
14. R. E. Carter, F. Reines, R. Wagner and M. E. Wyman, Phys. Rev. 113, 280 (1959).

15. F. T. Avignone, III, Phys. Rev. D2, 2609 (1970).
16. F. T. Avignone, III and L. P. Hopkins, in Proc. of Conf. on Neutrino Physics, ed. by E. C. Fowler (Purdue Univ. Press, 1978).
17. B. R. Davis, P. Vogel, F. M. Mann and R. E. Schenter, Phys. Rev. C19, 2259 (1979).
18. L. R. Sulak et al., in Proc. of Inter. Conf. on Neutrino Physics and Astrophysics, Elbrus, USSR (1977).
19. H. Wachsmuth, CERN-EP/79-115 C (1979); also K. Winter (private communication).
20. A. Chudakov and G. Zatsepin (private communication).
21. Irvine-Michigan-Brookhaven collaboration (F. Reines et al.,); Harvard-Purdue-Wisconsin collaboration (J. Blandino et al.).
22. J. L. Osborne and E. C. M. Young in Cosmic Rays at Ground Level, ed. by A. W. Wolfendale, Institute of Physics, London (1973).
23. L. Wolfenstein, Phys. Rev. D17, 2369 (1978).
24. Considerations are in progress by D. Cline and B. Burman for such a neutrino oscillation experiment at LAMPF.

TABLE REFERENCES

- a San Onofre reactor experiment by Reines et al.³ in progress, with $L = 25-100$ m.
- b Possible LAMPF experiment with $E_{\nu_e}, E_{\bar{\nu}_\mu} = 30-50$ MeV and $L = 30-100$ m.
- c Brookhaven experiment¹⁸ in data analysis stage.
- d $\nu_e \rightarrow \nu_\tau$ oscillations can lead to a e/μ ratio different from unity in beam dump experiments (see e.g., ref. 2b and data of ref. 19).
- e The excellent agreement of observed and calculated $\nu_e/\bar{\nu}_e$ flux at CERN and Fermilab indicates that most of the ν_e does not oscillate into ν_τ .
- f Deep mine experiments^{7,8} have detected about 130 neutrino events ($E \sim 10^4-10^6$ MeV, $L \sim 10^6-10^7$ m). An unaccountably large number of multitrack events were observed in the Kolar gold field experiment;⁷ assuming that these are not attributed to ν_μ , the event rate is about half the expected rate. In the Johannesburg mine experiment⁸ a ratio 1.6 ± 0.4 of expected to observed ν_μ events was found. The analysis in ref. 9 of these experiments is consistent with $\langle P(\nu_\mu \rightarrow \nu_\mu) \rangle \sim 0.5$. A new deep mine experiment is operating at Baksan, USSR which is sensitive to ν_μ flux through the earth.²⁰
- g Deep mine experiments in construction²¹ will detect neutrinos of energies $E \sim 10^2-10^3$ MeV using very large water detectors placed in deep mines. At these energies the composition²² of the ν -flux from π , K , and μ decays of the secondary cosmic ray component in the atmosphere is roughly $(2\nu_\mu + \nu_e)/3$. Upward events in the detector will have $L \simeq 10^6-10^7$ m and downward events will have $L \simeq 10^4$ m. The charged-current scattering of ν_e on electrons significantly modifies vacuum oscillation predictions only for deep mine events which have $E(\text{MeV}) \gtrsim 10^6 \delta m^2 (\text{eV}^2)$; see ref. 23.

TABLE 1
Experimental Limits on Neutrino Oscillations and Neutrino Flux Predictions

<u>Observable</u>	<u>Source Refs.</u>	<u>L E m MeV</u>	<u>Present Limit</u>	<u>A</u>	<u>Solution</u>	<u>C</u>
$\langle P(\nu_e \rightarrow \nu_e) \rangle$	S 6	10^{10}	$\gtrsim \frac{1}{4}, \lesssim \frac{1}{2}$	0.41	0.33	0.41
$P(\bar{\nu}_e \rightarrow \bar{\nu}_e)$	R 3,4	1-3	> 0.5	0.6-1.0	0.8-1.0	0.8 mean
	R a	5-20		0.1-0.9	0.05-0.5	0.1-0.9
$P(\nu_e \rightarrow \nu_e)$	A	0.04	> 0.85 e	1.0	1.0	0.9
	M 12	0.3	1.1 ± 0.4	0.95	1.0	0.8 mean
	M b	1-3		0.6-1.0	0.8-1.0	0.8 mean
$P(\bar{\nu}_\mu \rightarrow \bar{\nu}_e)$	M 12	0.3	< 0.04	10^{-4}	10^{-3}	10^{-3}
	M b	3		0.03	0.11	0.03
$P(\nu_\mu \rightarrow \nu_e) / P(\nu_\mu \rightarrow \nu_\mu)$	A 10,11	0.04	$< 10^{-3}$	10^{-6}	10^{-5}	10^{-4}
	A 18 c	1-7		0-0.2	0-0.8	0-0.2
$P(\nu_e \rightarrow \nu_\tau)$	A d	0.04	< 0.2 e	10^{-3}	10^{-5}	0.1
$P(\nu_\mu \rightarrow \nu_\tau) / P(\nu_\mu \rightarrow \nu_\mu)$	A 13	0.04	$< 2.5 \times 10^{-2}$	10^{-5}	10^{-5}	10^{-3}
$\langle P(\nu_\mu \rightarrow \nu_\mu) \rangle$	D f	$10^2 - 10^3$	~ 0.5	0.51	0.51	0.51
$\langle P(\nu_c \rightarrow \nu_\mu) \rangle$	D g	$10^3 - 10^5$		0.48	0.44	0.48
$\langle P(\nu_c \rightarrow \nu_e) \rangle$	D g	$10^3 - 10^5$		0.42	0.33	0.42
$P(\nu_c \rightarrow \nu_\mu)$	D g	$10 - 10^2$		0.3-0.7	0.3-0.7	0.3-0.7
$P(\nu_c \rightarrow \nu_e)$	D g	$10 - 10^2$		0.2-0.6	0.2-0.6	0.2-0.6

Notation: S(solar), R(reactor), M(meson factory), A(accelerator), D(deep mine); $\nu_c \approx (2\nu_\mu + \nu_e)/3$.

FIGURE CAPTIONS

Fig. 1 The $\bar{\nu}_e$ reactor flux measurements of Reines et al. at $L = 11.2$ m (ref. 3) and $L = 6$ m (ref. 4) compared with the calculated spectra of refs. 3, 4, 14-17.

Fig. 2 Transition probability $P(\bar{\nu}_e \rightarrow \bar{\nu}_e)$ versus L/E deduced from the ratio of the observed to the calculated $\bar{\nu}_e$ reactor flux from refs. 16-17. The curve represents neutrino oscillations with an eigenmass difference squared of $\delta m^2 = 1$ eV² (SOLUTION A of Eq. (5)).

Fig. 3 Subasymptotic neutrino oscillations for all channels based on SOLUTION A in Eq. (5). Arrows on the right-hand side denote asymptotic mean values.

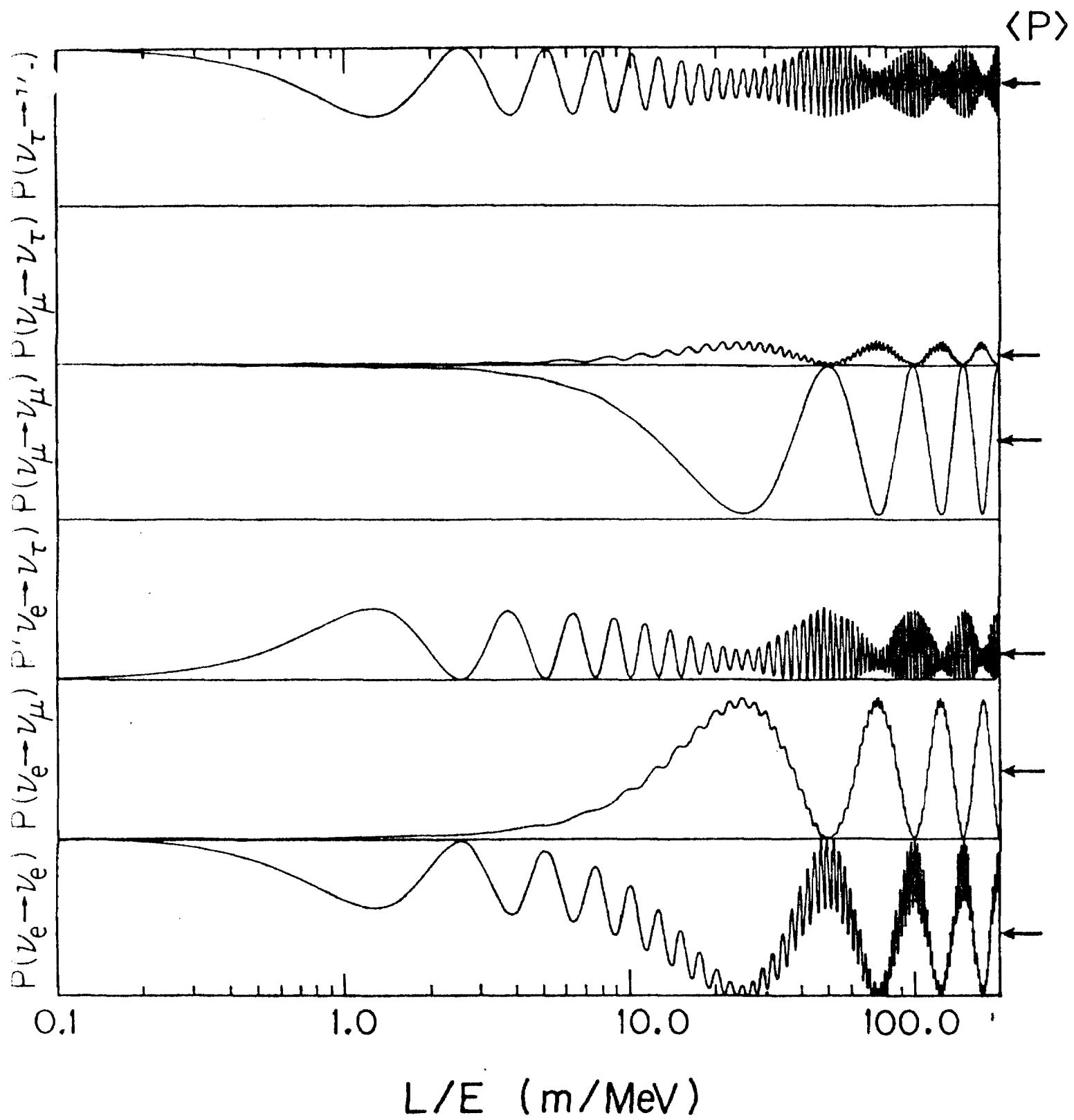


Fig. 3

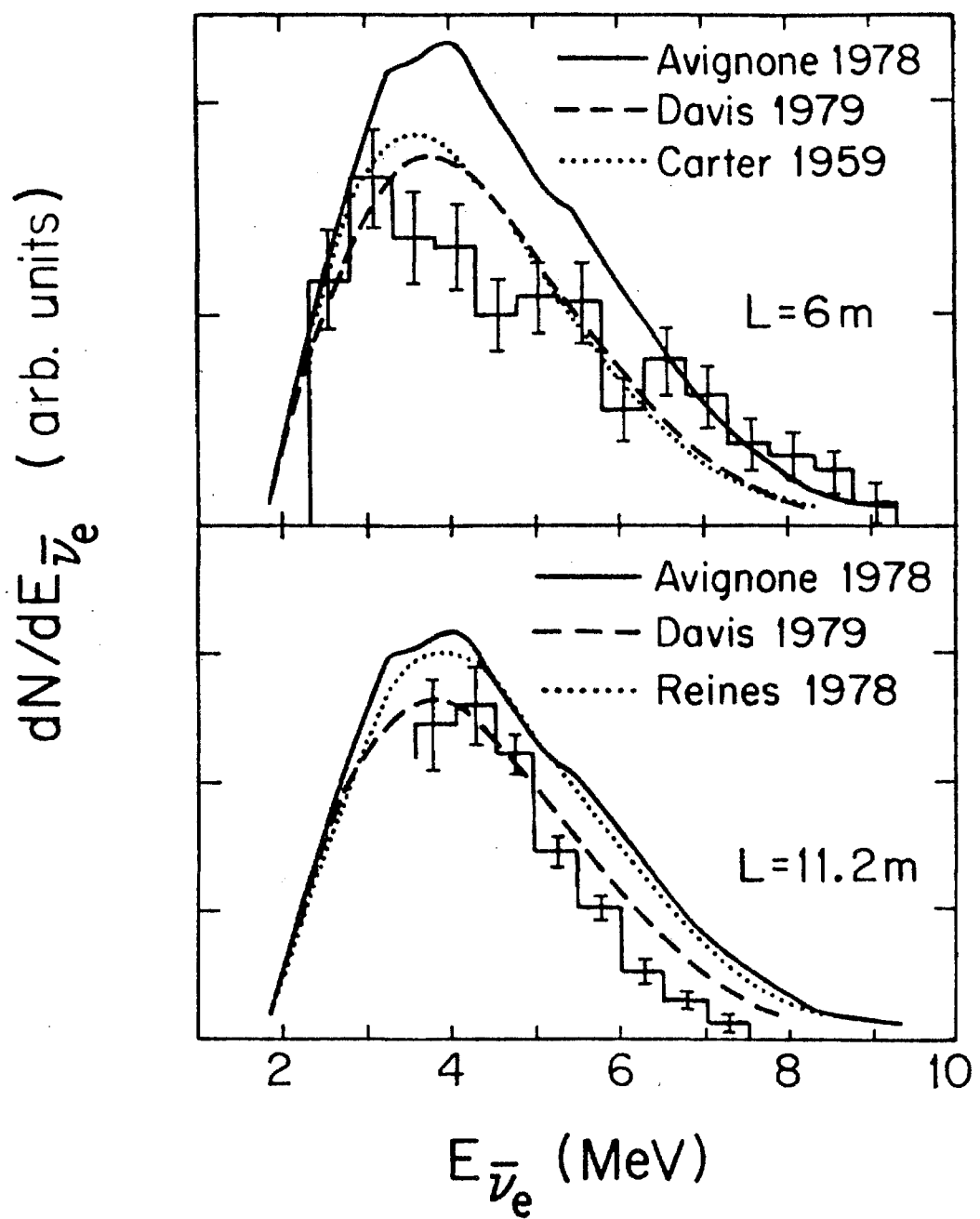


Fig. 1

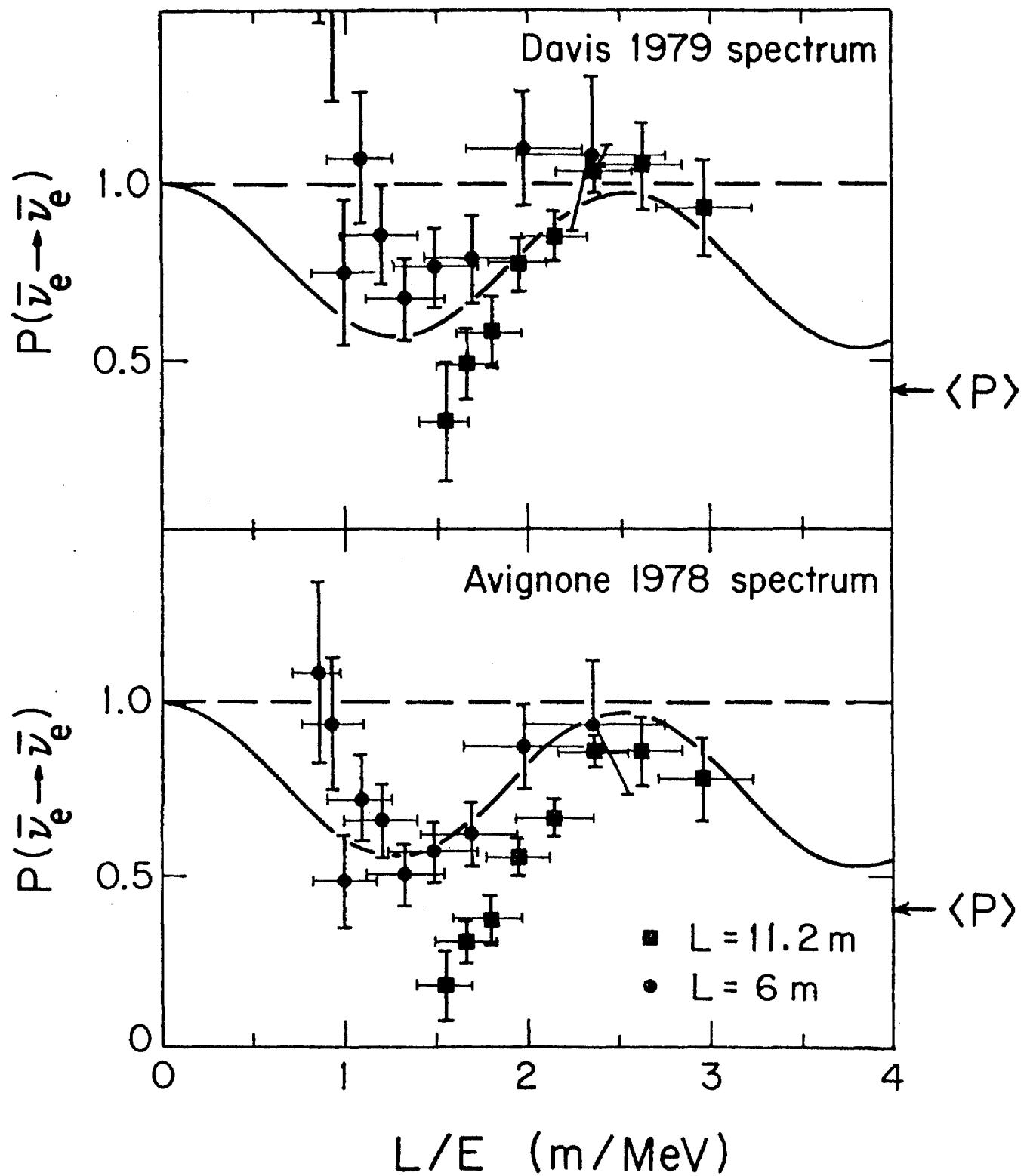


Fig. 2

COO-881-146

April 1980

MASS AND MIXING SCALES OF NEUTRINO OSCILLATIONS

V. Barger and K. Whisnant

Physics Department, University of Wisconsin, Madison, Wisconsin 53706 USA

D. Cline

Fermilab, Batavia, Illinois 60510 and
Physics Department, University of Wisconsin, Madison, Wisconsin 53706 USA

R. J. N. Phillips

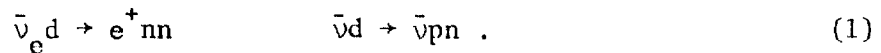
Rutherford Laboratory, Chilton, Didcot, Oxon, England

ABSTRACT

The extraction of neutrino oscillation parameters from the ratio of rates $(\bar{\nu}_e d \rightarrow e^+ nn)/(\bar{\nu} d \rightarrow \nu pn)$ is considered in the context of oscillations proposed to account for previous reactor data. The possibility that only ν_e, ν_μ oscillations occur is shown to be barely compatible with present limits on $\nu_\mu \rightarrow \nu_e$ transitions. Predictions for $\nu_e, \nu_\mu \rightarrow \nu_\tau$ oscillations are made for future accelerator experiments.

Neutrino oscillations¹⁻³ are of great interest because of the light they may shed on neutrino mass scales and mixing angles. The solar neutrino puzzle²⁻⁴ may indicate oscillations and a e/μ discrepancy in the CERN beam dump experiment has also been speculated upon⁵. Recently we presented⁶ a reexamination of all neutrino flux data, including the old reactor $\bar{\nu}_e$ measurements by Reines and collaborators.⁷ We drew the conclusion that the oscillation probability $P(\bar{\nu}_e \rightarrow \bar{\nu}_e)$ falls to 0.5 or lower in the neighborhood of $L/E = 1.5 \text{ m/MeV}$, where L is the distance from the source and E is the energy. Interpreting this as an oscillation effect, we showed that neutrino-mixing with a leading mass squared difference of the order of 1 eV^2 matched the reactor data in some detail (solution A of ref. 6). Qualitatively different classes of solutions were considered for comparison, with a δm^2 considerably smaller (solution B) or considerably larger (solution C) than 1 eV^2 .

Further evidence for neutrino oscillations from reactor experiments comes from the simultaneous consideration of charged current (CC) and neutral current (NC) deuteron disintegration reactions⁸



The neutral current process is immune to oscillations, being the same for all types of antineutrinos in the standard theory and effectively monitors the initial $\bar{\nu}$ flux. The ratio of CC/NC rates is rather insensitive to theoretical uncertainties in the calculated $\bar{\nu}_e$ spectrum from the reactor (the principle uncertainty hitherto) and can be used to extract neutrino oscillation parameters. In the present letter we calculate the NC/CC ratios predicted for this experiment by the solutions of ref. 6 and discuss the constraint on δm^2 and mixing angles. The possibility of having oscillations only in the ν_e, ν_μ system is

shown to be barely compatible with reactor data and present experimental limits on $\nu_\mu \rightarrow \nu_e$ transitions. For oscillations of three neutrinos, predictions of $\nu_e, \nu_\mu \rightarrow \nu_\tau$ oscillations are made for future accelerator experiments.

The spectrum averaged cross sections for deuteron disintegration have the form

$$\langle \sigma \rangle = \int_0^\infty dE_r \int_{E_{th}}^\infty dE_{\bar{\nu}} \rho(E_{\bar{\nu}}) f(E_{\bar{\nu}}) \frac{d\sigma}{dE_r} \quad (2)$$

where $\rho(E_{\bar{\nu}})$ is the $\bar{\nu}_e$ flux at $L = 0$ and $f = P(\bar{\nu}_e \rightarrow \bar{\nu}_e)$ at $L/E_{\bar{\nu}}$ for the CC case and $f = \frac{1}{2}$ for the NC case. The variable E_r is the energy of relative motion of the final state nucleons; the recoil energy of the two-nucleon system can be neglected to a 1% approximation. The differential cross sections are⁹

$$\frac{d\sigma}{dE_r} = \frac{g_A^2 G_F^2 M_N^{3/2}}{2\pi^3} J_d^2(E_r) (E_{\bar{\nu}} - E_{th} + m) [(E_{\bar{\nu}} - E_{th} + m)^2 - m^2]^{1/2} E_r^{1/2} \quad (3)$$

where M_N is the nucleon mass and $m = m_e$ for the CC and $m = 0$ for the NC.

The threshold energies are

$$E_{th}^{CC} = 4.030 \text{ MeV} + E_r \quad (4)$$

$$E_{th}^{NC} = 2.225 \text{ MeV} + E_r$$

In Eq. (2) the quantity J_d is the overlap integral of deuteron wave functions describing the 3S ground state and the 1S continuum state, given by⁹

$$J_d = \frac{1.52 \times 10^{-3} (43.1 + 0.83 E_r) \text{ MeV}^{-3/2}}{(E_r + 2.225) [E_r + (0.19 E_r + 0.27)^2]^{1/2}} \quad (5)$$

with E_r in MeV units. With the exponential fall-off of $\rho(E_{\bar{\nu}})$ folded in, the dominant contribution to $\langle\sigma\rangle$ comes from $E_r < 0.3$ MeV and $E_{\bar{\nu}} - E_{\bar{\nu}}^{\text{th}} \approx 0.5-3.5$ MeV. Thus oscillation effects can be measured in the range 4.6 - 7.6 MeV. We calculate the ratio

$$R_d \equiv \frac{\langle\sigma(\bar{\nu}_e d \rightarrow e^+ nn)\rangle}{\langle\sigma(\bar{\nu}_e d \rightarrow \bar{\nu}_e pn)\rangle} \quad (6)$$

with and without oscillations.

At $L \approx 11.2$ m, $R_d(\text{osc})/R_d(\text{no osc})$ measures $P(\bar{\nu}_e \rightarrow \bar{\nu}_e)$ over the range $L/E \approx 1.5 - 2.4$, which is the region in which our analysis of the $\bar{\nu}_e p \rightarrow e^+ n$ data shows an oscillation effect.⁶ Figure 1 shows the predictions, assuming that only one eigenmass-difference plays a significant role in the reactor range, for which

$$P(\bar{\nu}_e \rightarrow \bar{\nu}_e) = 1 - \sin^2 2\alpha \sin^2(1.27 \delta m^2 L/E) \quad (7)$$

with δm^2 in eV^2 units and L/E in m/MeV. The curves in Fig. 1 versus δm^2 represent mixing angles for which $\sin^2 2\alpha = 0.19$ (α = Cabibbo angle), 0.50, 0.80 and 1.0. These calculations are based on the Avignone-1978 reactor spectrum;¹⁰ closely similar results are obtained with the Davis et al. spectrum.¹¹ Assuming ideal acceptance and allowing one standard deviation from the measured value of⁸

$$R_d(\text{osc})/R_d(\text{no osc}) = 0.43 \pm 0.17 \quad (8)$$

values of δm^2 are permitted in the ranges

$$0.3 < \delta m^2 < 1.1 \text{ eV}^2 \quad \delta m^2 > 1.7 \text{ eV}^2 \quad (9)$$

for appropriate mixing angles α . The solution classes A and C of ref. 6 satisfy these criteria. For the preferred class A solutions, our analysis⁶ of the $\bar{\nu}_e p \rightarrow e^+ n$ data at $L = 11.2$ m gives the ranges

$$0.80 < \delta m^2 < 1.05 \text{ eV}^2 \quad (10)$$

$$0.4 < \sin^2 2\alpha < 0.9 .$$

Results similar to Eqs. (9) and (10) were independently obtained in ref. 8. Figure 2 shows predictions for $R_d(\text{osc})/R_d(\text{no osc})$ versus L for other reactor experiments, based on solution A with $\delta m^2 = 0.8$ eV² and the spectrum of ref. 10.

Stringent limits^{12,13} exist on $\nu_\mu \rightarrow \nu_e$ and $\bar{\nu}_\mu \rightarrow \bar{\nu}_e$ oscillations at $L/E \approx 0.04$ m/MeV and on $\bar{\nu}_\mu \rightarrow \bar{\nu}_e$ oscillations at $L/E \approx 0.3$ m/MeV. If oscillations occurred only between ν_e and ν_μ states and if a single δm^2 is dominant below $L/E = 3$ m/MeV (as in solutions A and C of ref. 6), we can write

$$P(\nu_\mu \rightarrow \nu_e) = P(\bar{\nu}_\mu \rightarrow \bar{\nu}_e) = P_0 \sin^2(1.27 \delta m^2 L/E) \quad (11)$$

with the experimental bound

$$P_0 < 0.3/(\delta m^2)^2 . \quad (12)$$

The corresponding bound on the mixing angle is

$$\sin^2 2\alpha < 0.3/(\delta m^2)^2 . \quad (13)$$

For $\delta m^2 \sim 1$ eV², this is just on the borderline of admissibility by the existing reactor data.

Applying similar considerations to oscillations of three neutrinos, probability conservation leads to the predictions

$$P(\nu_e \rightarrow \nu_\tau) = P(\bar{\nu}_e \rightarrow \bar{\nu}_\tau) = [\sin^2 2\alpha - P_0] \sin^2(1.27 \delta m^2 L/E) . \quad (14)$$

$$P(\nu_\mu \rightarrow \nu_\tau) = P(\bar{\nu}_\mu \rightarrow \bar{\nu}_\tau) = [P_0 / (4 \sin^4 \alpha)] P(\nu_e \rightarrow \nu_\tau) .$$

Thus three neutrino oscillations can be tested by detecting ν_τ , $\bar{\nu}_\tau$ produced in a ν_e , ν_μ beam that is free of ν_τ and $\bar{\nu}_\tau$. The ν_τ , $\bar{\nu}_\tau$ are detected through the interactions

$$\begin{aligned} \nu_\tau n &\rightarrow \tau^- X^+ \\ \bar{\nu}_\tau p &\rightarrow \tau^+ X^0 . \end{aligned} \quad (15)$$

Figure 3 shows predictions for $P(\nu_e \rightarrow \nu_\tau)$ for the L/E range of high energy accelerators (the two curves for solution A corresponding to P_0 between 0 and 0.3, with $\delta m^2 = 1 \text{ eV}^2$). $P(\nu_\mu \rightarrow \nu_\tau)$ depends critically on P_0 and can be larger than $P(\nu_e \rightarrow \nu_\tau)$.

Solution C has been of primary interest in connection with the e/μ ratio of beam dump experiments.⁵ By increasing the scale of the δm^2 , it is possible to construct an alternate version of solution C (solution C') which can explain both reactor and beam results by having a short wavelength oscillation (such as $\delta m_{13}^2 \approx 50 \text{ eV}^2$) superimposed on a long wavelength oscillation ($\delta m_{12}^2 \approx 1 \text{ eV}^2$). Representative six-quark mixing angles for such a solution are

$$\theta_1 = 30^\circ \quad \theta_2 = 50^\circ \quad \theta_3 = 55^\circ \quad \delta = 0^\circ . \quad (16)$$

Solution C' gives $R_d(\text{osc})/R_d(\text{no osc}) = 0.59$ at $L = 11.2 \text{ m}$; the minimum value of $P(\bar{\nu}_e \rightarrow \bar{\nu}_e)$ in the reactor range is 0.47 when averaged over the short wavelength oscillation. Predictions of $P(\nu_e \rightarrow \nu_\tau)$ for this solution are also given in Fig. 3.

Acknowledgements

We thank W. Sullivan for asking a pertinent question. We also thank S. Pakvasa for discussions and J. Leveille and D. Winn for transmitting information.

This research was supported in part by the University of Wisconsin Research Committee with funds granted by the Wisconsin Alumni Research Foundation, and in part by the Department of Energy under contract EY-76-C-02-0881, COO-881-111.

By acceptance of this article, the publisher and/or recipient acknowledges the U. S. government's right to retain a nonexclusive, royalty-free license in and to any copyright covering this paper.

REFERENCES

1. Z. Maki, M. Nakagawa and S. Sakata, *Prog. Theor. Phys.* 28, 247 (1962).
2. B. Pontecorvo, *Soviet Phys. JETP* 53, 1717 (1967); V. Gribov and B. Pontecorvo, *Phys. Lett.* 28B, 493 (1969).
3. For recent reviews of theory and experiment see S. M. Bilenky and B. Pontecorvo, *Phys. Reports* 41, 225 (1978).
4. R. Davis, Jr., J. C. Evans and B. T. Cleveland, *Proc. of the Conf. on Neutrino Physics*, ed. by E. C. Fowler (Purdue Univ. Press, 1978).
5. A. de Rujula et al., CERN TH-2788 (1979); H. Wachsmuth, CERN Report EP/79-115C (1979); K. Winter (private communication).
6. V. Barger et al., UW-Madison Report COO-881-135 (1980); to be published in *Phys. Lett.*
7. F. Reines, Unification of Elementary Forces and Gauge Theories (eds. D. B. Cline and F. E. Mills), Harwood Academic Publishers, p. 103 (1978); F. Nezrick and E. Reines, *Phys. Rev.* 142, 852 (1966).
8. F. Reines, H. W. Sobel and E. Pasierb, Evidence for Neutrino Instability, Univ. Cal.-Irvine preprint (1980); F. Reines et al., *Phys. Rev. Lett.* 43, 96 (1979); V. Barger and D. Cline, Flux-Independent Analysis of Neutrino Oscillations (February 1980, unpublished).
9. S. A. Fayans, L. A. Mikaelyan and Y. L. Dobryin, *J. Phys. G.: Nucl. Phys.* 5, 209 (1979); T. Ahrens and T. P. Lang, *Phys. Rev. C3*, 979 (1971).
10. F. T. Avignone, III and L. P. Hopkins, in *Proc. of Conf. on Neutrino Physics*, ed. by E. C. Fowler (Purdue Univ. Press, 1978).
11. B. R. Davis, P. Vogel, F. M. Mann and R. E. Schenter, *Phys. Rev. C19*, 2259 (1979).
12. J. Blietschau et al., *Nucl. Phys.* B133, 205 (1978).
13. A. N. Cnops et al., *Phys. Rev. Lett.* 40, 144 (1978).

FIGURE CAPTIONS

Figure 1 Neutrino oscillation results for the quantity $R_d(\text{osc})/R_d(\text{no osc})$ with R_d as defined in Eq. (6).

Figure 2 Predictions for $R_d(\text{osc})/R_d(\text{no osc})$ versus distance L from the reactor core, based on solution A with $\delta m^2 = 0.8 \text{ eV}^2$.

Figure 3 Predicted $\nu_e \rightarrow \nu_\tau$ transition probability for the L/E range of high energy accelerators. The δm^2 values are 1 eV^2 for solution A, 10 eV^2 for C, 50 eV^2 and 1 eV^2 for C'.

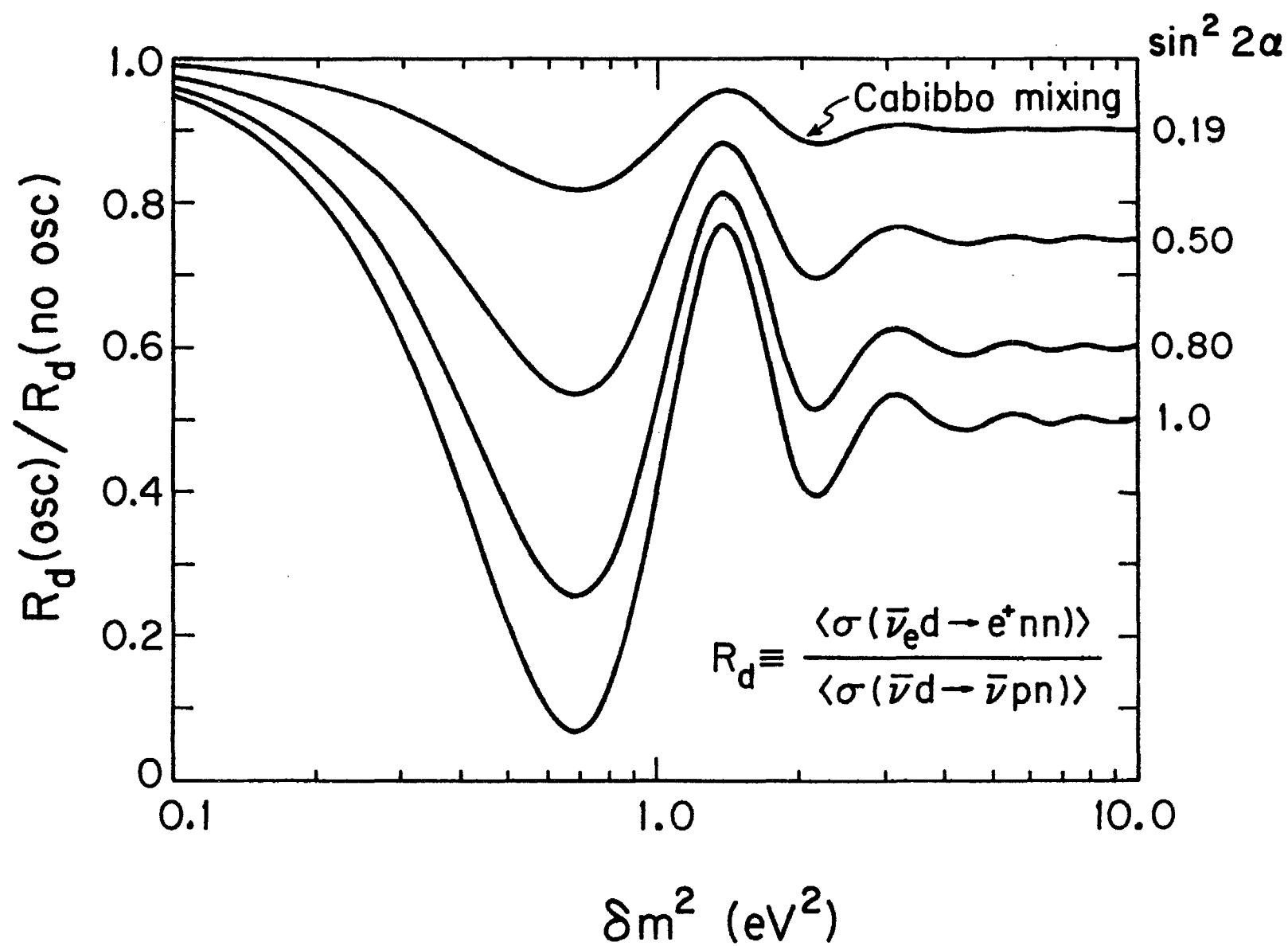


Figure 1

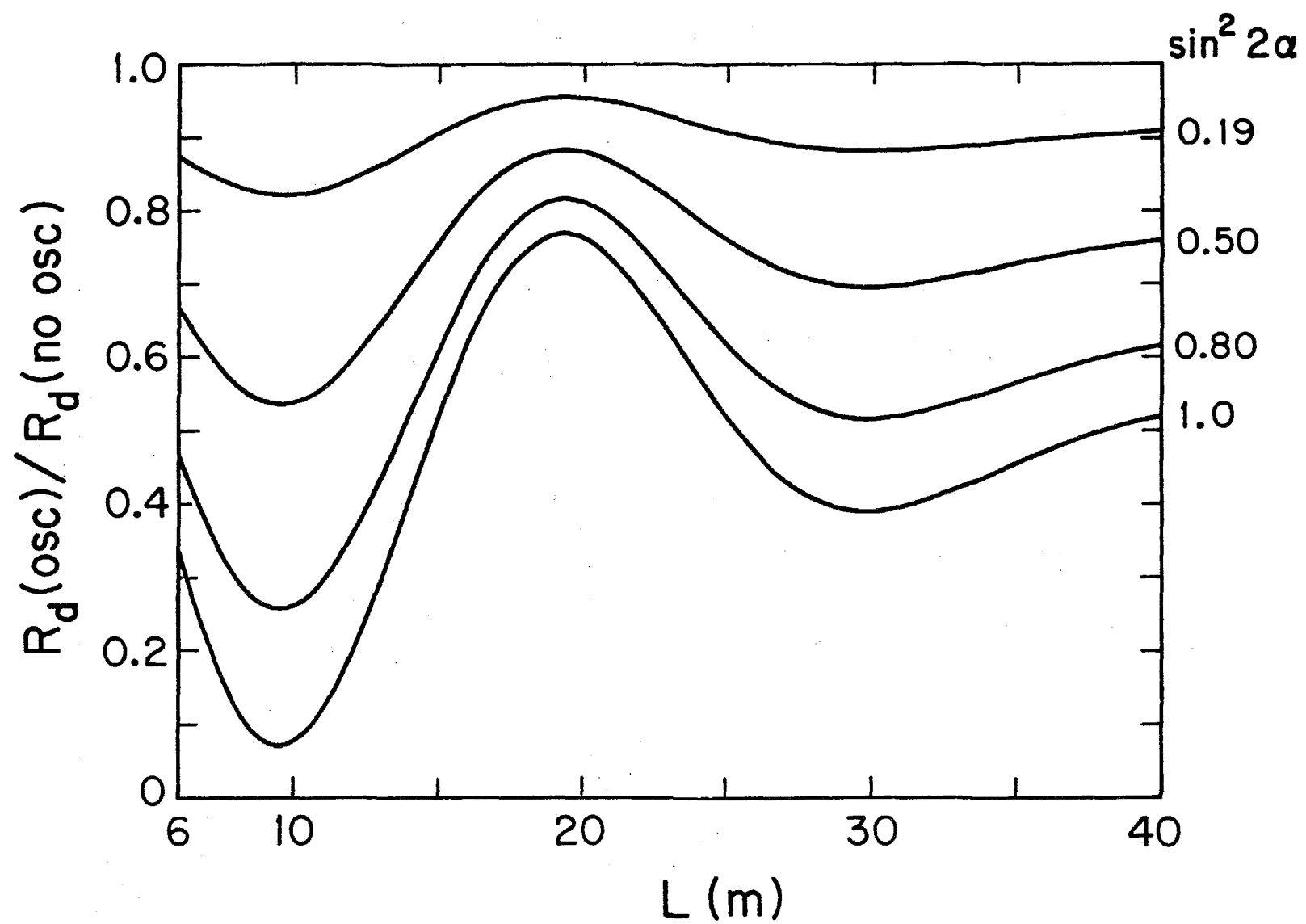


Figure 2

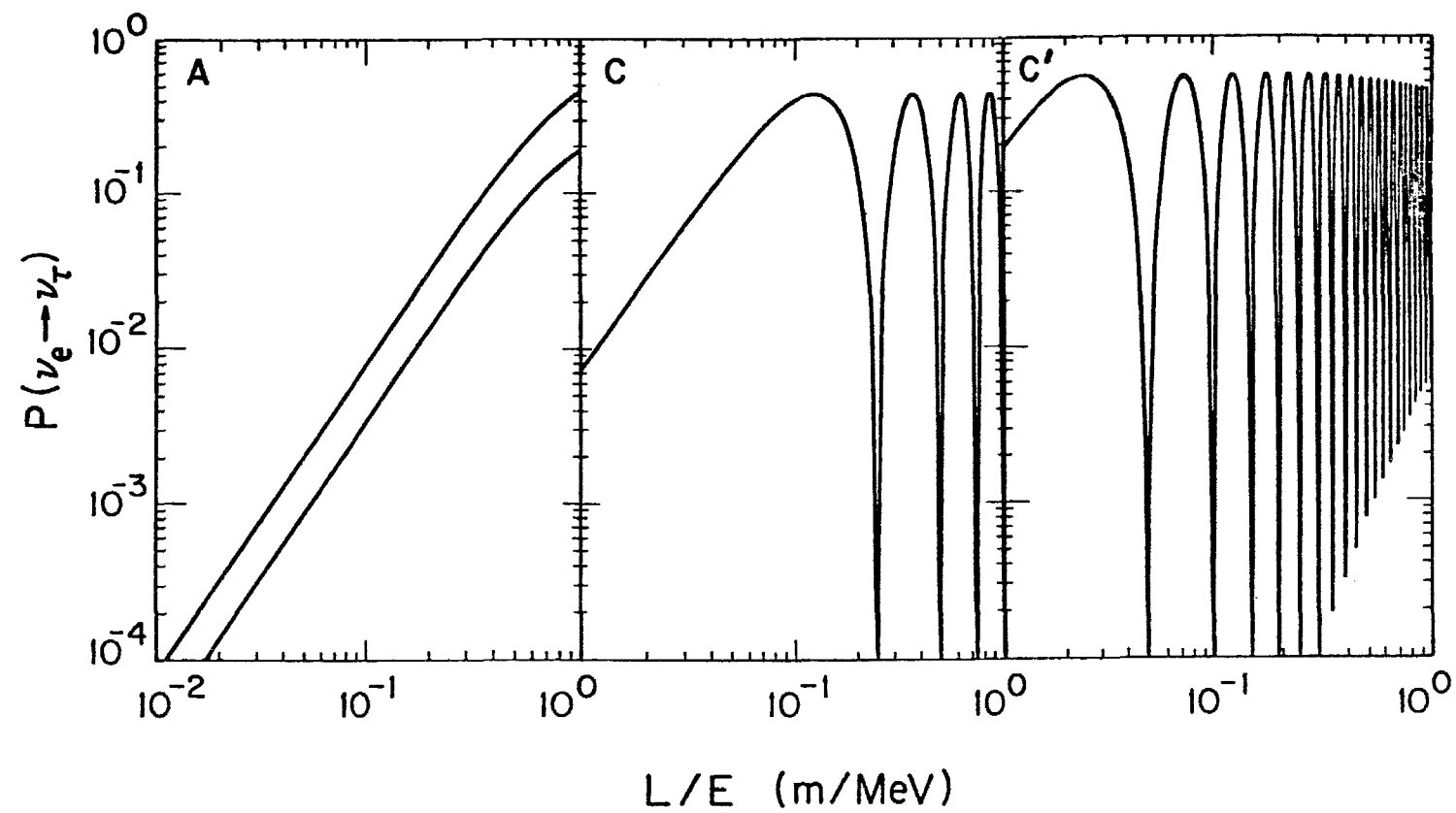


Figure 3

An Experiment to Search for Neutrino Oscillations

Using a ν_e Enriched Beam

U. Camerini, C. Canada, D. Cline, G. Bauer, W. Fry, R. Loveless,
J. Mathews, R. Morse, M. Mohammadi, A. More, D.D. Reeder
A. Szentgyorgi, H. Wachsmuth

University of Wisconsin, Madison, Wisconsin

C. Kourkoumelis, A. Markou, L.K. Resvanis
University of Athens, Athens, Greece

R. Huson, D. Ljung, J. Schmidt, W. Smart, R. Stefanski, E. Treadwell
Fermilab, Batavia, Illinois

M. Baldo-Ceolin, F. Bobisut, E. Calimani, G. Puglierin, A. Sconza
Instituto di Fisica, Universita di Padova, Padova, Italy*

*Universita di Padova's participation is subject to Italian authorities' approval.

Contents

1. Physics Goals
2. Beam Description
3. Detector and Event Rates
4. τ Search
 - A. Kinematic Analysis
 - B. Visible Decay
5. Ratio of Electron to Muon Events
6. Ratio of Events Without and With Charged Leptons $R(\frac{N_0}{N_\ell})$
7. Summary

Appendices

- A.
- B.
- C.

1. Physics Goals

We propose to search for neutrino oscillations. The possibility of neutrino oscillations has long been recognized.¹ A recent analysis of the experimental situation indicates that oscillations may exist with shorter wavelengths than previously considered. (See appendices.) The oscillations are periodic in L/E where L is the path length and E is the neutrino energy. Since the path length is fixed for our experiment, the energy dependence of a possible oscillation effect must be measured. The signals for oscillations would be the disappearance of one kind of neutrino and/or the reappearance of another kind.

The current experimental limits are shown in Figure 1 in which we plot the probability $\nu_\alpha \rightarrow \nu_\beta$ against L/E . The oscillation of ν_μ into ν_e or ν_τ has low experimental limits. In contrast, the oscillation of ν_e is essentially unmeasured. Several experiments which use reactor neutrinos, solar neutrinos, and neutrinos produced in accelerator beam dumps have obtained results which suggest that ν_e disappear, possibly by oscillation.²

In order to investigate ν_e oscillations we propose to use an ν_e enriched beam obtained from K_L^0 decay and the 15' heavy liquid bubble chamber. The signals for oscillations would be:

a) The detection of ν_τ . As described below about one third of the ν_τ CC interactions can be identified by kinematical considerations and the probability of $\nu_e \rightarrow \nu_\tau$ can be measured to a sensitivity of 1-2%.

The τ lepton may also be directly detected by observation of its decay vertex. About 6% of τ decays will be visible.

b) The ratio of electron to muon events $[R(e/\mu)]$.

Although less sensitive than a) for the reaction $\nu_e \rightarrow \nu_\tau$, this measurement could detect the oscillation of ν_{eL} into $\bar{\nu}_{eL}$ which then has zero interaction cross section. (This possibility is discussed in Appendix C).

c) The ratio of lepton-less events (neutral

current type) to charged current events, $[R(\frac{N_0}{N_\ell})]$.

The search for ν_e oscillations cannot be made at this sensitivity using a conventionally focussed neutrino beam, e.g. horn focussed or Quad triplet focussed. In the conventional beams the ratio of ν_μ or ν_e is about 100 to 1, thus the backgrounds in the ν_τ measurement are increased one hundred fold. Furthermore the ratio of neutral current events to charged current events becomes completely insensitive to ν_e phenomena.

2. Beam Description

Previous accelerator experiments have been insensitive to ν_e oscillations due to low ν_e flux or very large accompanying ν_μ flux. We propose to construct a $\nu_e/\bar{\nu}_e$ beam with a ν_e/ν_μ ratio close to unity. A beam with this feature was previously designed.^{3,4} Figure 2 shows the beam arrangement. The Sign Selected Bare Target (SSBT) train used for the HPWF neutrino experiment could be modified for this electron neutrino beam. The main idea of the beam is to sweep all charged particles out of the beam with a dipole placed just downstream of the target. A second dipole farther downstream sweeps out the charged decay products from K_s^0 decays. Electron neutrinos are produced from $K_L^0 \rightarrow \pi^- e^+ \nu_e$ (or $\rightarrow \pi^+ e^- \bar{\nu}_e$) decay. Figure 3 shows a Monte Carlo calculation of the neutrino fluxes in a beam using 400 GeV incident protons. The neutral kaon production is assumed to be the average of K^+ and K^- production. The muon neutrino background from $K_{\mu 3}^0$ decay and π and K decays is also shown. Note that above about 20 GeV the electron neutrino flux is comparable to the muon neutrino flux.

3. Detector and Event Rates

The 15' bubble chamber and the two-plane EMI form an excellent detector for neutrino events. The use of the heavy liquid bubble chamber has the following well-known advantages:

- 1) excellent identification of electrons ($\sim 95\%$) and muons ($\sim 80\%$) with both sign and momentum determination and $\sim 80\%$ γ detection.
- 2) good efficiency for observing and measuring complicated exclusive channels.
- 3) excellent visibility of the vertex. It might be possible to see the τ lepton decay vertex depending on τ momentum spectra and lifetime. The addition of a high resolution camera to the stereo triad would considerably enhance this possibility.
- 4) unbiased data taking. The detection of events and energy resolution are independent of the kinematic characteristics and/or the event energy, which allows the experiment to cover a wide range of L/E.

We propose a heavy mix of neon in hydrogen to optimize event rates. As a goal we wish to obtain $1000 \nu_e$ charged current interactions in order to be sensitive to $P(\nu_e + \nu_\tau) \sim 1-2\%$. This requires approximately 10^{19} protons on target at 400 GeV.

TABLE 1

Event rates

expected for 15 ton and 10^{19} protons on 1 λ_{abs} target

	CC ^(a)			NC ^(b)			e/ μ ratio		
	10-40	>40	total	10-40	>40	total	10-40	>40	total
ν_e	150	870	1020	45	260	305			
$\bar{\nu}_e$	75	420	495	25	143	168			
ν_μ	240	960	1200	72	288	360	.63	.91	.85
$\bar{\nu}_\mu$	125	330	455	43	112	155	.60	1.25	1.09
ν_τ ^(c)			<4						

(a). From spectra in fig. 3 assuming $\sigma^{\nu} = 0.62E \times 10^{-38}$, $\sigma^{\bar{\nu}}/\sigma^{\nu} = 0.48$.75 prompt ν_e , ν_μ (36 $\bar{\nu}_e$, $\bar{\nu}_\mu$) events are included (CERN beam dump result).(b). NC/CC = 0.30 for ν , 0.34 for $\bar{\nu}$.(c). Assumes $\overline{FF}/\overline{DD} = 0.1$, $\text{BR}(F \rightarrow \tau \nu) = 0.03$.

Assuming 3×10^{13} protons per pulse, a dedicated run could complete this experiment in five weeks with 300K photographs. Table 1 shows the expected number of events for such a run.

4. τ Search

a. Kinematic Analysis

We propose to identify the presence of ν_τ and $\bar{\nu}_\tau$ through the characteristic τ decay signatures. These decays fall into two general categories (shown in Figure 4) according to the types of background we must eliminate. Decays 1 and 2 appear as somewhat unusual charged current events with missing neutrinos. The other reactions resemble neutral currents in that they have no charged lepton, only a missing neutrino. Table 2 shows the τ decay modes with the estimated efficiency and the ultimate sensitivity of each channel. This sensitivity has been corrected for τ threshold effects, which reduce the cross section for ν_τ CC interactions with respect to ν_μ CC interactions by 22% (Figure 5) averaged over our neutrino spectrum.⁵

Table 2

<u>τ decay mode</u>	<u>BR</u>	<u>Det. Eff.</u>	<u>Bckgrd</u>	<u>Sensitivity</u>
1. $e\nu\bar{\nu}$	17%	10.7%	0.3%	20%
2. $\mu\nu\bar{\nu}$	17%	8.7%	0.3%	23%
3. $\pi\nu$	9%	30.0%	0.3%	14%
4. $\rho\nu$	22%	\sim 50.0%	0.05%	1.5%
5. $\pi\rho^0\nu$	4%	\sim 50.0%	0.1%	6%
6. $n\pi\nu$	31%	\sim 50.0%	2.0%	17%

Leptonic Decays (decays 1 and 2)

The missing neutrinos typically have a large transverse momentum (p_{\perp}) directed oppositely to the hadronic transverse momentum. We identify three independent variables which can distinguish a τ decay from an ordinary CC event: the missing transverse momentum (p_{\perp}^0); the angle (ϕ) between the lepton transverse momentum and the p_{\perp} ; and the longitudinal momentum of the lepton. Generally, we follow the analysis discussed by Albright et al.⁶ although we include additional information from the lepton longitudinal momentum to achieve better background rejection.

To estimate the background we use a sample of 1500 CC events (average energy ~ 30 GeV) from Exp. 28 and plot the missing p_{\perp} vs. ϕ (Figure 6). The electrons from τ decay are calculated by assuming the CC muons were τ 's, then allowing these τ 's to decay into $e\bar{v}v$. This analysis has the advantage that the hadron shower includes resolution effects and thus provides a realistic picture of the difficulties of separating ν_{τ} interactions from the normal CC events.

By requiring that missing p_{\perp}^0 be greater than 1.6 GeV/c and ϕ be ~~less~~ greater than 2.0 radians the background is 0.3% of ν_e CC events, whereas we identify 10.7% of the $\tau \rightarrow e\bar{v}v$ decays. By choosing a less restrictive cut ($p_{\perp}^0 > 0.8$, $\phi < 2.0$) we include 34% of the events with leptonic modes and the background increases to 4.1% of $\nu_e(\nu_{\mu})$ CC events. Clearly, we can further increase the τ detection efficiency albeit with increased background.

A potential difficulty is that the mismeasurement of the electron energy could result in mimicking the τ signature. The electron identification relies on the observation of bremsstrahlung gammas in the H_2 -Neon mix. It is possible that the electron might radiate a large fraction of its energy before its curvature can be measured. This results in missing momentum along the electron direction, exactly the signature for a τ event. By searching for gammas with the appropriate dip and azimuth we may detect this "lost" electron energy. Even more important is the removal of these gammas from the hadron shower. To illustrate our ability to correct the electron energy we plot $\gamma\gamma$ invariant mass distribution from E-546 data (Figure 7). The FWHM for the π^0 mass is 30 MeV.

The sensitivity of the experiment can be determined by choosing a cut which maximizes the signal to noise, such as the first example ($p_T^0 > 1.6$, $\phi < 2.0$). For 1000 ν_e events the CC background is three events. A sample of six events (three background events plus three real τ events) would correspond to 160 ν_τ interactions after correcting for detection efficiency and branching ratio. This sample would correspond to ν_e oscillation into ν_τ of 20%. We anticipate that $\tau \rightarrow \mu\nu\nu$ decays give equivalent numbers although we note the muon detection efficiency is somewhat smaller than that for the electron.

Hadronic Decays

$\tau \rightarrow \rho v$ (decay 4)

For this mode the τ decay gives one charged track and two γ 's with large transverse momentum with respect to the other hadrons (p_{th}). We expect to see both γ 's $\sim 60\%$ of the time. These tracks can be fitted to a ρ^\pm , which will then have a large p_{th} . Our ability to correct the γ energy (see Figure 7) allows us good resolution on the ρ mass. Since we choose events with a large $p_{th} \pi^0$, we anticipate few problems with multiple γ pairings.

With a fitted ρ at large p_{th} we estimate less than .05% background due to NC interactions (see $\tau \rightarrow \pi v$ analysis). So the observation of a single $\tau \rightarrow \rho v$ event (detection eff. $\sim .50$, BR = .22) implies only 10 ν_τ interactions. If there were originally 1000 ν_e , we are sensitive to a 1-2% oscillation into ν_τ . This is the most sensitive channel and sets the experimental limit. This channel is not available for most counter experiments, particularly those utilizing a hadronic calorimeter.

$\tau \rightarrow \pi v$ (decay 3)

We expect one charged track with large p_{th} . We again identify three independent variables to distinguish $\tau \rightarrow \pi v$ events: transverse momentum of π , longitudinal momentum of π , and the angle (θ) between the π transverse momentum p_{tv} and the missing p_{tv}^0 . To estimate the background we use the same E-28 data sample and treat the muon as unseen. The π vector is computed by assuming the muon was a tau which decayed into πv .

In the plane transverse to the neutrino direction we determine the transverse axis (TA) of the event (pseudo-thrust analysis). The transverse momentum, p_{tv} , of each track is projected onto this axis and plotted vs. the longitudinal momentum for $\theta < 2.0$ radians. From these data we estimate a background to $\tau \rightarrow \pi\nu$ of 0.3% of NC events. The τ detection efficiency for these cuts is 30% (see Figure 8). Since the total NC sample is expected to be 1,000 events we anticipate three background events. If we detect six events (three background, three real $\tau \rightarrow \pi\nu$ decays) this channel is sensitive to a 14% ν_e oscillation.

$\tau \rightarrow \pi$'s (decays 5 \rightarrow 7)

These decay channels are similar to $\pi\nu$ if the pions from decay can be separated from the hadrons. The pseudo-thrust analysis can be used to identify candidates which can be fitted to $A_1 \rightarrow \pi\rho$, $\pi\pi\pi$. We estimate the sensitivity of these channels is about 17%.

4.b. Visible Decay

The expected lifetime of the τ lepton is 2.8×10^{-13} sec., assuming full V-A coupling. Therefore, with the conventional optical system of the 15' bubble chamber we expect to see the decay vertex in 5-10% of the τ decays. Although the decays are predominately one-pronged which makes identification more difficult, this is partly compensated by the separation of the lepton from the hadron shower. We base our estimate on our experience in E-546 in which we identified greater than four examples of charmed particle decay.

A single high resolution camera operated in conjunction with the conventional triad would improve our resolution significantly over about one-half the fiducial volume. Subject to availability and operating cost considerations, we propose to utilize this high resolution camera.

5. Ratio of Electron to Muon Events

Two different oscillation phenomena lead to an observed e/μ ratio which differs from the value expected from the beam fluxes (see Table 1).

a) $\nu_e \rightarrow \nu_\tau$

In this case the ratio becomes

$$R\left(\frac{e}{\mu}\right) = \frac{\phi_e \left\{ [1 - P(\nu_\tau)] \sigma_{cc} + 0.17 P(\nu_\tau) \sigma_{cc}^\tau \right\}}{\phi_\mu \sigma_{cc} + 0.17 \phi_e P(\nu_\tau) \sigma_{cc}^\tau}$$

where $P(\nu_\tau)$ is the probability of the ν_e oscillating into ν_τ , σ_{cc} is the cross section for ν_e and ν_μ , σ_{cc}^τ is the corresponding cross section for ν_τ interactions, ϕ_e is the ν_e flux and ϕ_μ is the ν_μ flux. For example if $P(\nu_\tau) = .3$, and σ_{cc}^τ for our spectrum is $0.78 \sigma_{cc}$, then R becomes

$$R\left(\frac{e}{\mu}\right) = \frac{.7 + .17(.78)}{1 + .17(.78)} = .74 (\phi_e/\phi_\mu)$$

to be compared with $R\left(\frac{e}{\mu}\right) = \phi_e/\phi_\mu$ for no oscillation.

b. $\nu_{eL} \rightarrow \bar{\nu}_{eL}$ (see Appendix C)

For this case the V-A theory predicts that the $\bar{\nu}_{eL}$ will not interact. Hence $R\left(\frac{e}{\mu}\right)$ becomes

$$R\left(\frac{e}{\mu}\right) = \frac{\phi_e [1 - P(\bar{\nu}_{eL})] \sigma_{cc}}{\phi_\mu \sigma_{cc}}$$

As in the previous example, for $P(\bar{\nu}_{eL}) = .3$, $R(\frac{e}{\mu})$ becomes $0.7 (\phi_e/\phi_\mu)$, comparable to the previous ratio. However, the two phenomena would be distinguished by the observation of the ν_τ interaction.

The experimental significance of this ratio depends strongly on the knowledge of ϕ_e and ϕ_μ . From particle production data and beam geometry we believe ϕ_e/ϕ_μ can be determined to 5%. We are currently studying this question. If this can be achieved, the e/μ ratio would be sensitive to an oscillation of $\leq 10\%$ of the ν_e .

6. Ratio of Events Without and With Charged Leptons $R(\frac{N_0}{N_\ell})$

The ratio of events without (N_0) and with (N_ℓ) a charged lepton is also sensitive to $\nu_e \rightarrow \nu_\tau$ oscillations. We define the relevant parameters:

$R_\mu(\frac{NC}{CC})$, $R_e(\frac{NC}{CC})$ - the ratio of neutral to charged current interactions

$R_\tau(\frac{NC}{CC})$ - neutral to charged ratio for ν_τ interactions ($\sim .38$ corrected for the threshold effect)

σ_{CC} - CC cross section for ν_e and ν_τ

σ_{CC}^τ - CC cross section for ν_τ ($\sim .78 \sigma_{CC}$ integrated over the spectrum)

$P(\nu_\tau)$ - probability of ν_e oscillation into ν_τ

$P(\bar{\nu}_{eL})$ - probability of ν_e oscillation into $\bar{\nu}_{eL}$

ϕ_e, ϕ_μ - primary flux of ν_e, ν_μ

a) $\nu_e \rightarrow \nu_\tau$

The ratio $N(\frac{N_0}{N_\ell})$ can be calculated by summing contributions:

$$R(\frac{N_0}{N_\ell}) = \frac{\left\{ \phi_\mu \sigma_{CC} R_\mu(\frac{NC}{CC}) + \phi_e \sigma_{CC} R_e(\frac{NC}{CC}) [1 - P(\nu_\tau)] + .66 \phi_e P(\nu_\tau) \sigma_{CC}^\tau + \phi_e P(\nu_\tau) \sigma_{CC}^\tau R_\tau(\frac{NC}{CC}) \right\} / \left\{ \phi_\mu \sigma_{CC} + \phi_e \sigma_{CC} [1 - P(\nu_\tau)] + .34 \phi_e \sigma_{CC}^\tau P(\nu_\tau) \right\}}$$

Without oscillation, the ratio $R\left(\frac{N_O}{N_\ell}\right) = 0.3$, independent of the flux ratio, ϕ_e/ϕ_μ . However, if $P(v_\tau) = .3$ and $\phi_e = \phi_\mu$

$$R\left(\frac{N_O}{N_\ell}\right) = 0.42$$

If $\phi_e = \frac{1}{Z}\phi_\mu$, and $P(v_\tau) = 0.3$,

$$R\left(\frac{N_O}{N_\ell}\right) = 0.38$$

so the ratio R is relatively insensitive to the flux ratio.

Assuming $\phi_e = \phi_\mu$ we can solve for $P(v_\tau)$ as a function of the measured ratio, $R\left(\frac{N_O}{N_\ell}\right)$.

$$P(v_\tau) = \frac{2R - .6}{.73R + .51}$$

For a measured $R = 0.40 \pm .02$ we can measure $\frac{\Delta P}{P} \sim .20$.

It should be noted that if the measured ratio $R\left(\frac{N_O}{N_\ell}\right)$ deviates from that measured in a v_μ beam, and if no v_τ CC interactions are observed, then μ -e universality is violated in the NC sector.

b) $\nu_e \rightarrow \bar{\nu}_{eL}$

In this case the ratio becomes

$$R\left(\frac{N_0}{N_\lambda}\right) = \frac{\phi_\mu \sigma_{CC} R_\mu \left(\frac{NC}{CC}\right) + \phi_e \sigma_{CC} R_e \left(\frac{NC}{CC}\right) [1 - P(\bar{\nu}_{eL})]}{\phi_\mu \sigma_{CC} + \phi_e \sigma_{CC} [1 - P(\bar{\nu}_{eL})]}$$

which is independent of $P(\bar{\nu}_{eL})$. Hence this ratio can never observe an oscillation into a channel which does not interact.

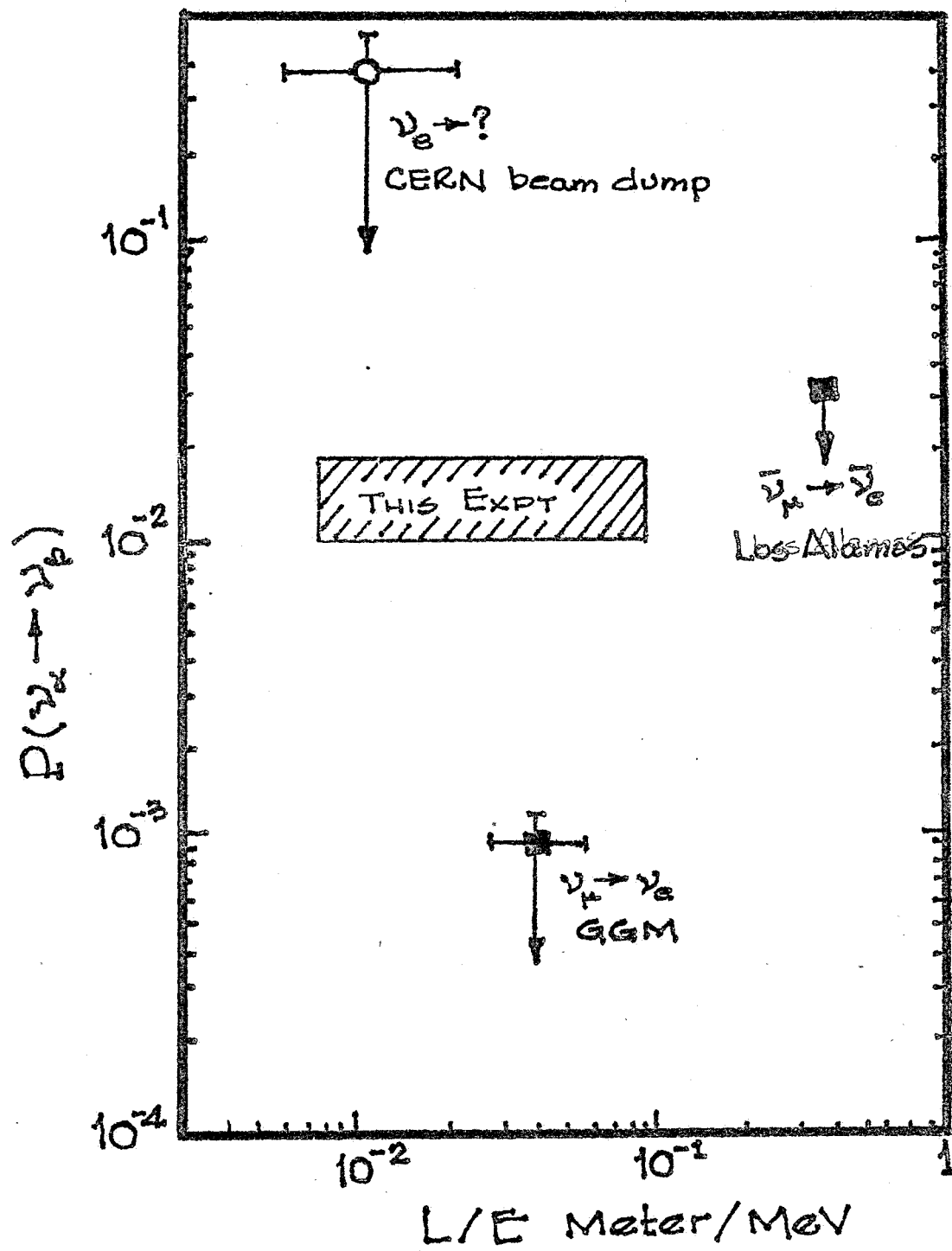


FIGURE 1

BTSS Beam modified for K_L^0

C1 - magnet protection collimator

C-2, C-3 - ± 2 mrad xy collimators (no cooling)

Dump - 3 m Al block (water cooled)

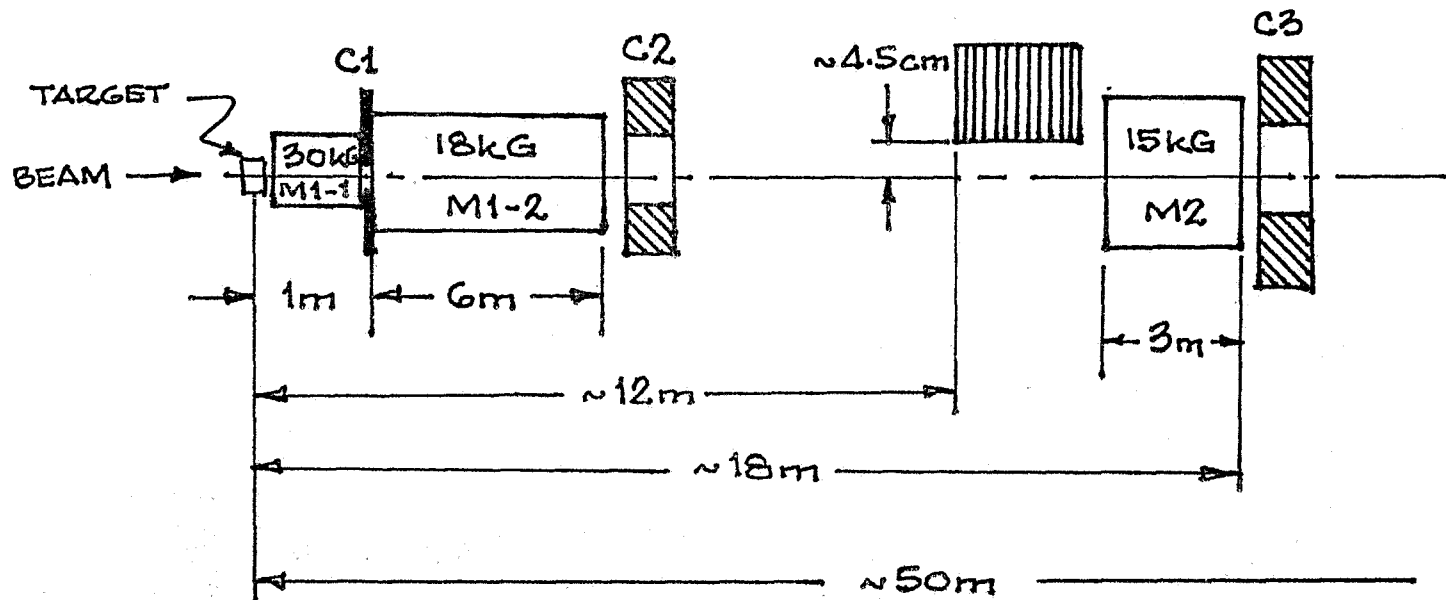


FIGURE 2

FLUXES FROM K_L^0 BEAM

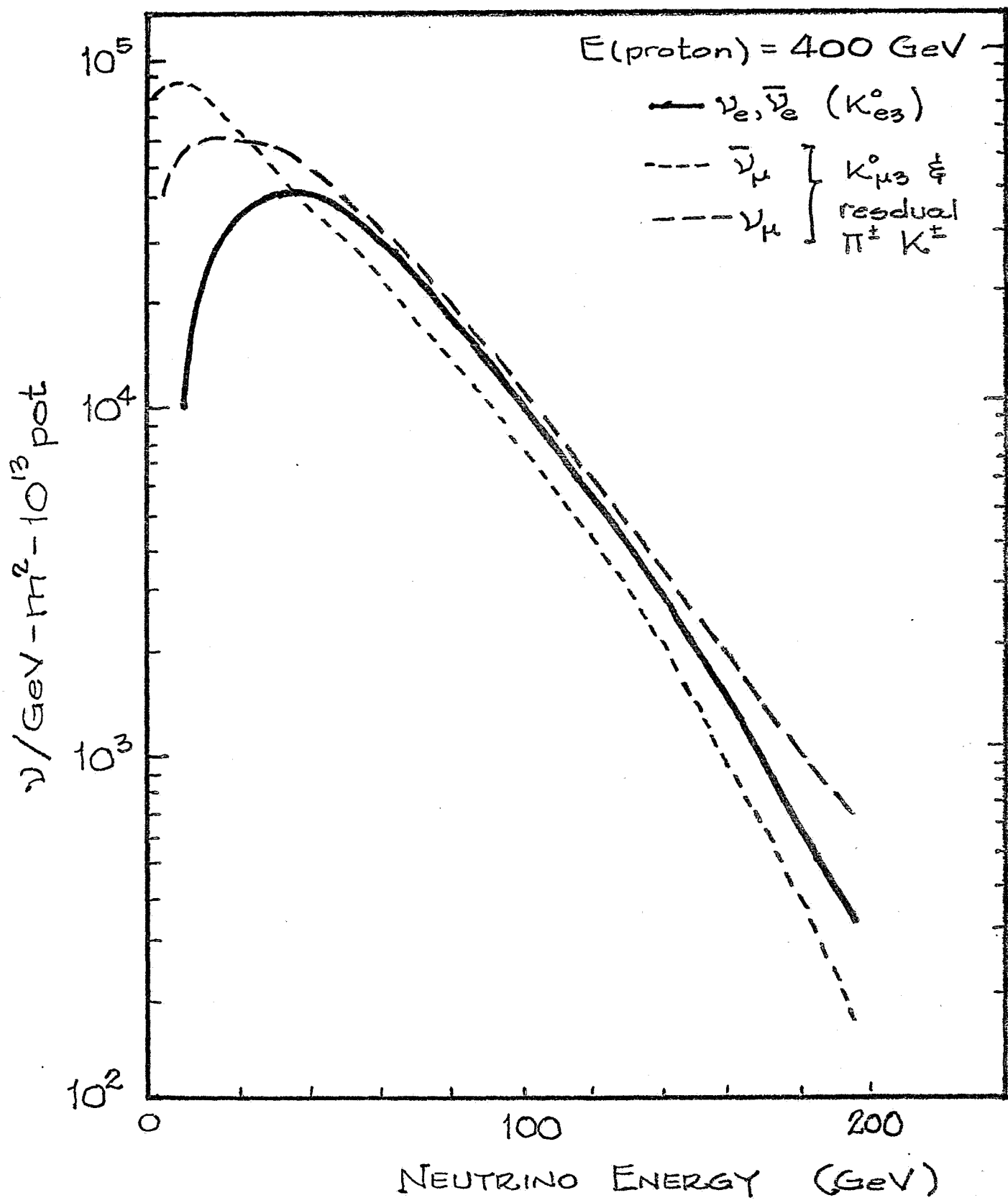


FIGURE 3

τ Signatures

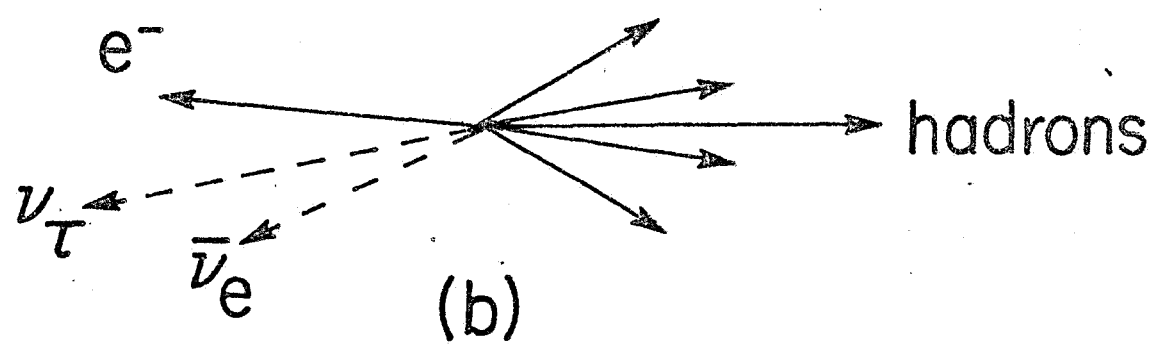
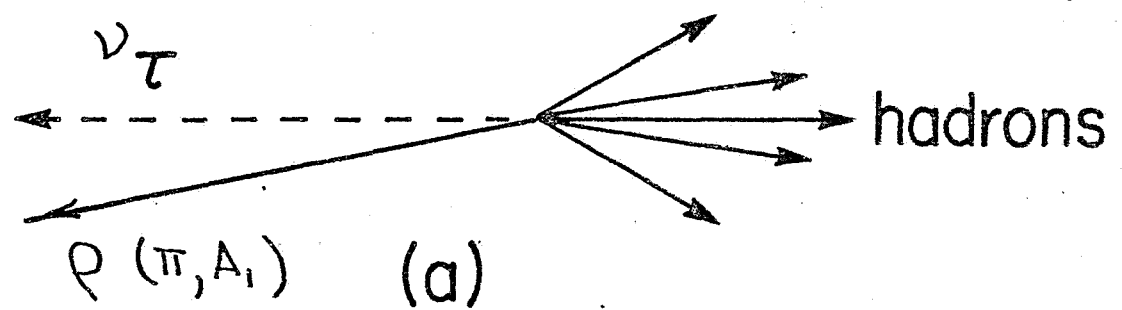
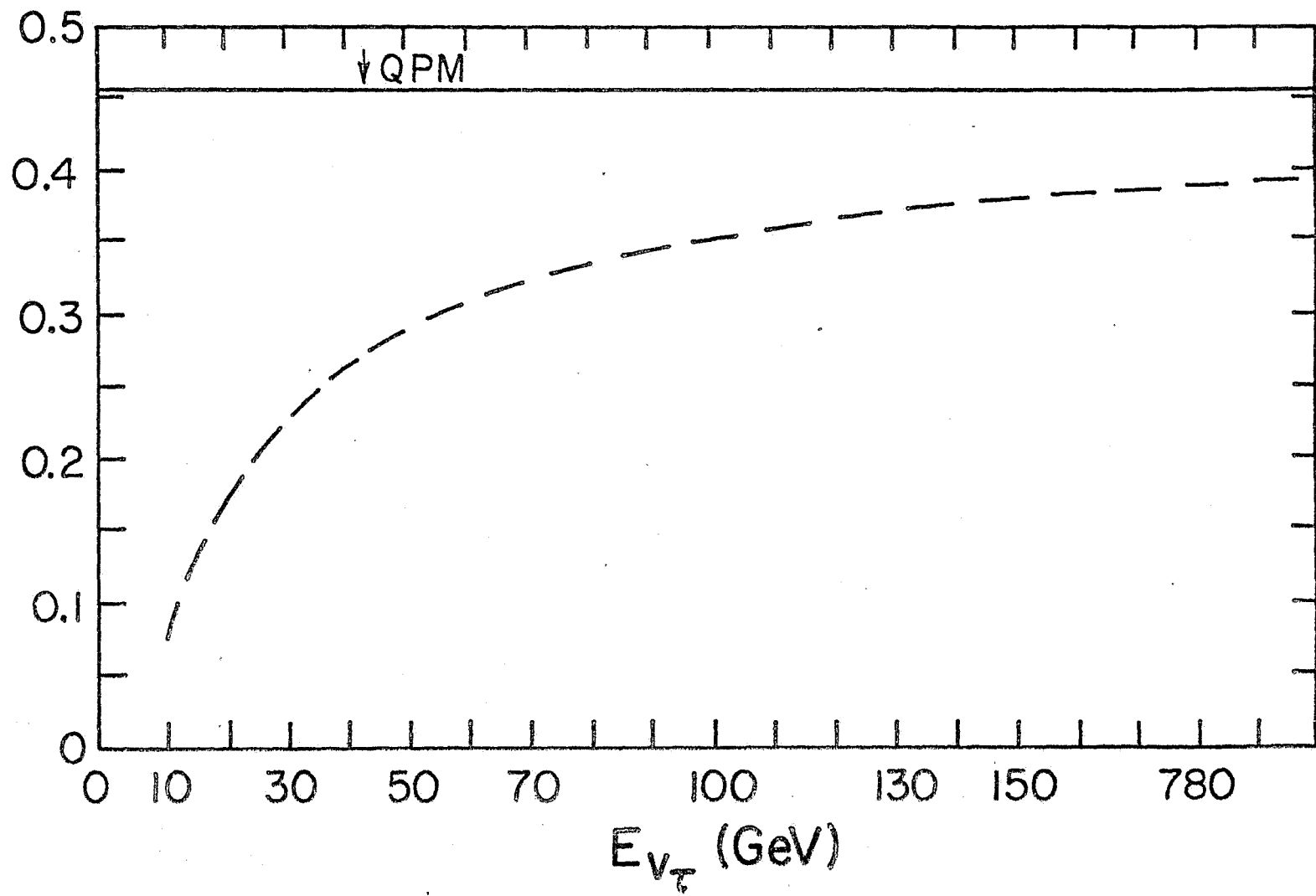


FIGURE 4

FIGURE 5



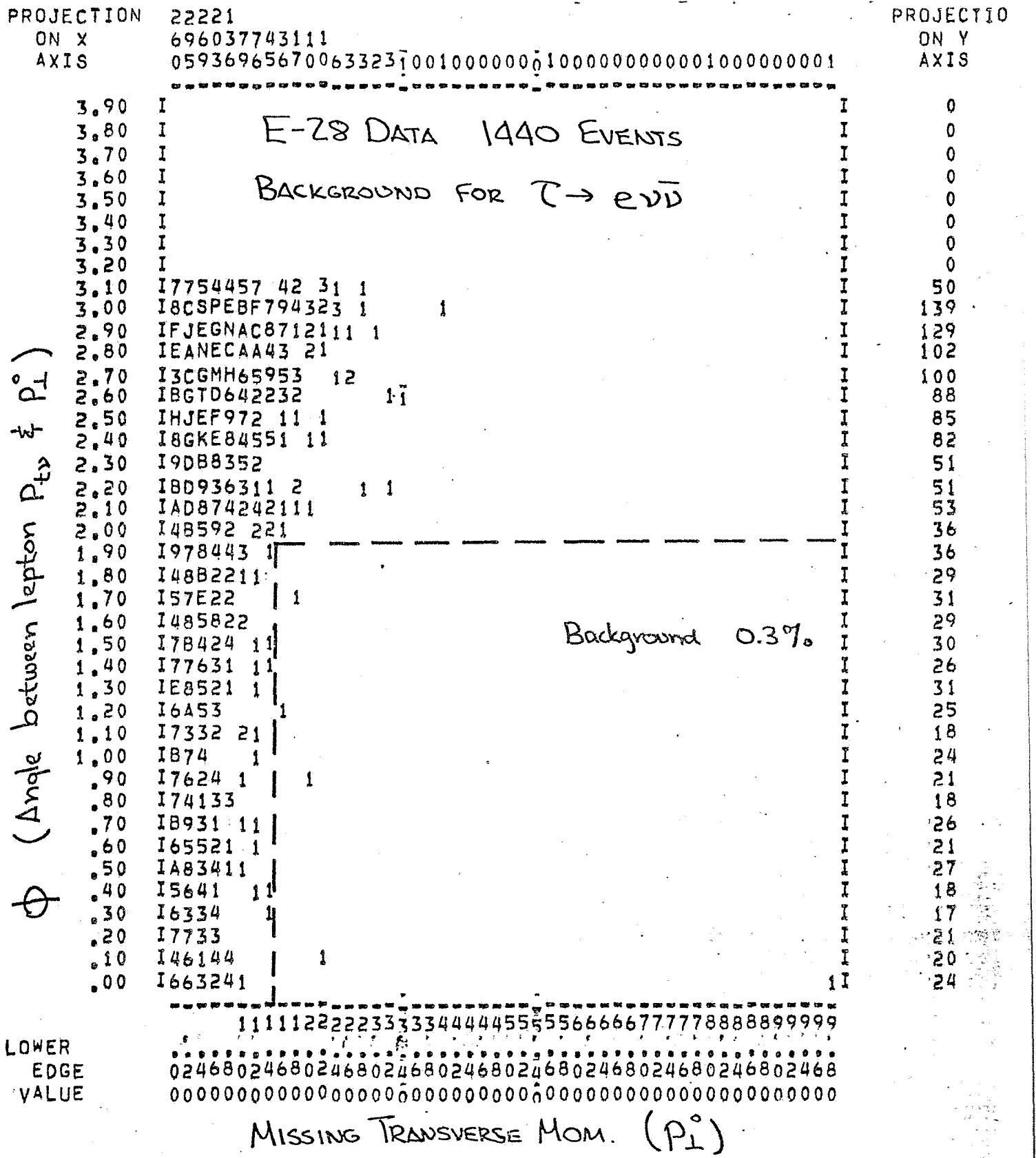


FIGURE 6a

PROJECTION

122211

ON X 43140619653111 1
AXIS 4815933484155360

ON Y
AXIS

τ Signal 10.7%

LOWER
EDGE
VALUE

MISSING TRANSVERSE MOM. (PI⁰)

GAMMA-GAMMA MASS SPECTRUM

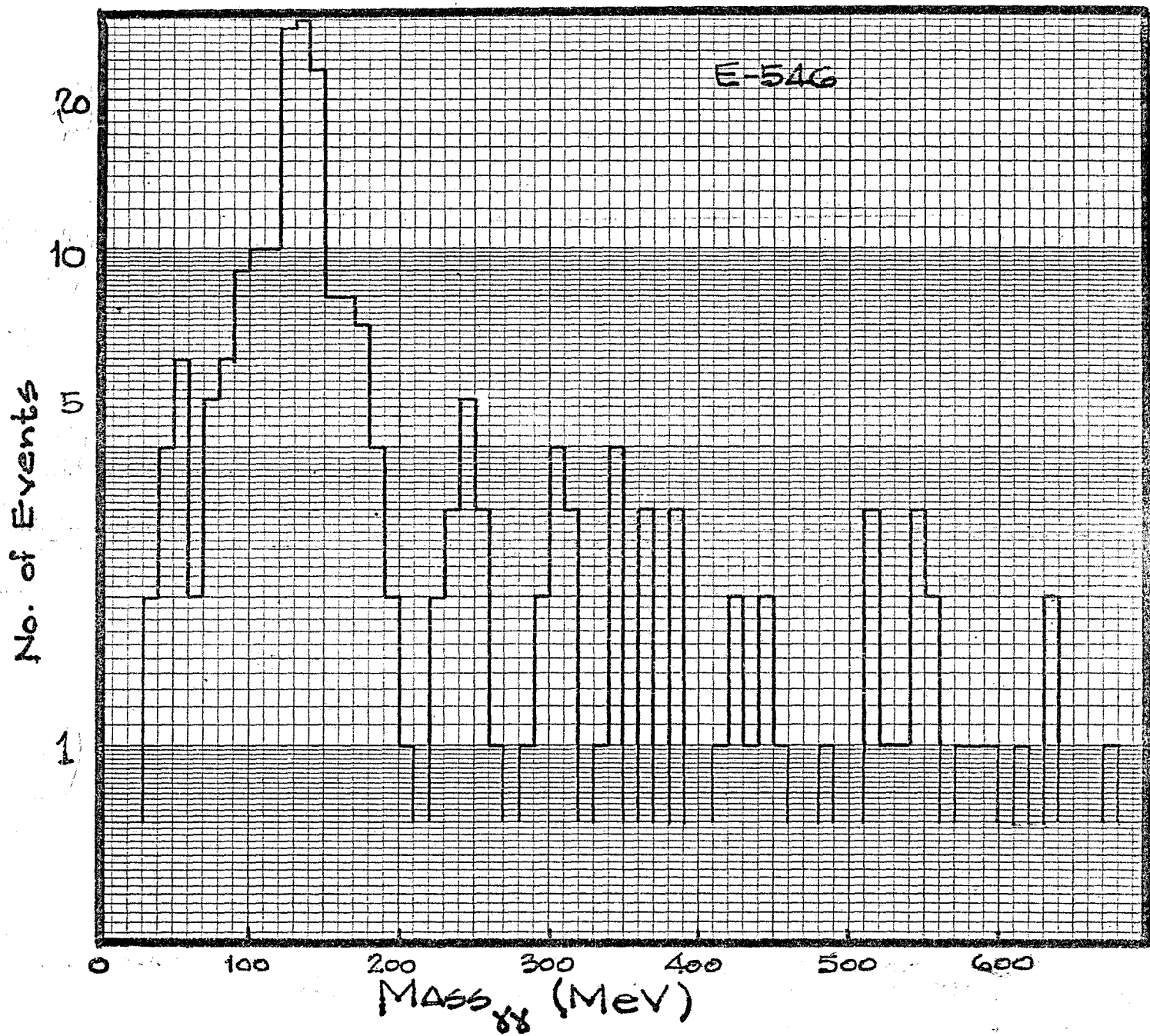


FIGURE 7

PROJECTION 11
ON X 06353211
AXIS 53323410

E-28 DATA 1440 EVENTS

"NC" BACKGROUND

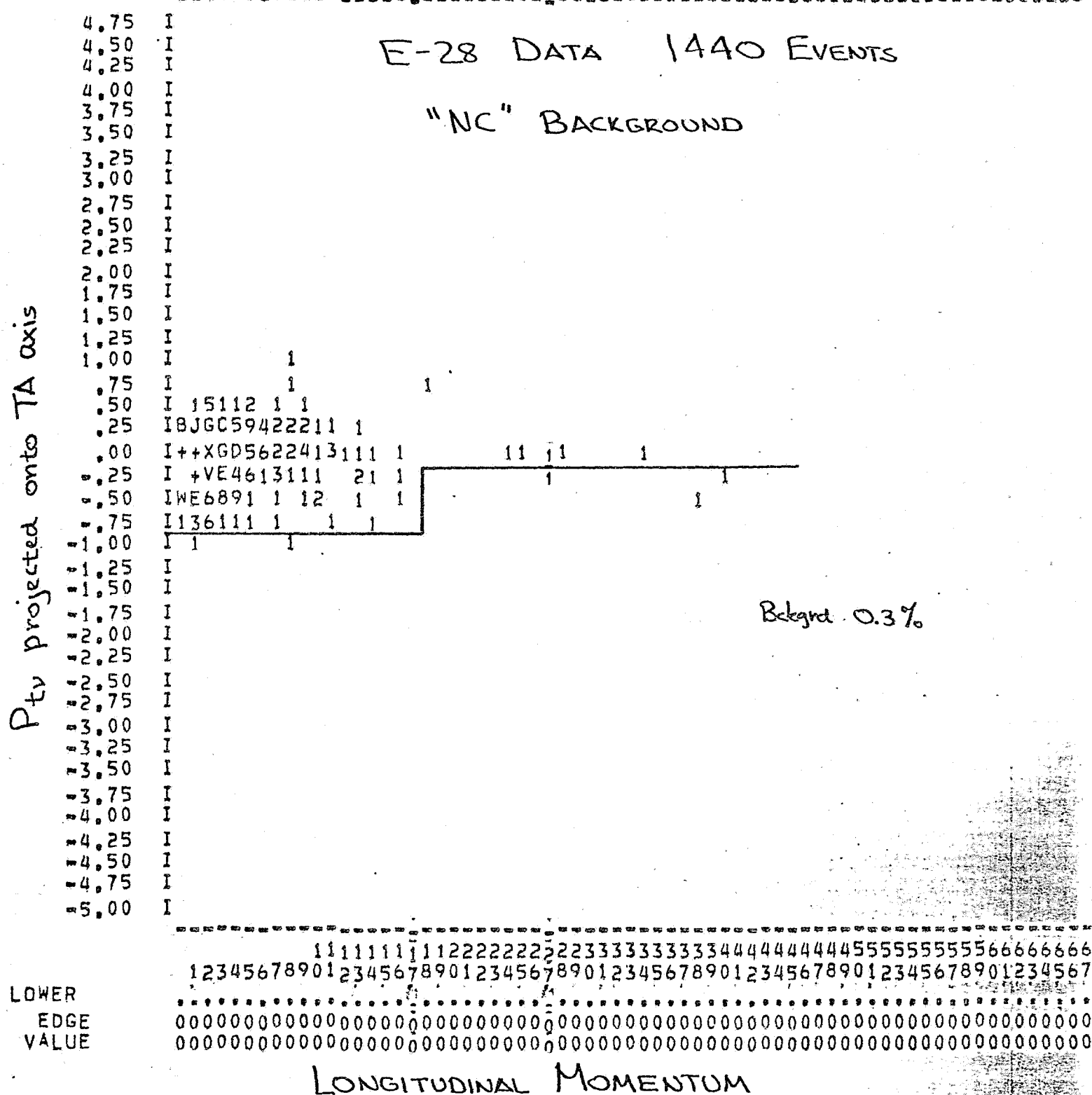


FIGURE 8a

PROJECTION 111
ON X 0418864332221122211
AXIS 620718915749691313788727525683348342202144030100002300101012100011110

E-28 DATA 1440 EVENTS

SIMULATED $\tau \rightarrow \pi\nu$

P_{tr} projected onto TA axis

-5
LOWER
EDGE
VALUE

T signal 30%

LONGITUDINAL MOMENTUM (GeV)

FIGURE 8b

REFERENCES

1. B. Pontecorvo, Soviet Phys. JETP 53, 1717(1967); V. Gribov and B. Pontecorvo, Phys. Lett. 28B, 493(1969).
For thorough recent review of theory and experiment see
(a) S.M. Bilenky and B. Pontecorvo, Phys. Reports 41, 225 (1978); (b) A. de Rujula et al., CERN TH-2788 (1979).
2. F. Reines, Unification of Elementary Forces and Gauge Theories (eds. D.B. Cline and F.E. Mills), Harwood Academic Publishers, p. 103 (1978); F. Reines, private communication to D. Cline of $E > 5.5$ MeV data (1978); S.Y. Nakamura et al., Proc. of the Inter. Neutrino Conf., Aachen (ed. by H. Faissner et al.), Vieweg (1977).
F. Nezrick and E. Reines, Phys. Rev. 142, 852 (1966).
R. Davis Jr., J.C. Evans and B.T. Cleveland, Proc. of the Conf. on Neutrino Physics, ed by E.C. Fowler (Purdue Univ. Press, 1978).
H. Wachsmuth, Proceedings of the International Symposium on Lepton and Photon Interactions at High Energies, FNAL (1980) pg. 541.
3. D. Treille, R. Turlay, K. Winter, CERN/ECFA/72/4, Vol. 1 (1972) p. 167.
4. S. Mori, S. Pruss, and R. Stefanski, TM-725 (April, 1977).
S. Mori, "Improved Electron Neutrino Beam:", TM-769.
5. K. Bonnardt, "Lepton Mass Effects in Production of Heavy Leptons by Neutrinos in Deep Inelastic Processes", Karlsruhe Preprint, TKP/9-5 (1979).
6. C. Albright, R. Shrock, and J. Smith, Phys. Rev. D20, 2177(1979).
7. H.C. Ballagh et al., Physics Letters 89B, 423 (1980).

POSSIBLE INDICATIONS OF NEUTRINO OSCILLATIONS

V. Barger, K. Whisnant

Physics Department, University of Wisconsin, Madison, Wisconsin 53706 USA

D. Cline

Physics Department, University of Wisconsin, Madison, Wisconsin 53706 USA
and Fermilab, Batavia, Illinois 60510 USA

R. J. N. Phillips

Rutherford Laboratory, Chilton, Didcot, Oxon, England

ABSTRACT

We analyze neutrino oscillations of the ν_e , ν_μ , ν_τ system. Presently available reactor antineutrino data contain indications of oscillations, that have hitherto escaped attention, corresponding to an eigenmass squared difference of $\delta m^2 = 1 \text{ eV}^2$. Two other classes of oscillation solutions are contrasted and further experimental tests are indicated. All the δm^2 must be greater than 10^{-3} eV^2 to explain solar and deep mine observations.

The interesting possibility of neutrino oscillations has long been recognized¹ but no clear signal has yet been established.² In this Letter we observe, however, that the reactor antineutrino data of Reines et al.^{3,4} are consistent with an oscillation effect of shorter wavelength than hitherto considered. Solar neutrino observations and deep mine neutrino data reinforce the indication that neutrino oscillations occur, and constrain their parameters.

Neutrino oscillations depend on differences in mass m_i between the neutrino mass eigenstates ν_i . The latter are related to the weak charged current eigenstates ν_α (distinguished by Greek suffices) through a unitary transformation $|\nu_\alpha\rangle = U_{\alpha i} |\nu_i\rangle$. Starting with an initial neutrino ν_α of energy E , the probability for finding a neutrino ν_β after a path length L can be compactly written (for $E^2 \gg m_i^2$):

$$P(\nu_\alpha \rightarrow \nu_\beta) = \delta_{\alpha\beta} + \sum_{i < j} 2 |U_{\alpha i} U_{\beta i} U_{\alpha j} U_{\beta j}| [(\cos(\Delta_{ij} - \phi_{\alpha\beta ij})) - \cos \phi_{\alpha\beta ij}] \quad (1)$$

where $\phi_{\alpha\beta ij} = \arg(U_{\alpha i} U_{\beta i}^* U_{\alpha j}^* U_{\beta j})$ and $\Delta_{ij} = \frac{1}{2}(m_i^2 - m_j^2)L/E$. For a diagonal transition or an off-diagonal transition with CP conservation (U real), we obtain the simple formula

$$P(\nu_\alpha \rightarrow \nu_\beta) = \delta_{\alpha\beta} - \sum_{i < j} 4 U_{\alpha i} U_{\beta i}^* U_{\alpha j}^* U_{\beta j} \sin^2(\frac{1}{2}\Delta_{ij}) \quad (2)$$

With L/E in m/MeV and m_i in eV units, the oscillation argument in radians is

$$\frac{1}{2}\Delta_{ij} = 1.27 \delta m_{ij}^2 L/E \quad (3)$$

where $\delta m_{ij}^2 \equiv m_i^2 - m_j^2$. For antineutrinos replace U by U^* above.

The oscillations are periodic in L/E . Oscillations arising from a given δm_{ij}^2 can be most readily mapped out at L/E values of order $1/\delta m_{ij}^2$. The

experimentally accessible ranges of L/E in m/MeV are $\sim 10^{10}$ (solar), $\sim 10-10^5$ (deep mine), 1-7 (low energy accelerators), 1-20 (reactors), 0.3-3. (meson factories), and 0.01-0.05 (high energy accelerators). After many cycles, detectors cannot measure L or E precisely enough to resolve individual oscillations and are sensitive only to average values. In the limit $L/E \gg (m_i^2 - m_j^2)^{-1}$ for all $i \neq j$, the average asymptotic values are given by

$$\langle P(\nu_\alpha \rightarrow \nu_\beta) \rangle = \sum_i |U_{\alpha i} U_{\beta i}^*|^2. \quad (4)$$

Since only ν_e , ν_μ , and ν_τ neutrino types are known, we specialize to a three neutrino world. The matrix U can then be parameterized in the form introduced by Kobayashi and Maskawa,⁵ in terms of angles $\theta_1, \theta_2, \theta_3$ with ranges $(0, \pi/2)$ and phase δ with range $(-\pi, \pi)$. In our present analysis we neglect CP violation (thus $\delta = 0$ or $\pm \pi$). To limit the regions of the $\theta_i, \delta m_{ij}^2$ parameter space, we consider first the constraints placed by solar, deep mine and accelerator data.

Solar neutrino observations and deep mine experiments: The solar neutrino data⁶ suggest that $\langle P(\nu_e \rightarrow \nu_e) \rangle \simeq 0.3-0.5$ at $L/E \sim 10^{10}$ m/MeV. For three neutrinos, Eq. (4) gives

$$\langle P(\nu_e \rightarrow \nu_e) \rangle = c_1^4 + s_1^4 c_3^4 + s_1^4 s_3^4 \quad (5)$$

where $c_i = \cos \theta_i$ and $s_i = \sin \theta_i$. The minimum value of Eq. (5) is 1/3 and this requires $c_1 = 1/\sqrt{3}$, $c_3 = 1/\sqrt{2}$. For $\langle P(\nu_e \rightarrow \nu_e) \rangle$ to be near its minimum, all mass differences must satisfy $\delta m^2 \gg 10^{-10}$ eV². At this minimum all transition averages are specified, independent of θ_2 ; in particular $\langle P(\nu_\mu \rightarrow \nu_\mu) \rangle = 1/2$. In fact, there are indications from deep mine experiments⁷⁻⁹ that $\langle P(\nu_\mu \rightarrow \nu_\mu) \rangle \sim 1/2$ (see footnote f in Table 1). Since the ν_μ

neutrinos detected in deep mines have traversed terrestrial distances, this measurement suggests that all $\delta m^2 \gtrsim 10^{-3}$ eV². Based on these considerations we may suppose that the true solution is not far from the above θ_1 , θ_3 values. If we only require $\langle P(\nu_e \rightarrow \nu_e) \rangle < 0.5$, then θ_1 and θ_3 are constrained to a region approximated by the triangle $\theta_1 > 35^\circ$, $\theta_3 > \theta_1 - 45^\circ$, and $\theta_3 < 135^\circ - \theta_1$.

$\nu_\mu \rightarrow \nu_e$, ν_τ oscillations: Stringent experimental limits exist on these transitions¹⁰⁻¹³ at L/E in the range 0.01 to 0.3 m/MeV (see Table 1). For $\delta m^2 \ll 1$ eV², these oscillations do not appear until L/E $\gg 1$ m/MeV. With a single $\delta m^2 \gtrsim 1$ eV², these oscillations can be suppressed by choice of θ_2 (if θ_1, θ_3 are taken as above).

Reactor $\bar{\nu}_e$ -oscillations: The $\bar{\nu}_e$ flux at distances L = 6 m and 11.2 m from a reactor core center was measured by Reines et al.,^{3,4} using the known cross section for the inverse beta-decay reaction $\bar{\nu}_e p \rightarrow e^+ n$. The reactor $\bar{\nu}_e$ flux at the core has been calculated using semi-empirical methods.¹⁴⁻¹⁷ The ratio of measured flux at L to the calculated flux measures $P(\bar{\nu}_e \rightarrow \bar{\nu}_e)$. Neutrino oscillation interpretations of the data thereby depend on the calculated spectrum about which there is some uncertainty.

Figure 1 shows a comparison of the measured $\bar{\nu}_e$ flux at L = 6 m and L = 11.2 m with calculated spectra. We note that the Avignone-1978 calculated flux¹⁶ accommodates best the L = 6 m measurements for $E_{\bar{\nu}_e} > 6$ MeV. The data for $P(\bar{\nu}_e \rightarrow \bar{\nu}_e)$ obtained with the Avignone-1978¹⁶ and Davis et al.¹⁷ calculated spectra are shown in Fig. 2. The horizontal error bars in Fig. 2 take into account the finite size of the reactor core source. We observe that $P(\bar{\nu}_e \rightarrow \bar{\nu}_e)$ seems to follow an oscillation pattern with one node in the range of L/E covered by the measurements. The possibility of such a solution

in which a short wavelength oscillation occurs was not considered by Reines et al.³ in their analysis of the 11.2 m data based on a similar calculated spectrum.¹⁵

The oscillation in Fig. 2 is well-described by the formula

$P(\bar{\nu}_e \rightarrow \bar{\nu}_e) = 1 - 0.44 \sin^2(1.27 L/E)$. This corresponds to a mass difference $\delta m^2 = 1 \text{ eV}^2$, which we can arbitrarily identify as δm_{13}^2 . A non-zero δm_{12}^2 with $\delta m_{12}^2 \ll \delta m_{13}^2$, is required to bring $\langle P(\bar{\nu}_e \rightarrow \bar{\nu}_e) \rangle$ down asymptotically to the solar neutrino result. The value of δm_{12}^2 is not tightly constrained, other than the indication from deep mine measurements of $\langle P(\bar{\nu}_\mu \rightarrow \bar{\nu}_\mu) \rangle$ that $\delta m_{12}^2 \gtrsim 10^{-3} \text{ eV}^2$. A solution which accommodates all known constraints is

δm_{13}^2	δm_{12}^2	θ_1	θ_2	θ_3	δ	(5)	
<u>SOLUTION A:</u>	1.0 eV^2	0.05 eV^2	45°	25°	30°	0°	.

The predictions for subasymptotic transition probabilities are shown in Fig. 3.

A more conservative interpretation of the reactor $\bar{\nu}_e$ data could be that $P(\bar{\nu}_e \rightarrow \bar{\nu}_e)$ falls to around 0.7-0.8 in the range of L/E considered, but that oscillatory behavior is not established. If so, two other classes of solution are possible: Class B, where $\bar{\nu}_e \rightarrow \bar{\nu}_e$ is suppressed by the onset of a long wavelength oscillation, that may have its first node well beyond $L/E = 1 \text{ m/MeV}$; Class C, where $\bar{\nu}_e \rightarrow \bar{\nu}_e$ is suppressed by a short wavelength oscillation, that may have many nodes below $L/E = 1 \text{ m/MeV}$. Illustrative solutions of these classes are as follows (we emphasize that their parameters are less constrained than in Class A).

	δm_{13}^2	δm_{12}^2	θ_1	θ_2	θ_3	δ	
<u>SOLUTION B:</u>	0.15 eV ²	0.05 eV ²	55°	0°	45°	0°	(6)
<u>SOLUTION C:</u>	10 eV ²	0.05 eV ²	45°	25°	30°	0°	.

We note that equivalent solutions to Eqs. (5) and (6) are obtained with $\delta m_{13}^2 \leftrightarrow \delta m_{12}^2$, $\delta = \pi$, and $\theta_3 \rightarrow \frac{\pi}{2} - \theta_3$ with θ_1 , θ_2 unchanged. Table 1 presents a capsule summary of the present experimental limits on oscillations and summarizes predictions of solutions A, B and C for existing and planned experiments. For the L/E range of the CERN beam dump experiment,¹⁹ a $\delta m^2 \gtrsim 10$ eV² is required to yield an e/ μ ratio that is significantly less than unity.^{2b} In solution C, which has a δm^2 in that range, the mixing angles are nearly the same as those contained in ref. 2b. Solution A has the same mixing matrix as solution C, but the smaller value of δm_{13}^2 leads to visible oscillations in reactor experiments rather than in high energy beam dump experiments.

New reactor experiments: Reactor measurements³ in the L/E range 5-20 m/MeV could provide information on δm_{12}^2 . For $\delta m_{12}^2 \ll 0.05$ eV² solutions A and C predict no appreciable deviation from a $1/r^2$ fall-off of the average flux at $L/E > 5$ m/MeV.

New meson factory experiments: Since the decays of stopped μ^+ mesons provide well-known ν_e and $\bar{\nu}_\mu$ spectra, meson factory experiments at $L/E \sim 1-3$ m/MeV²⁴ could confirm the existence of $\nu_e \rightarrow \nu_e$ oscillations and place further constraints on $\bar{\nu}_\mu \rightarrow \bar{\nu}_e$ oscillations.

Summary: Reactor $\bar{\nu}_e$ data provide indications of neutrino oscillations with mass scale $\delta m^2 = 1$ eV². Solar and deep mine results suggest that the other mass scale is in the range $\delta m^2 \gtrsim 10^{-3}$ eV².

Acknowledgements

This research was supported in part by the University of Wisconsin Research Committee with funds granted by the Wisconsin Alumni Research Foundation, and in part by the Department of Energy under contract DE-AC02 76ER00881, COO-881-135.

By acceptance of this article, the publisher and/or recipient acknowledges the U. S. Government's right to retain a nonexclusive, royalty-free license in and to any copyright covering this paper.

REFERENCES

1. B. Pontecorvo, Soviet Phys. JETP 53, 1717 (1967); V. Gribov and B. Pontecorvo, Phys. Lett. 28B, 493 (1969).
2. For thorough recent reviews of theory and experiment see (a) S.M. Bilenky and B. Pontecorvo, Phys. Reports 41, 225 (1978); (b) A. de Rujula et al., CERN TH-2788 (1979).
3. F. Reines, Unification of Elementary Forces and Gauge Theories (eds. D. B. Cline and F. E. Mills), Harwood Academic Publishers, p. 103 (1978); F. Reines, private communication to D. Cline of $E > 5.5$ MeV data (1978); S. Y. Nakamura et al., Proc. of the Inter. Neutrino Conf., Aachen (ed. by H. Faissner et al.), Vieweg (1977).
4. F. Nezrick and E. Reines, Phys. Rev. 142, 852 (1966).
5. M. Kobayashi and T. Maskawa, Prog. Theor. Phys. 49, 652 (1973). We follow the convention in V. Barger and S. Pakvasa, Phys. Rev. Lett. 42, 1585 (1979).
6. R. Davis Jr., J. C. Evans and B. T. Cleveland, Proc. of the Conf. on on Neutrino Physics, ed. by E. C. Fowler (Purdue Univ. Press, 1978).
7. M. R. Krishnaswamy et al., Proc. Phys. Soc. Lond. A323, 489 (1971).
8. M. F. Crouch et al., Phys. Rev. D18, 2239 (1978).
9. L. V. Volkova and G. T. Zatsepin, Sov. J. Nucl. Phys. 14, 117 (1972).
10. E. Bellotti et al., Lett. Nuovo Cim. 17, 553 (1976).
11. J. Blietschau et al., Nucl. Phys. B133, 205 (1978).
12. S. E. Willis et al., Phys. Rev. Lett. 44, 522 (1980).
13. A. M. Cnops et al., Phys. Rev. Lett. 40, 144 (1978).
14. R. E. Carter, F. Reines, R. Wagner and M. E. Wyman, Phys. Rev. 113, 280 (1959).

15. F. T. Avignone, III, Phys. Rev. D2, 2609 (1970).
16. F. T. Avignone, III and L. P. Hopkins, in Proc. of Conf. on Neutrino Physics, ed. by E. C. Fowler (Purdue Univ. Press, 1978).
17. B. R. Davis, P. Vogel, F. M. Mann and R. E. Schenter, Phys. Rev. C19, 2259 (1979).
18. L. R. Sulak et al., in Proc. of Inter. Conf. on Neutrino Physics and Astrophysics, Elbrus, USSR (1977).
19. H. Wachsmuth, CERN-EP/79-115 C (1979); also K. Winter (private communication).
20. A. Chudakov and G. Zatsepin (private communication).
21. Irvine-Michigan-Brookhaven collaboration (F. Reines et al.,); Harvard-Purdue-Wisconsin collaboration (J. Blandino et al.).
22. J. L. Osborne and E. C. M. Young in Cosmic Rays at Ground Level, ed. by A. W. Wolfendale, Institute of Physics, London (1973).
23. L. Wolfenstein, Phys. Rev. D17, 2369 (1978).
24. Considerations are in progress by D. Cline and B. Burman for such a neutrino oscillation experiment at LAMPF.

TABLE REFERENCES

- a San Onofre reactor experiment by Reines et al.³ in progress, with $L = 25-100$ m.
- b Possible LAMPF experiment with $E_{\nu_e}, E_{\bar{\nu}_e} = 30-50$ MeV and $L = 30-100$ m.
- c Brookhaven experiment¹⁸ in data analysis stage.
- d $\nu_e \rightarrow \nu_\tau$ oscillations can lead to a e/μ ratio different from unity in beam dump experiments (see e.g., ref. 2b and data of ref. 19).
- e The excellent agreement of observed and calculated $\nu_e/\bar{\nu}_e$ flux at CERN and Fermilab indicates that most of the ν_e does not oscillate into ν_τ .
- f Deep mine experiments^{7,8} have detected about 130 neutrino events ($E \sim 10^4-10^6$ MeV, $L \sim 10^6-10^7$ m). An unaccountably large number of multitrack events were observed in the Kolar gold field experiment;⁷ assuming that these are not attributed to ν_μ , the event rate is about half the expected rate. In the Johannesburg mine experiment⁸ a ratio 1.6 ± 0.4 of expected to observed ν_μ events was found. The analysis in ref. 9 of these experiments is consistent with $\langle P(\nu_\mu \rightarrow \nu_\mu) \rangle \sim 0.5$. A new deep mine experiment is operating at Baksan, USSR which is sensitive to ν_μ flux through the earth.²⁰
- g Deep mine experiments in construction²¹ will detect neutrinos of energies $E \sim 10^2-10^3$ MeV using very large water detectors placed in deep mines. At these energies the composition²² of the ν -flux from π , K , and μ decays of the secondary cosmic ray component in the atmosphere is roughly $(2\nu_\mu + \nu_e)/3$. Upward events in the detector will have $L \simeq 10^6-10^7$ m and downward events will have $L \simeq 10^4$ m. The charged-current scattering of ν_e on electrons significantly modifies vacuum oscillation predictions only for deep mine events which have $E(\text{MeV}) \gtrsim 10^6 \delta m^2 (\text{eV}^2)$; see ref. 23.

TABLE 1

Experimental Limits on Neutrino Oscillations and Neutrino Flux Predictions

<u>Observable</u>	<u>Source Refs.</u>	<u>L E</u>	<u>m MeV</u>	<u>Present Limit</u>	<u>A</u>	<u>Solution</u>	<u>B</u>	<u>C</u>
$\langle P(\nu_e \rightarrow \nu_e) \rangle$	S 6	10^{10}		$\gtrsim \frac{1}{4}, \lesssim \frac{1}{2}$	0.41	0.33	0.41	
$P(\bar{\nu}_e \rightarrow \bar{\nu}_e)$	R 3,4	1-3		> 0.5	0.6-1.0	0.8-1.0	0.8 mean	
	R a	5-20			0.1-0.9	0.05-0.5	0.1-0.9	
$P(\nu_e \rightarrow \nu_e)$	A	0.04		> 0.85 e	1.0	1.0	0.9	
	M 12	0.3		1.1 ± 0.4	0.95	1.0	0.8 mean	
	M b	1-3			0.6-1.0	0.8-1.0	0.8 mean	
$P(\bar{\nu}_\mu \rightarrow \bar{\nu}_e)$	M 12	0.3		< 0.04	10^{-4}	10^{-3}	10^{-3}	
	M b	3			0.03	0.11	0.03	
$P(\nu_\mu \rightarrow \nu_e)/P(\nu_\mu \rightarrow \nu_\mu)$	A 10,11	0.04		$< 10^{-3}$	10^{-6}	10^{-5}	10^{-4}	
	A 18 c	1-7			0-0.2	0-0.8	0-0.2	
$P(\nu_e \rightarrow \nu_\tau)$	A d	0.04		< 0.2 e	10^{-3}	10^{-5}	0.1	
$P(\nu_\mu \rightarrow \nu_\tau)/P(\nu_\mu \rightarrow \nu_\mu)$	A 13	0.04		$< 2.5 \times 10^{-2}$	10^{-5}	10^{-5}	10^{-3}	
$\langle P(\nu_\mu \rightarrow \nu_\mu) \rangle$	D f	10^2-10^3		~ 0.5	0.51	0.51	0.51	
$\langle P(\nu_c \rightarrow \nu_\mu) \rangle$	D g	10^3-10^5			0.48	0.44	0.48	
$\langle P(\nu_c \rightarrow \nu_e) \rangle$	D g	10^3-10^5			0.42	0.33	0.42	
$P(\nu_c \rightarrow \nu_\mu)$	D g	$10-10^2$			0.3-0.7	0.3-0.7	0.3-0.7	
$P(\nu_c \rightarrow \nu_e)$	D g	$10-10^2$			0.2-0.6	0.2-0.6	0.2-0.6	

Notation: S(solar), R(reactor), M(meson factory), A(accelerator), D(deep mine); $\nu_c \approx (2\nu_\mu + \nu_e)/3$.

FIGURE CAPTIONS

Fig. 1 The $\bar{\nu}_e$ reactor flux measurements of Reines et al. at $L = 11.2$ m (ref. 3) and $L = 6$ m (ref. 4) compared with the calculated spectra of refs. 3, 4, 14-17.

Fig. 2 Transition probability $P(\bar{\nu}_e \rightarrow \bar{\nu}_e)$ versus L/E deduced from the ratio of the observed to the calculated $\bar{\nu}_e$ reactor flux from refs. 16-17. The curve represents neutrino oscillations with an eigenmass difference squared of $\delta m^2 = 1$ eV² (SOLUTION A of Eq. (5)).

Fig. 3 Subasymptotic neutrino oscillations for all channels based on SOLUTION A in Eq. (5). Arrows on the right-hand side denote asymptotic mean values.

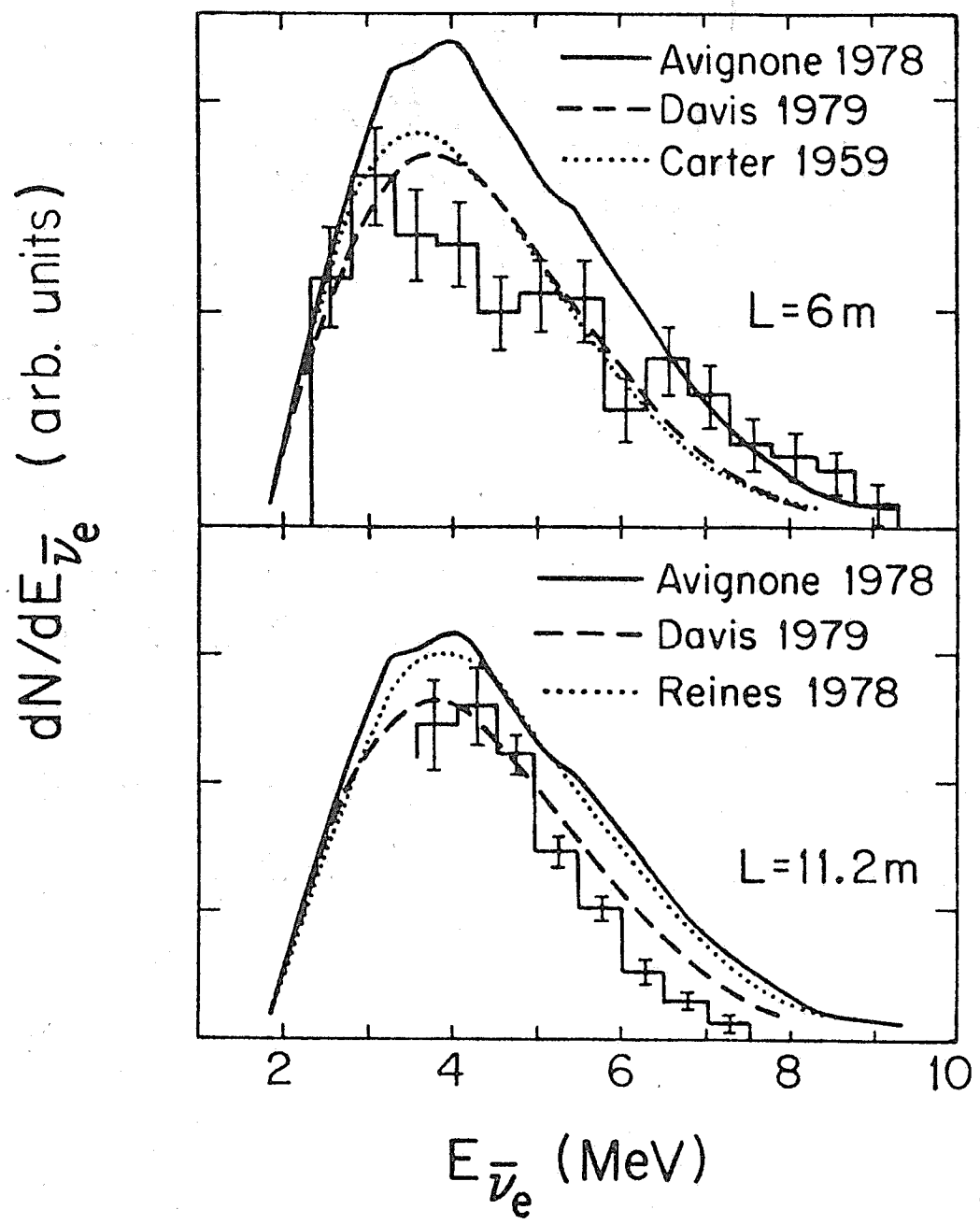


Fig. 1

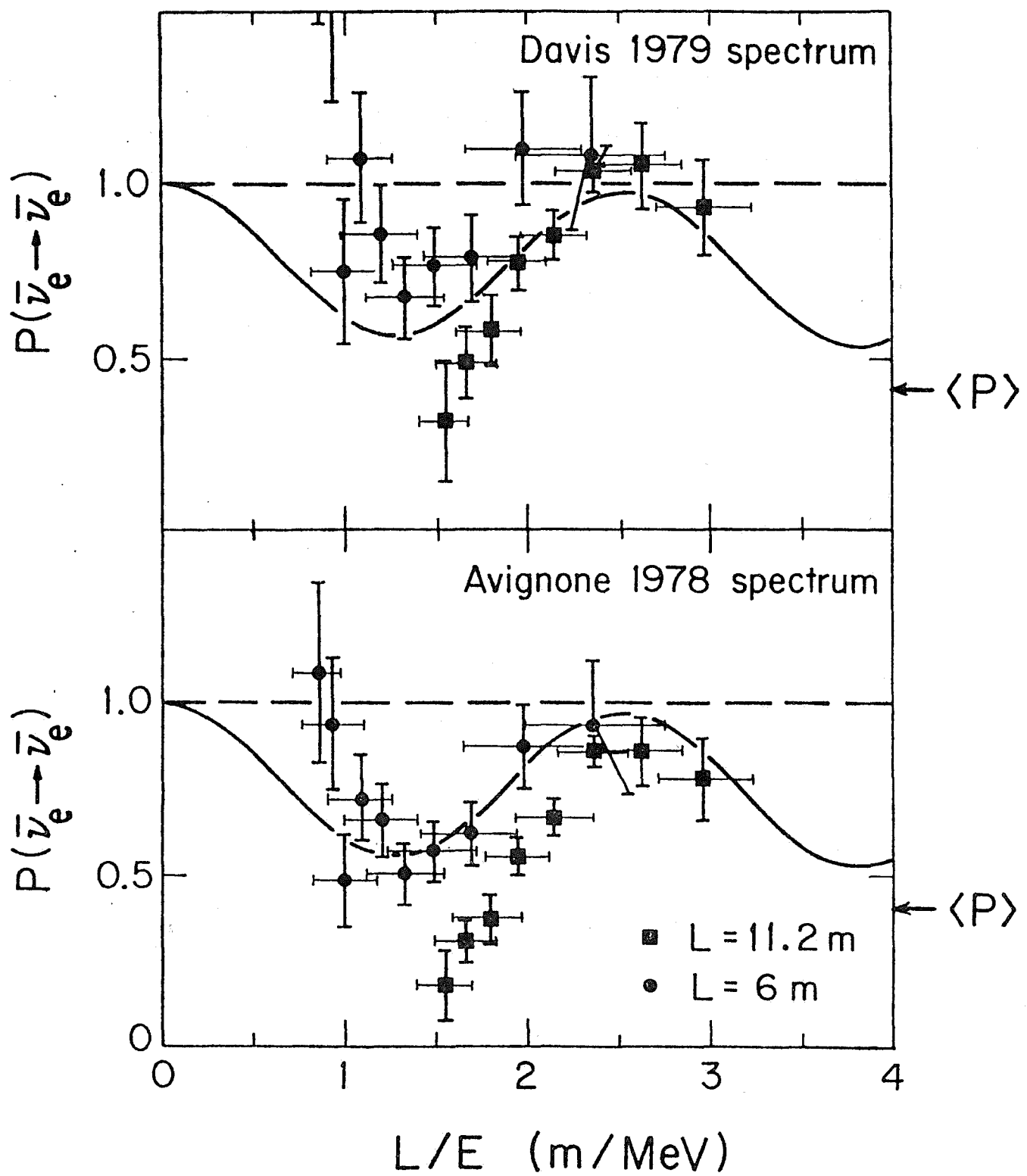


Fig. 2

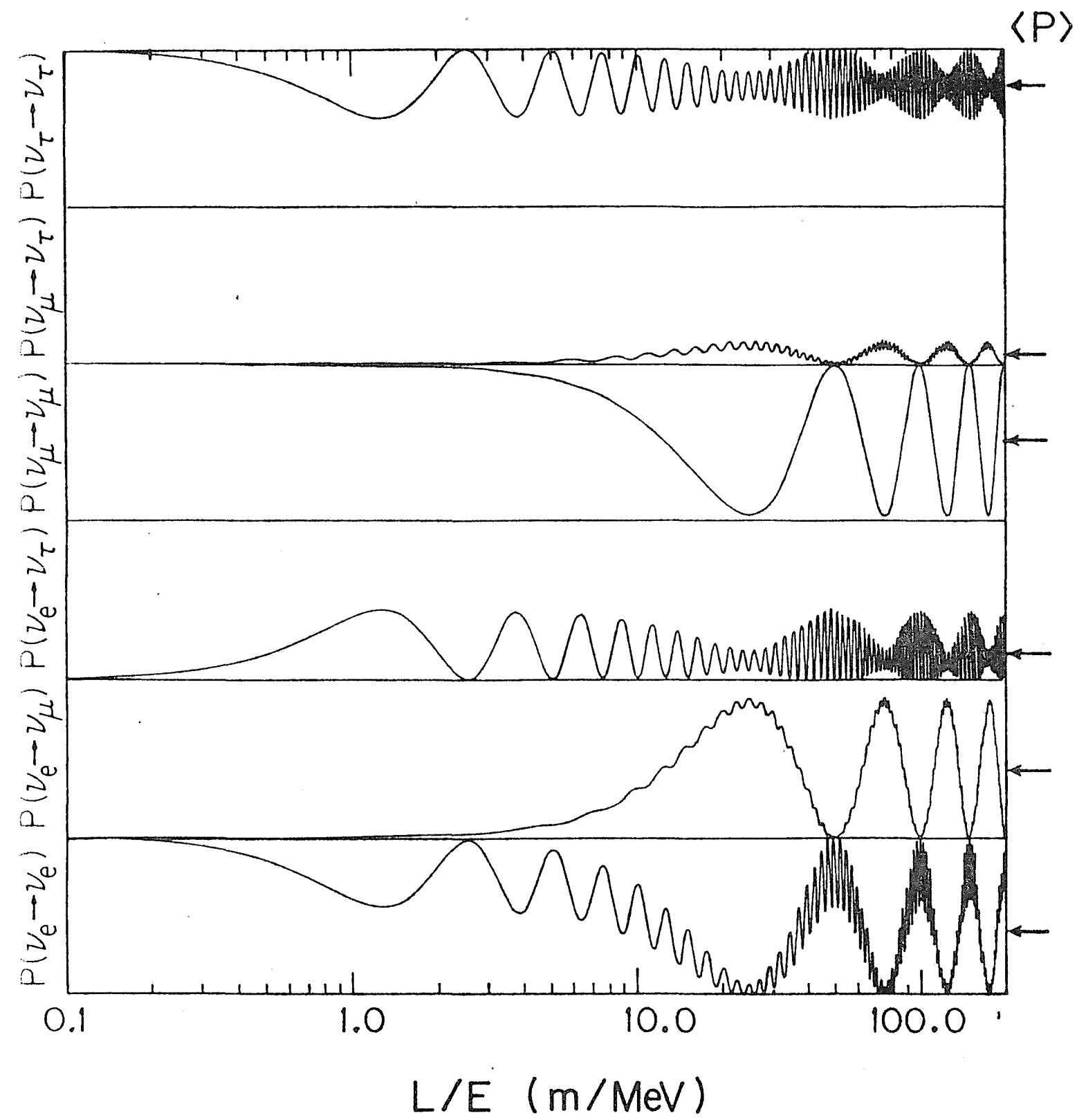


Fig. 3

APPENDIX B

COO-881-146

April 1980

MASS AND MIXING SCALES OF NEUTRINO OSCILLATIONS

V. Barger and K. Whisnant

Physics Department, University of Wisconsin, Madison, Wisconsin 53706 USA

D. Cline

Fermilab, Batavia, Illinois 60510 and

Physics Department, University of Wisconsin, Madison, Wisconsin 53706 USA

R. J. N. Phillips

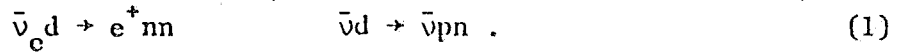
Rutherford Laboratory, Chilton, Didcot, Oxon, England

ABSTRACT

The extraction of neutrino oscillation parameters from the ratio of rates $(\bar{\nu}_e d \rightarrow e^+ nn)/(\bar{\nu} d \rightarrow \nu p n)$ is considered in the context of oscillations proposed to account for previous reactor data. The possibility that only ν_e, ν_μ oscillations occur is shown to be barely compatible with present limits on $\nu_\mu \rightarrow \nu_e$ transitions. Predictions for $\nu_e, \nu_\mu \rightarrow \nu_\tau$ oscillations are made for future accelerator experiments.

Neutrino oscillations¹⁻³ are of great interest because of the light they may shed on neutrino mass scales and mixing angles. The solar neutrino puzzle²⁻⁴ may indicate oscillations and a e/μ discrepancy in the CERN beam dump experiment has also been speculated upon⁵. Recently we presented⁶ a reexamination of all neutrino flux data, including the old reactor $\bar{\nu}_e$ measurements by Reines and collaborators.⁷ We drew the conclusion that the oscillation probability $P(\bar{\nu}_e \rightarrow \bar{\nu}_e)$ falls to 0.5 or lower in the neighborhood of $L/E = 1.5 \text{ m/MeV}$, where L is the distance from the source and E is the energy. Interpreting this as an oscillation effect, we showed that neutrino-mixing with a leading mass squared difference of the order of 1 eV^2 matched the reactor data in some detail (solution A of ref. 6). Qualitatively different classes of solutions were considered for comparison, with a δm^2 considerably smaller (solution B) or considerably larger (solution C) than 1 eV^2 .

Further evidence for neutrino oscillations from reactor experiments comes from the simultaneous consideration of charged current (CC) and neutral current (NC) deuteron disintegration reactions⁸



The neutral current process is immune to oscillations, being the same for all types of antineutrinos in the standard theory and effectively monitors the initial $\bar{\nu}$ flux. The ratio of CC/NC rates is rather insensitive to theoretical uncertainties in the calculated $\bar{\nu}_e$ spectrum from the reactor (the principle uncertainty hitherto) and can be used to extract neutrino oscillation parameters. In the present letter we calculate the NC/CC ratios predicted for this experiment by the solutions of ref. 6 and discuss the constraint on δm^2 and mixing angles. The possibility of having oscillations only in the ν_e, ν_μ system is

shown to be barely compatible with reactor data and present experimental limits on $\nu_\mu \rightarrow \nu_e$ transitions. For oscillations of three neutrinos, predictions of $\nu_e, \nu_\mu \rightarrow \nu_\tau$ oscillations are made for future accelerator experiments.

The spectrum averaged cross sections for deuteron disintegration have the form

$$\langle \sigma \rangle = \int_0^\infty dE_r \int_{E_{th}}^\infty dE_{\bar{\nu}} \rho(E_{\bar{\nu}}) f(E_{\bar{\nu}}) \frac{d\sigma}{dE_r} \quad (2)$$

where $\rho(E_{\bar{\nu}})$ is the $\bar{\nu}_e$ flux at $L = 0$ and $f = P(\bar{\nu}_e \rightarrow \bar{\nu}_e)$ at $L/E_{\bar{\nu}}$ for the CC case and $f = \frac{1}{2}$ for the NC case. The variable E_r is the energy of relative motion of the final state nucleons; the recoil energy of the two-nucleon system can be neglected to a 1% approximation. The differential cross sections are⁹

$$\frac{d\sigma}{dE_r} = \frac{g_A^2 G_F^2 M_N^{3/2}}{2\pi^3} J_d^2(E_r) (E_{\bar{\nu}} - E_{th} + m) [(E_{\bar{\nu}} - E_{th} + m)^2 - m^2]^{1/2} E_r^{1/2} \quad (3)$$

where M_N is the nucleon mass and $m = m_e$ for the CC and $m = 0$ for the NC.

The threshold energies are

$$E_{th}^{CC} = 4.030 \text{ MeV} + E_r \quad (4)$$

$$E_{th}^{NC} = 2.225 \text{ MeV} + E_r$$

In Eq. (2) the quantity J_d is the overlap integral of deuteron wave functions describing the 3S ground state and the 1S continuum state, given by⁹

$$J_d = \frac{1.52 \times 10^{-3} (43.1 + 0.83 E_r) \text{ MeV}^{-3/2}}{(E_r + 2.225) [E_r + (0.19 E_r + 0.27)^2]^{1/2}} \quad (5)$$

with E_r in MeV units. With the exponential fall-off of $\rho(E_{\bar{v}})$ folded in, the dominant contribution to $\langle\sigma\rangle$ comes from $E_r < 0.3$ MeV and $E_{\bar{v}} - E_{th} \approx 0.5-3.5$ MeV. Thus oscillation effects can be measured in the range 4.6 - 7.6 MeV. We calculate the ratio

$$R_d \equiv \frac{\langle\sigma(\bar{\nu}_e d \rightarrow e^+ nn)\rangle}{\langle\sigma(\bar{\nu}_e d \rightarrow \bar{\nu}_e pn)\rangle} \quad (6)$$

with and without oscillations.

At $L \approx 11.2$ m, $R_d(\text{osc})/R_d(\text{no osc})$ measures $P(\bar{\nu}_e \rightarrow \bar{\nu}_e)$ over the range $L/E \approx 1.5 - 2.4$, which is the region in which our analysis of the $\bar{\nu}_e p \rightarrow e^+ n$ data shows an oscillation effect.⁶ Figure 1 shows the predictions, assuming that only one eigenmass-difference plays a significant role in the reactor range, for which

$$P(\bar{\nu}_e \rightarrow \bar{\nu}_e) = 1 - \sin^2 2\alpha \sin^2(1.27 \delta m^2 L/E) \quad (7)$$

with δm^2 in eV^2 units and L/E in m/MeV. The curves in Fig. 1 versus δm^2 represent mixing angles for which $\sin^2 2\alpha = 0.19$ (α = Cabibbo angle), 0.50, 0.80 and 1.0. These calculations are based on the Avignone-1978 reactor spectrum;¹⁰ closely similar results are obtained with the Davis et al. spectrum.¹¹ Assuming ideal acceptance and allowing one standard deviation from the measured value of⁸

$$R_d(\text{osc})/R_d(\text{no osc}) = 0.43 \pm 0.17 \quad (8)$$

values of δm^2 are permitted in the ranges

$$0.3 < \delta m^2 < 1.1 \text{ eV}^2 \quad \delta m^2 > 1.7 \text{ eV}^2 \quad (9)$$

for appropriate mixing angles α . The solution classes A and C of ref. 6 satisfy these criteria. For the preferred class A solutions, our analysis⁶ of the $\bar{\nu}_e p \rightarrow e^+ n$ data at $L = 11.2$ m gives the ranges

$$0.80 < \delta m^2 < 1.05 \text{ eV}^2 \quad (10)$$

$$0.4 < \sin^2 2\alpha < 0.9$$

Results similar to Eqs. (9) and (10) were independently obtained in ref. 8. Figure 2 shows predictions for $R_d(\text{osc})/R_d(\text{no osc})$ versus L for other reactor experiments, based on solution A with $\delta m^2 = 0.8 \text{ eV}^2$ and the spectrum of ref. 10.

Stringent limits^{12,13} exist on $\nu_\mu \rightarrow \nu_e$ and $\bar{\nu}_\mu \rightarrow \bar{\nu}_e$ oscillations at $L/E \approx 0.04 \text{ m/MeV}$ and on $\bar{\nu}_\mu \rightarrow \bar{\nu}_e$ oscillations at $L/E \approx 0.3 \text{ m/MeV}$. If oscillations occurred only between ν_e and ν_μ states and if a single δm^2 is dominant below $L/E = 3 \text{ m/MeV}$ (as in solutions A and C of ref. 6), we can write

$$P(\nu_\mu \rightarrow \nu_e) = P(\bar{\nu}_\mu \rightarrow \bar{\nu}_e) = P_0 \sin^2(1.27 \delta m^2 L/E) \quad (11)$$

with the experimental bound

$$P_0 < 0.3/(\delta m^2)^2. \quad (12)$$

The corresponding bound on the mixing angle is

$$\sin^2 2\alpha < 0.3/(\delta m^2)^2. \quad (13)$$

For $\delta m^2 \sim 1 \text{ eV}^2$, this is just on the borderline of admissibility by the existing reactor data.

Applying similar considerations to oscillations of three neutrinos, probability conservation leads to the predictions

$$P(v_e \rightarrow v_\tau) = P(\bar{v}_e \rightarrow \bar{v}_\tau) = [\sin^2 2\alpha - P_0] \sin^2(1.27 \delta m^2 L/E) .$$

(14)

$$P(v_\mu \rightarrow v_\tau) = P(\bar{v}_\mu \rightarrow \bar{v}_\tau) = [P_0 / (4 \sin^4 \alpha)] P(v_e \rightarrow v_\tau) .$$

Thus three neutrino oscillations can be tested by detecting v_τ , \bar{v}_τ produced in a v_e , v_μ beam that is free of v_τ and \bar{v}_τ . The v_τ , \bar{v}_τ are detected through the interactions

$$v_\tau n \rightarrow \tau^- X^+$$

(15)

$$\bar{v}_\tau p \rightarrow \tau^+ X^0 .$$

Figure 3 shows predictions for $P(v_e \rightarrow v_\tau)$ for the L/E range of high energy accelerators (the two curves for solution A corresponding to P_0 between 0 and 0.3, with $\delta m^2 = 1 \text{ eV}^2$). $P(v_\mu \rightarrow v_\tau)$ depends critically on P_0 and can be larger than $P(v_e \rightarrow v_\tau)$.

Solution C has been of primary interest in connection with the e/μ ratio of beam dump experiments.⁵ By increasing the scale of the δm^2 , it is possible to construct an alternate version of solution C (solution C') which can explain both reactor and beam results by having a short wavelength oscillation (such as $\delta m_{13}^2 \approx 50 \text{ eV}^2$) superimposed on a long wavelength oscillation ($\delta m_{12}^2 \approx 1 \text{ eV}^2$). Representative six-quark mixing angles for such a solution are

$$\theta_1 = 30^\circ \quad \theta_2 = 50^\circ \quad \theta_3 = 55^\circ \quad \delta = 0^\circ . \quad (16)$$

Solution C' gives $R_d(\text{osc})/R_d(\text{no osc}) = 0.59$ at $L = 11.2 \text{ m}$; the minimum value of $P(\bar{v}_e \rightarrow \bar{v}_e)$ in the reactor range is 0.47 when averaged over the short wavelength oscillation. Predictions of $P(v_e \rightarrow v_\tau)$ for this solution are also given in Fig. 3.

Acknowledgements

We thank W. Sullivan for asking a pertinent question. We also thank S. Pakvasa for discussions and J. Leveille and D. Winn for transmitting information.

This research was supported in part by the University of Wisconsin Research Committee with funds granted by the Wisconsin Alumni Research Foundation, and in part by the Department of Energy under contract EY-76-C-02-0881, COO-881-111.

By acceptance of this article, the publisher and/or recipient acknowledges the U. S. government's right to retain a nonexclusive, royalty-free license in and to any copyright covering this paper.

REFERENCES

1. Z. Maki, M. Nakagawa and S. Sakata, *Prog. Theor. Phys.* 28, 247 (1962).
2. B. Pontecorvo, *Soviet Phys. JETP* 53, 1717 (1967); V. Gribov and B. Pontecorvo, *Phys. Lett.* 28B, 493 (1969).
3. For recent reviews of theory and experiment see S. M. Bilenky and B. Pontecorvo, *Phys. Reports* 41, 225 (1978).
4. R. Davis, Jr., J. C. Evans and B. T. Cleveland, *Proc. of the Conf. on Neutrino Physics*, ed. by E. C. Fowler (Purdue Univ. Press, 1978).
5. A. de Rujula et al., CERN TH-2788 (1979); H. Wachsmuth, CERN Report EP/79-115C (1979); K. Winter (private communication).
6. V. Barger et al., UW-Madison Report COO-881-135 (1980); to be published in *Phys. Lett.*
7. F. Reines, Unification of Elementary Forces and Gauge Theories (eds. D. B. Cline and F. E. Mills), Harwood Academic Publishers, p. 103 (1978); F. Nezrick and E. Reines, *Phys. Rev.* 142, 852 (1966).
8. F. Reines, H. W. Sobel and E. Pasierb, *Evidence for Neutrino Instability*, Univ. Cal.-Irvine preprint (1980); F. Reines et al., *Phys. Rev. Lett.* 43, 96 (1979); V. Barger and D. Cline, *Flux-Independent Analysis of Neutrino Oscillations* (February 1980, unpublished).
9. S. A. Fayans, L. A. Mikaelyan and Y. L. Dobryin, *J. Phys. G.: Nucl. Phys.* 5, 209 (1979); T. Ahrens and T. P. Lang, *Phys. Rev. C3*, 979 (1971).
10. F. T. Avignone, III and L. P. Hopkins, in *Proc. of Conf. on Neutrino Physics*, ed. by E. C. Fowler (Purdue Univ. Press, 1978).
11. B. R. Davis, P. Vogel, F. M. Mann and R. E. Schenter, *Phys. Rev. C19*, 2259 (1979).
12. J. Blietschau et al., *Nucl. Phys. B133*, 205 (1978).
13. A. N. Cnops et al., *Phys. Rev. Lett.* 40, 144 (1978).

FIGURE CAPTIONS

Figure 1 Neutrino oscillation results for the quantity $R_d(\text{osc})/R_d(\text{no osc})$ with R_d as defined in Eq. (6).

Figure 2 Predictions for $R_d(\text{osc})/R_d(\text{no osc})$ versus distance L from the reactor core, based on solution A with $\delta m^2 = 0.8 \text{ eV}^2$.

Figure 3 Predicted $\nu_e \rightarrow \nu_\tau$ transition probability for the L/E range of high energy accelerators. The δm^2 values are 1 eV^2 for solution A, 10 eV^2 for C, 50 eV^2 and 1 eV^2 for C'.

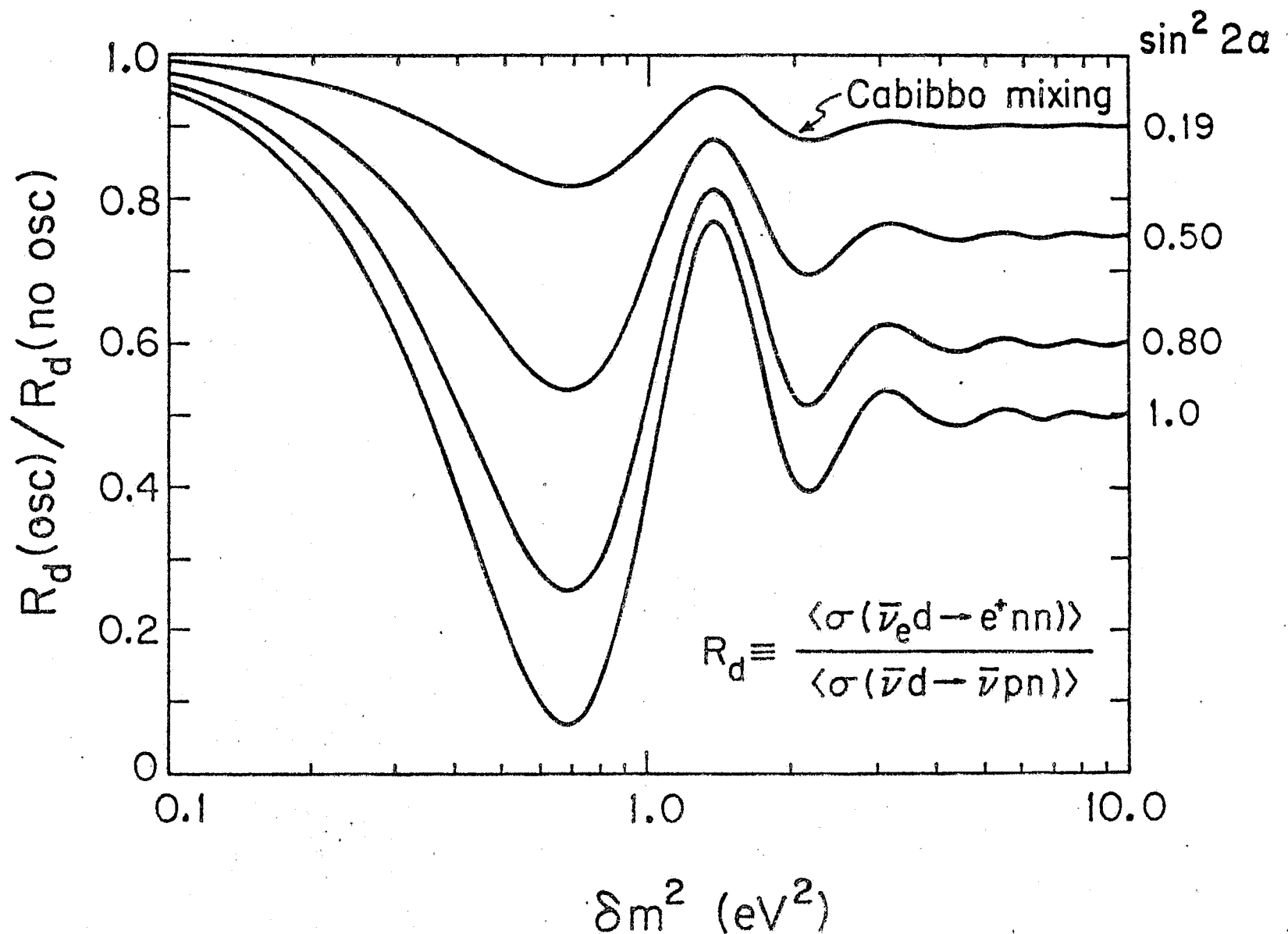


Figure 1

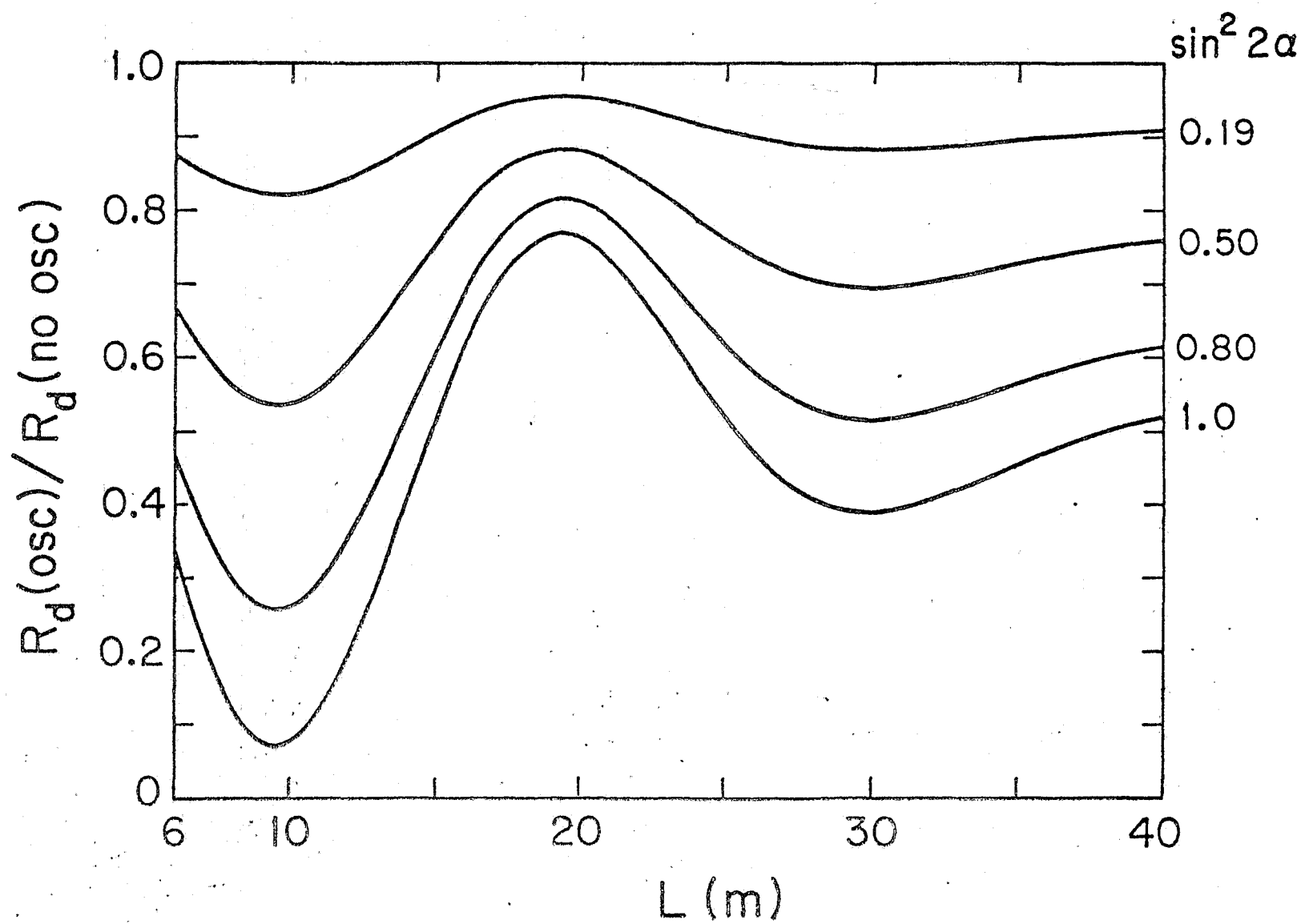


Figure 2

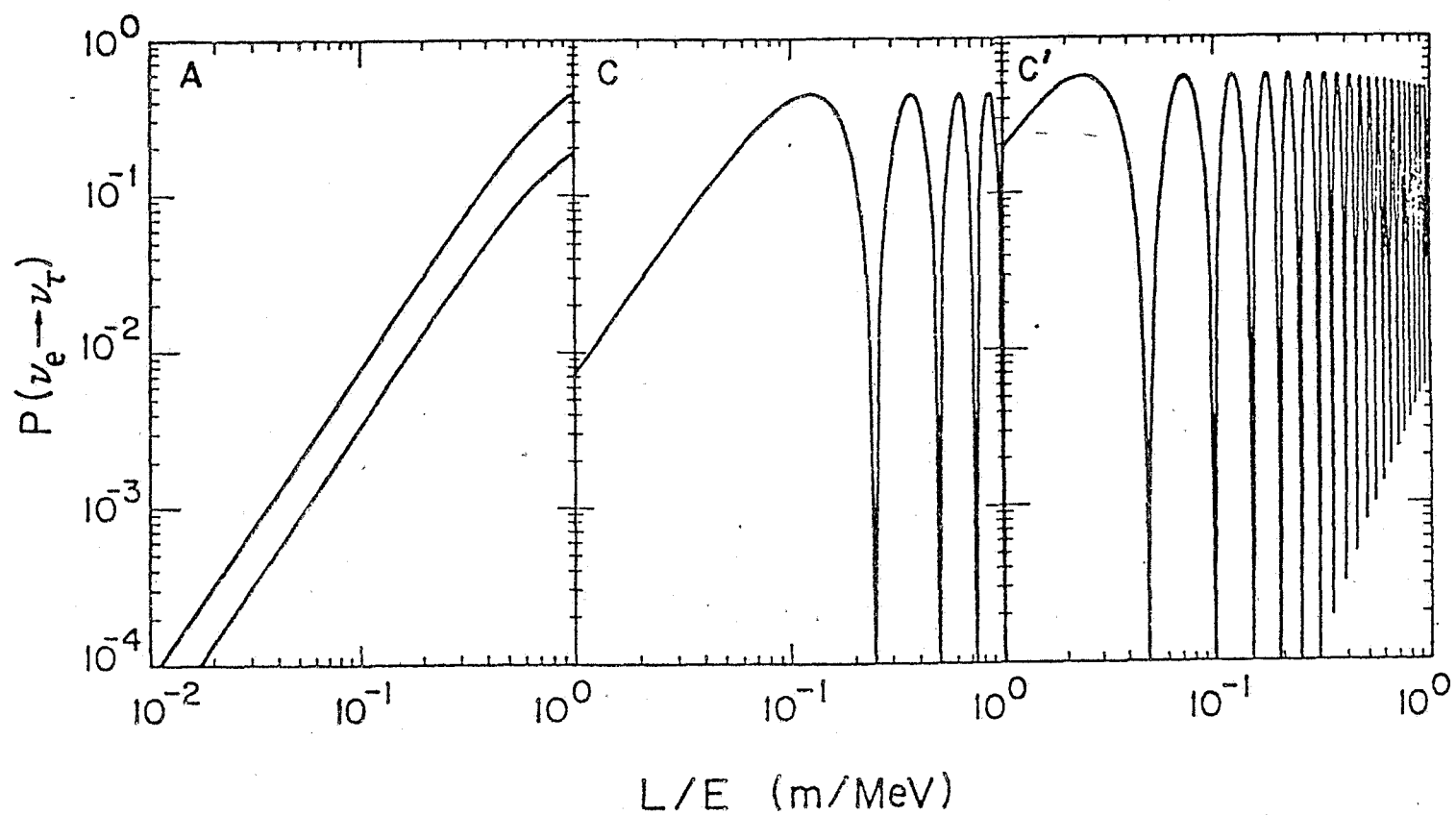


Figure 3

COO-881-149

May 1980

CONSEQUENCES OF MAJORANA AND DIRAC MASS MIXING FOR NEUTRINO OSCILLATIONS

V. Barger, P. Langacker*, J. P. Leveille

Department of Physics, University of Wisconsin-Madison
Madison, Wisconsin 53706

and

S. Pakvasa

Department of Physics and Astronomy, University of Hawaii at Manoa
Honolulu, Hawaii 96822

ABSTRACT

We consider a second class of neutrino oscillations which can arise when both Majorana and Dirac neutrino mass terms exist. These oscillations mix neutrino members of weak current doublets with singlets of the same helicity. A depletion of a neutrino beam results, with apparent non-conservation of probability. Possible relevance to current oscillation experiments is discussed.

*On leave from the University of Pennsylvania, Philadelphia, PA 19174.

The success and appeal of grand unified theories¹ have given a new theoretical impetus to the question of neutrino mass.² Moreover, recent analyses of reactor and beam dump data have revealed the exciting possibility that neutrino oscillations exist.³⁻⁵ The standard formalism^{6,7} for neutrino oscillations is based on oscillations of the type $\nu_{eL} \leftrightarrow \nu_{\mu L} \leftrightarrow \nu_{\tau L}$, which mix flavors without change of chirality or lepton number; hereafter we refer to these as first class oscillations. In this Letter we consider the possibility of a second class of neutrino oscillations,⁸ involving transitions of the type $\nu_L \leftrightarrow \eta_L$ which mix neutral members of weak isospin doublets ν_L with singlets η_L . In the standard $SU(2) \times U(1)$ model, the usual right-handed singlets would be $\eta_R^c = C(\bar{\eta}_L)^T$ where C is the charge conjugation matrix. To avoid confusion, we emphasize at the outset that second class oscillations are not of the helicity-flip type $\nu_{eL} \leftrightarrow \nu_{eR}^c$, where ν_{eR}^c (usually denoted by $\bar{\nu}_e$) is the right-handed antineutrino produced in μ^- decay; ν_{eL} and ν_{eR}^c are related by charge conjugation, and ν_{eR}^c is an $SU(2)$ doublet member along with e^+ . In general, second class oscillations can involve transitions among different doublet and singlet flavors.

Neutrino mass terms can be either of Majorana or Dirac type. At least some grand unified theories suggest² that both may be present simultaneously.⁸ Dirac mass terms are of the form $\bar{\nu}_L \eta_R^c$ while Majorana mass terms are of the forms $\bar{\nu}_L \nu_R^c$ and $\bar{\eta}_L \eta_R^c$, which violate lepton number by two units.⁹ Diagonalization of the mass matrix for a single lepton family yields two Majorana (i.e., self-conjugate) mass eigenstates. Assuming that both masses are small, neutrino oscillations will occur between the doublet and singlet gauge eigenstates of the same helicity. Since singlet fields are decoupled from gauge bosons, these second class oscillations deplete neutrino beams, giving the appearance of probability non-conservation. In the general case of several

lepton flavors, both first and second class oscillations can occur.

In the following we first develop the formalism for second class oscillations involving a single lepton family. We then address possible phenomenological implications for neutrino oscillation experiments, comparing expectations from first and second class oscillations. Finally, we develop the formalism for the situation when both classes of oscillations are present. Our considerations are specifically based on a V-A structure for the charged weak current, in which case helicity flip oscillations¹⁰ are suppressed by $(m_\nu/E)^2$ and are negligible.

For simplicity we first consider the consequences of having both Majorana and Dirac neutrino mass terms in a single family version of the standard $SU(2) \times U(1)$ model. The left-handed leptons are $(\nu, e^-)_L$, e_L^+ and η_L . The associated charge conjugate neutrino fields are defined as $\nu_R^c \equiv C(\bar{\nu}_L)^T$ and $\eta_R^c \equiv C(\bar{\eta}_L)^T$, where $C = i\gamma^2\gamma^0$ is the charge conjugation matrix. The general form of the Lagrangian mass term is

$$L_{\text{mass}} = -\frac{1}{2}[a(\bar{\nu}_L \nu_R^c) + d(\bar{\nu}_L \eta_R^c + \bar{\eta}_L \nu_R^c) + s(\bar{\eta}_L \eta_R^c)] + \text{h.c.} \quad (1)$$

In Eq. (1) we have made use of the identity $\bar{\nu}_L \eta_R^c = \bar{\eta}_L \nu_R^c$ to reduce the number of independent constants. Defining the doublets $\omega_L^\alpha \equiv (\nu_L, \eta_L)$ and $\omega_R^\alpha \equiv (\nu_R^c, \eta_R^c)$, we can write

$$L_{\text{mass}} = -\frac{1}{2}\bar{\omega}_L^\alpha M^{\alpha\beta} \omega_R^\beta + \text{h.c.} \quad (2)$$

with mass matrix

$$M = \begin{pmatrix} a & d \\ d & s \end{pmatrix}. \quad (3)$$

For symmetry breaking with the standard Higgs doublet representation, the

parameter d is non-zero but a vanishes; a non-zero value for a can be obtained by adding a Higgs triplet; s is due to a singlet Higgs or a bare mass term.

The diagonalized mass matrix is $M_D = U_L^\dagger M U_R$ where U_L and U_R are unitary transformations of the ω_L and ω_R^c fields. Since M is symmetric, $U_R = U_L^* K^\dagger$ with K a symmetric unitary matrix. For non-degenerate mass eigenvalues, K is a diagonal matrix of phases, $K_{ij} = e^{-i\phi_i} \delta_{ij}$. By appropriate choice of the matrix K , we can take U_L to be a real rotation matrix. The relation of mass eigenstates ν_{iL} to ω_L^α is

$$\omega_L^\alpha = U_L^{\alpha i} \nu_{iL} \quad (i = 1, 2) . \quad (4)$$

The corresponding right-handed transformation is

$$\omega_R^{\alpha c} = C(\overline{\omega_L^\alpha})^T = U_R^{\alpha i} K_{ij} \nu_{jR}^c \equiv U_R^{\alpha i} \tilde{\nu}_{iR}^c \quad (5)$$

where

$$\tilde{\nu}_{iR}^c \equiv K_{ij} \nu_{jR}^c = K_{ij} C(\overline{\nu_{jL}})^T . \quad (6)$$

The free Lagrangian for the neutral leptons is diagonal in the basis $\nu_i = \nu_{iL} + \tilde{\nu}_{iR}^c$. From Eq. (6) we find $\tilde{\nu}_i^c = \nu_i$, where $\nu_i^c \equiv K_{ij} C(\bar{\nu}_j)^T$. Hence the ν_i are Majorana neutrino fields since they are self-conjugate.¹¹ The combined Dirac and Majorana mass terms in the Lagrangian produce two Majorana eigenstates which in general have different masses m_1 and m_2 . When $m_1 \neq m_2$, there is no conserved lepton number.

From Eq. (4), the weak eigenstates ν_L and η_L are linear superpositions of the two Majorana mass eigenstates

$$\nu_L = \cos\alpha \nu_{1L} + \sin\alpha \nu_{2L} \quad (7)$$

$$\eta_L = -\sin\alpha \nu_{1L} + \cos\alpha \nu_{2L}$$

where $\cos\alpha = (U_L)^{11}$, $\sin\alpha = (U_L)^{12}$. The singlet state η_L does not couple to gauge bosons and interacts with fermions only via Higgs couplings. The doublet member ν_L has the usual charged and neutral current couplings. In the mass eigenstate basis, the neutral current is non-diagonal.

We mention two limiting cases of Eq. (3). If $a = 0$, $s = 0$, the Lagrangian possesses an invariance $(\nu_L, e_L, \eta_R^c) \rightarrow e^{i\beta}(\nu_L, e_L, \eta_R^c)$, corresponding to lepton number conservation; note that η_L is an antilepton in this case. The Majorana states are then degenerate ($m_1 = m_2$) and combine to form a single massive Dirac field. Another interesting limit is $a = 0$, $|s| \gg |d|$ which occurs naturally in some grand unified theories.² In this case the mass eigenvalues are $m_1 = |d|^2/s$ and $m_2 = |s|$, and U_L is a unit matrix, to leading order in $|d|/|s|$. If $|d|$ is a typical fermion mass ~ 1 GeV and $|s|$ is the unification mass scale $\sim 10^{14}$ GeV, the state m_2 cannot be produced and effectively decouples.

Our primary considerations are for another logical possibility in which both m_1 and m_2 are small compared to the electron mass. This possibility has interesting implications for neutrino oscillations. Since the mass eigenstates propagate differently in time, $\nu_{eL} \rightarrow \eta_{eL}$ oscillations occur. These "second class" oscillations conserve helicity. At a distance L from a source of ν_{eL} , the probability (for energy $E \gg m_1, m_2$) of finding ν_{eL} is

$$P(\nu_{eL} \rightarrow \nu_{eL}) = 1 - \sin^2 2\alpha \sin^2(\frac{1}{2}\Delta) \quad (8)$$

where the oscillation argument is $\frac{1}{2}\Delta = 1.27 \delta m^2 L/E$, with $\delta m^2 = m_1^2 - m_2^2$ in

eV^2 units and L/E in m/MeV units. The oscillations result in a depletion of an electron neutrino beam, or equivalently a deviation from a $1/r^2$ law for a point ν_{eL} source. Moreover, since η_{eL} is effectively non-interacting, probability conservation would appear to be experimentally violated by an amount $P(\nu_{eL} \rightarrow \eta_{eL}) = 1 - P(\nu_{eL} \rightarrow \nu_{eL})$, in contrast to first class oscillations where a depletion in $\nu_{eL} \rightarrow \nu_{eL}$ coincides with $\nu_{eL} \rightarrow \nu_{\mu L}$, $\nu_{\tau L}, \dots$ transitions which are in principle observable.

In second class oscillations, both the charged current (CC) $\nu_{eL} p \rightarrow e^- X$ and neutral current (NC) $\nu_{eL} p \rightarrow \nu_{eL} X$ cross sections oscillate

$$\sigma(L)/\sigma(L=0) = P(\nu_{eL} \rightarrow \nu_{eL}; L/E) \quad (9)$$

and the ratio $\sigma_{\text{NC}}/\sigma_{\text{CC}}$ is unaffected in the one family case. This contrasts with first class oscillations where σ_{CC} and $\sigma_{\text{NC}}/\sigma_{\text{CC}}$ oscillate, but σ_{NC} does not. Corresponding statements apply to ν_{eR}^c cross sections.

We now turn to possible phenomenological implications of second class oscillations for current experiments.

Solar: Lepton number violating oscillations have the capability of explaining the deficiency in the ratio of observed to expected solar neutrinos.¹² With first and second class oscillations among three families, the minimum probability for $\nu_e \rightarrow \nu_e$ transitions is 1/6.

Reactor: The cross sections for an initial ν_{eR}^c beam scattering on proton and deuteron targets indicate depletions^{3,4} in $\sigma_{\text{CC}}(p)$, $\sigma_{\text{CC}}(d)$ and $\sigma_{\text{CC}}(d)/\sigma_{\text{NC}}(d)$ but not (at the $\approx 20\%$ uncertainty level) in $\sigma_{\text{NC}}(d)$. To explain both the σ_{CC} and $\sigma_{\text{CC}}/\sigma_{\text{NC}}$ results, first class oscillations are required with $\delta m^2 \approx 1 \text{ eV}^2$.

Beam dump: Charged and neutral current events are produced by prompt neutrinos created in the dump. Since the prompt neutrinos originate from

decays of charmed particles, identical ν_e and ν_μ spectra and numbers are generated. The charged and neutral current interactions of the prompt neutrinos are measured in bubble chamber and counter experiments¹³ at CERN at a distance $L \approx 800-900$ m downstream.

In the bubble chamber experiment, the measured e/μ ratio¹³ is $R(e/\mu) = 0.48^{+0.24}_{-0.16}$. Such deviations of the e/μ ratio from unity may indicate a $P(\nu_e \rightarrow \nu_e)$ depletion arising from oscillations.^{3,5} For the CERN beam dump $L/E \approx 0.01$ m/MeV, so the mass scale of the oscillations would be $\delta m^2 \approx 100$ eV². To discuss such oscillations we assume a prompt neutrino beam with equal parts of ν_{eL} and $\nu_{\mu L}$, neglecting any ν_{eR}^c and $\nu_{\mu R}^c$ contributions for simplicity.

For second class oscillations of the ν_e family alone, the e/μ ratio is given by

$$R(e/\mu) = [\langle P(\nu_e \rightarrow \nu_e) \sigma_{CC} \rangle] / \langle \sigma_{CC} \rangle \quad (10)$$

where σ_{CC} is the inclusive production cross section for e or μ and $\langle \rangle$ denotes a spectrum average. For first class oscillations $\nu_e \rightarrow \nu_e$, $\nu_e \rightarrow \nu_\tau$ (stringent experimental limits exist on $\nu_\mu \rightarrow \nu_e$ and $\nu_\mu \rightarrow \nu_\tau$ oscillations in this L/E range), the corresponding prediction is

$$R(e/\mu) = \frac{\langle P(\nu_e \rightarrow \nu_e) \sigma_{CC} \rangle + 0.17 \langle P(\nu_e \rightarrow \nu_\tau) \sigma_{CC}^\tau \rangle}{\langle \sigma_{CC} \rangle + 0.17 \langle P(\nu_e \rightarrow \nu_\tau) \sigma_{CC}^\tau \rangle} \quad (11)$$

where σ_{CC}^τ is the inclusive τ cross section. For comparable mixing in the two classes, the predictions in Eqs. (10) and (11) are similar. One can discriminate experimentally between the classes of oscillations by ascertaining whether τ is produced and whether σ_{NC}/σ_{CC} changes.

The beam dump counter experiments measure the ratio $N(0\mu)/N(1\mu)$ of muonless to single muon events. With second class oscillations of the ν_e family the prediction is

$$N(0\mu)/N(1\mu) = [\langle (1 + P(\nu_e \rightarrow \nu_e)) \sigma_{NC} \rangle + \langle P(\nu_e \rightarrow \nu_e) \sigma_{CC} \rangle] / \langle \sigma_{CC} \rangle \quad (12)$$

in the limit of perfect acceptance. The corresponding prediction for first class oscillations is

$$\frac{N(0\mu)}{N(1\mu)} = \frac{2 \langle \sigma_{NC} \rangle + \langle P(\nu_e \rightarrow \nu_e) \sigma_{CC} \rangle + 0.83 \langle P(\nu_e \rightarrow \nu_\tau) \sigma_{CC}^T \rangle}{\langle \sigma_{CC} \rangle + 0.17 \langle P(\nu_e \rightarrow \nu_\tau) \sigma_{CC}^T \rangle} \quad (13)$$

Taking comparable mixing in the two classes (and hence similar $R(e/\mu)$ predictions), the value of $N(0\mu)/N(1\mu)$ is significantly lower for second class oscillations. A detailed analysis with experimental cuts could thereby differentiate between first and second class oscillations in this L/E range on the basis of measured $R(e/\mu)$ and $N(0\mu)/N(1\mu)$ values. Still other alternatives are simultaneous first and second class oscillations or first class oscillations involving additional families.

We next turn to the general case of first and second class oscillations involving three families of leptons. The neutral members of the weak doublets are ν_{eL} , $\nu_{\mu L}$ and $\nu_{\tau L}$. We assume an equal number of singlets η_{eL} , $\eta_{\mu L}$ and $\eta_{\tau L}$ (though there could be a different number).¹⁴ As in the single family case, we define vectors $\omega_L^\alpha = (\nu_{eL}, \nu_{\mu L}, \nu_{\tau L}, \eta_{eL}, \eta_{\mu L}, \eta_{\tau L})$ and $\omega_R^{\alpha c} = (\nu_{eR}^c, \nu_{\mu R}^c, \nu_{\tau R}^c, \eta_{eR}^c, \eta_{\mu R}^c, \eta_{\tau R}^c)$ with $\alpha = 1, \dots, 6$. The mass term can then be written as in Eq. (2) with

$$M = \begin{pmatrix} A & D \\ D^T & S \end{pmatrix}, \quad (14)$$

where A , S and D are 3×3 matrices. A and S are symmetric matrices, which implies M is symmetric also. To diagonalize M , we make the transformations analogous to Eqs. (4) and (5) with $i = 1, \dots, 6$. The Majorana fields $\nu_i = \nu_{iL} + \tilde{\nu}_{iR}^c$ are the physical eigenstates with masses m_i , $i = 1, \dots, 6$.

The unitary matrix U_L can be written in 3×3 matrix block form as

$$U_L = \begin{pmatrix} W & X \\ Y & Z \end{pmatrix} = U_R^* K^\dagger. \quad (15)$$

The matrix $W(Z)$ describes first class oscillations among the doublet (singlet) members; X and Y describe second class oscillations connecting doublets and singlets.

In the special cases of only Dirac mass terms ($A = S = 0$) or of only Majorana mass terms ($D = 0$), the freedom of choice of K can be used to set $X = Y = 0$. Hence only first class oscillations occur and the unitarity of U_L implies that W and Z are unitary. W describes the conventional flavor-changing oscillations; Z is essentially unobservable.

In the general case in which both first class and second class oscillations are present simultaneously, the unitarity of U_L no longer implies that W is unitary. This corresponds to the depletion effect of doublets oscillating into singlets, such as $\nu_{eL} \leftrightarrow \bar{\nu}_{eL}$, $\bar{\nu}_{\mu L}$, $\bar{\nu}_{\tau L}$. The crucial test of second class oscillations is the direct measurement of all flavors of produced neutrino doublet members to test for apparent probability non-conservation.

Acknowledgements

We thank M. Deshpande, E. Ma, R. J. N. Phillips, H. Wachsmuth and K. Whisnant for Discussions. This research was supported in part by the Department of Energy under contracts DE-AC02 76ER00881, COO-881-149 and DE-AC03-76ER00511.

By acceptance of this article, the publisher and/or recipient acknowledges the U. S. Government's right to retain a nonexclusive, royalty-free license in and to any copyright covering this paper.

REFERENCES

1. See for example, H. Georgi and S. Glashow, Phys. Rev. Lett. 32, 438 (1974); A. Buras et al., Nucl. Phys. B135, 66 (1978).
2. H. Georgi and D. V. Nanopoulos, Nucl. Phys. B155, 52 (1979); M. Gell-Mann et al., in Supergravity, ed. by P. van Nieuwenhuizen and D. Z. Freedman, North-Holland (1979); R. Barbieri et al., CERN TH 2776 (1979); E. Witten, HUTP-79/A076. For a different approach to the neutrino mass matrix, see R. H. Mohapatra and G. Senjanovic, Phys. Rev. Lett. 44, 912 (1980).
3. V. Barger et al., Phys. Lett. (in press); UW-Madison reports COO-881-135, 146, 148 (1980).
4. F. Reines et al., Univ. of Cal.-Irvine preprint (1980).
5. A. DeRujula et al., CERN report TH-2788 (1979).
6. Z. Maki et al., Prog. Theor. Phys. 28, 870 (1962); B. Pontecorvo, Phys. Lett. 28B, 493 (1969).
7. For a recent review see S. M. Bilenky and B. Pontecorvo, Phys. Reports 41, 225 (1978).
8. S. M. Bilenky and B. Pontecorvo, Lett. Nuovo Cim. 17, 569 (1976).
9. These Majorana mass terms can be rewritten as $\overline{\nu_L} C(\overline{\nu_L})^T$ and $\overline{\eta_L} C(\overline{\eta_L})^T$.
10. J. N. Bahcall and H. Primakoff, Phys. Rev. D18, 3463 (1978); A. Zee, Univ. of Penn. preprint UPR-0150T (1980).
11. By the transformation $\nu_i^! \equiv (K^{-\frac{1}{2}})_{ij} \nu_j$ we recover the conventional definition of Majorana fields, $\nu_i^{!c} = \nu_i^!$. However, we choose not to follow this convention in order to maintain a freedom of choice for U_L .
12. J. Bahcall, Sp. Sc. Rev. 24, 227 (1979); J. Bahcall and S. C. Frautschi, Phys. Lett. 29B, 623 (1969); R. Davis, Jr. et al., ed. by E. C. Fowler (Purdue Univ. Press, 1978).
13. H. Wachsmuth, CERN-EP/79-115C (1979).
14. Since the singlets are essentially non-interacting, they seem to have no astrophysical consequences.